Investigating the potential senomorphic properties of SCFA butyrate on aged T cells

by

Nia Paddison Rees

A thesis submitted to
the University of Birmingham
for the degree of
MSc Res Inflammation and Ageing

Institute of Inflammation and Ageing
College of Medical and Dental Sciences
University of Birmingham
June 2023

Abstract

Ageing is accompanied by remodelling of the T cell pool and a hallmark of immune ageing is the expansion of senescent T cells in aged hosts. Senescent T cells express markers of DNA damage and cell cycle arrest markers, elevated production of pro-inflammatory cytokines as a result of the senescence-associated secretory phenotype (SASP), and accumulation of dysfunctional mitochondria. Importantly, animal studies have brought to light the causal role of senescent T cell accumulation in driving ageing of non-lymphoid organs; highlighting the need to combat the build-up of senescent T cells with advancing age.

Advancing age is also characterised by changes in gut microbiome composition, one consequence of which is a reduction in short-chain fatty acid (SCFA) levels, the products of bacterial fermentation in the gut. Interestingly, our group have reported a negative correlation between stool butyrate levels and senescent CD4 and CD8 T cells in older adults. To elucidate this connection further, in this thesis, we have examined the effect of butyrate on T cell senescent features in healthy young ($\leq$ 35 years) and healthy old ($\geq$ 65 years) adults using an *in vitro* model of proliferation-induced senescence.

Evaluation of the potential anti-senescent effect of butyrate revealed significant reductions in the cell cycle arrest maker p53 and DNA damage marker γ-H2AX in aged T cells following 3 day culture with 1mM butyrate. We observed potential senomorphic properties of butyrate mediated via attenuation of SASP post butyrate treatment in aged T cells, alongside reductions in the expression of a key SASP regulator, the transcription factor nuclear factor kappa B (NF-κB) at both the gene and protein level. Additionally, our findings demonstrated the potential ability of butyrate to decrease mitochondrial mass and ROS production in the T cells of older adults, however this requires further investigation. Consequently, we present butyrate supplementation as a future senomorphic postbiotic treatment to delay the onset of the senescent phenotype and help reduce the healthspan-lifespan gap by combating immunesenescence.

Acknowledgements

I would like to acknowledge and express my thanks to Dr Niharika Duggal for all her support and supervision during my thesis, and for encouraging my enthusiasm for the gut microbiome and ageing throughout my years at the University of Birmingham.

I thank PhD student, and fellow researcher in the Duggal group, Jessica Conway for all her guidance and assistance in teaching me the laboratory techniques used in this thesis, alongside Ben Dugan, my laboratory technician, who was also a great help during my time in the lab.

I am extremely grateful to my family for their continuous encouragement and belief in me during my academic journey.

Finally, I would like to thank everyone at the Institute of Inflammation and Ageing that assisted with this research, in particular those who helped with blood sample donation and collection.

Table of Contents

List of Figures and Tables

1.0 Introduction

2.0 Materials and Methods

3.0 Results

4.0 Discussion

Appendix

List of Abbreviations

ABC	Age-associated B cell
AMP	Antimicrobial peptide
APCs	Antigen presenting cells
ARDs	Age-related diseases
β-HB	Beta-hydroxybutyrate
BCR	B cell receptor
Blimp-1	B lymphocyte-induced maturation protein 1
B_{regs}	Regulatory B cells
CCFs	Cytoplasmic chromatin fragments
cDCs	Conventional dendritic cells
CDKn1a	Cyclin dependent kinase inhibitor 1a
CM	Central memory
CRAMP	Cathelicidin-related antimicrobial peptide
CREB	cAMP response element-binding protein
CRP	C-reactive protein
cT_{reg}	Colonic regulatory T cell
CVD	Cardiovascular disease
CXCL	CXC motif chemokine ligand
DAMPs	Damage-associated molecular patterns
DCs	Dendritic cells
DSBs	Double strand breaks
EM	Effector memory
EMRA	Effector memory RA
FMT	Faecal microbiota transplant
γ-H2AX	Gamma-H2A histone family member X
GDF11	Growth differentiation factor 11
GI	Gastrointestinal
GPI	Glucose-6-phosphate isomerase
GPR	G-protein coupled receptor

GSK3β	Glycogen synthase kinase 3β
H_2O_2	Hydrogen peroxide
hASMCs	Human aortic smooth muscle cells
HDAC	Histone deacetylase
HFD	High fibre diet
HLA-DRB5	HLA class II histocompatibility antigen DR beta 5 chain
HLA-DQA2	HLA Class II histocompatibility antigen DQ alpha 2 chain
HSCs	Haematopoietic stem cells
HUVECs	Human umbilical vein endothelial cells
IECs	Intestinal epithelial cells
IFNα	Interferon-alpha
IFN-γ	Interferon-gamma
IL-1β	Interleukin-1 beta
IL-2	Interleukin 2
IL-2R	Interleukin 2 receptor
IL-6	Interleukin 6
IL-7	Interleukin 7
IL-8	Interleukin 8
IRF7	Interferon regulatory factor 7
IS	Immunological synapse
LBP	Lipopolysaccharide-binding protein
LC3	Microtubule associated protein 1 light-chain 3
LFD	Low fibre diet
LP	Lamina propria
LPS	Lipopolysaccharide
MAMPs	Microbe-associated molecular patterns
MAPK	Mitogen activated protein kinases
mDCs	Myeloid dendritic cells
MHC	Major histocompatibility complex
MLN	Mesenteric lymph node
MMP	Mitochondrial membrane potential

MRM	Multiple reaction mode
miRNAs	MicroRNAs
mtDNA	Mitochondrial DNA
mTORC1	Mammalian target of rapamycin complex 1
mTOR	Mammalian target of rapamycin
NF-kB	Nuclear factor kappa-light-chain-enhancer of activated B cells
NK	Natural killer
PBMCs	Peripheral blood mononuclear cells
PCs	Plasma cells
pDCs	Plasmacytoid cells
PI3K	Phosphoinositide 3-kinase
PSA	Polysaccharide A
ROS	Reactive oxygen species
RIG-I	Retinoic acid–inducible gene I
RILP	Rab-interacting lysosomal protein
S6	Ribosomal protein S6
S6K	Ribosomal protein S6 kinase
SASP	Senescence associated secretory phenotype
SCFAs	Short-chain fatty acids
SIgA	Secretory IgA
SLE	Systemic lupus erythematosus
SPF	Specific-pathogen-free
shRNAs	Short hairpin RNAs
T_{conv}	Conventional T cells
TCR	T cell receptor
TEC	Thymic epithelial cell
T_h	T helper cell
TLR	Toll-like receptor
TMAO	Trimethylamine-*N*-oxide
TMB	Tetramethylbenzidine
TNF-α	Tumour necrosis factor alpha
TRECs	T cell receptor excision circles

TREM-2	Triggering receptor expressed on myeloid cells 2
T_{reg}	Regulatory T cell
TSA	Trichostatin A
WT	Wild type
ZO-1	Zonula occludens-1

1.0 Introduction

1.1 Ageing population

Globally, lifespan (the total number of years lived) has extended considerably since the mid-twentieth century. As of 2020, life expectancy is now approximately 73 years of age, a 26-year increase from the life expectancy in 1950 (1). This prolonged lifespan has brought about a shift in the population demographic, with an inordinate growth in individuals over 70 (3). Despite this, a corresponding expansion in healthspan (the years lived disease-free) has not occurred due to the increasing incidence of chronic diseases with age, leading to the healthspan-lifespan gap which is estimated to be around 9 years (Figure 1) (1, 4). 80% of chronic disease-related deaths are attributable to diseases such as cancer, diabetes, cardiovascular disease (CVD) and chronic respiratory diseases with 58% of these deaths occurring in the over 70 age group (5).

Ageing is characterised by a loss of function in most organs such as cardiac, renal, pulmonary and cerebral in addition to a decline in endocrine and immune function (6). Physiological changes occurring with age are primarily determined by genetics however, they are also affected by environmental elements such as diet, exposure to microorganisms and exercise (7). So far, increases in lifespan have occurred due to advancements in reducing childhood mortality and recently it has been proposed that any further increase in lifespan will rely on extending the lives of the older population (8, 9). However, any extension of lifespan without the parallel increase in healthspan will only serve to widen the aforementioned healthspan-lifespan gap. Recognised as a priority by the UK government, it is imperative to focus on improving healthspan by reducing the years spent living with chronic disease in order to achieve a healthy lifespan (10, 11).

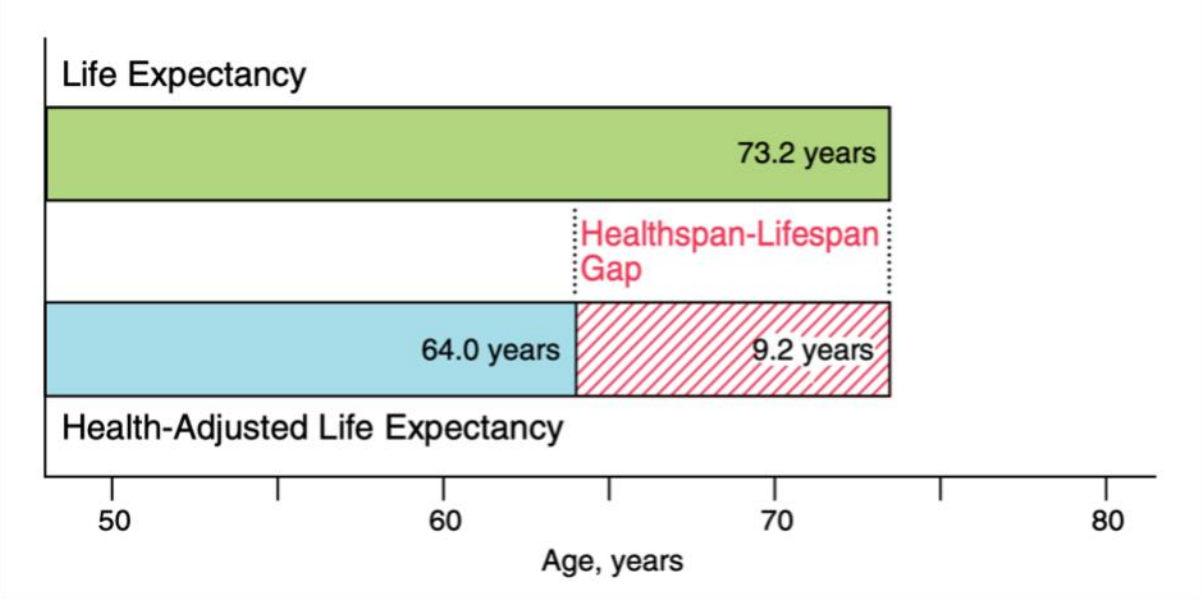

Figure 1. Healthspan-lifespan gap.
Despite life expectancy having increased to an average of 73.2 years, a significant proportion of this is spent in poor health. Therefore, the gap between the current life expectancy and total years spent healthy and disease-free (i.e., healthspan) is estimated at 9.2 years (1).

1.2 Immunesenescence

During the process of ageing, a remodelling of the innate and adaptive immune system occurs, resulting in an impaired ability to mount a robust immune response, termed immunesenescence (Figure 2) (12). Clinical implications of immunesenescence include increased susceptibility towards bacterial and viral infections (13), reduction in response to vaccinations (14) and an increased risk of chronic inflammatory conditions, such as rheumatoid arthritis (15) and cancers (16). Importantly, a recent study has recognised immunesenescence as a driver of the ageing process, demonstrating the causal role that an aged immune system has on systemic ageing (17).

1.2.1 Innate immune ageing

1.2.1 (a) Neutrophils

Neutrophils are the first immune cells to leave circulation and migrate to the site of infection and kill invading bacterial and fungal pathogens. However, with advancing age, the ability of neutrophils to migrate in response to a stimulus gradient, termed chemotaxis, has been shown to decrease (18, 19). Furthermore, aged neutrophils also display a reduced ability to phagocytose pathogens (20). Neutrophils mediate intracellular killing of pathogens via the antimicrobial enzymes and peptides present within intracellular granules, one of these being Cathelicidin-related antimicrobial peptide (CRAMP) (21). Lower concentrations of CRAMP were expressed at baseline in old mice compared to the young and whilst levels increased following *S. pneumoniae* infection, overall CRAMP levels remained significantly lower in old mice; together contributing towards the age-associated increased vulnerability to bacterial infections and elevated mortality (22).

1.2.1 (b) Monocytes/Macrophages

Responsible for the clearance of invading pathogens through the process of phagocytosis, macrophages are important immune effectors that are activated in both the early and late stages of infection (23). Although circulating monocyte numbers are preserved with age, an expansion of both the intermediate and pro-inflammatory non-classical $CD16^{+}$ monocyte

compartments is observed, paired with a decline in the classical subset (24). Such as with neutrophils, the ability of macrophages to phagocytose bacteria and apoptotic cells, a process known as efferocytosis, declines with age (25). A decline in phagocytic function of alveolar macrophages has been reported in aged mice and a decrease in efferocytosis capability with age is also seen in older humans (26, 27). Another feature of macrophage ageing is the shift toward a more pro-inflammatory phenotype. Aged monocytes display a decline in the production of pro-inflammatory cytokines (interferon-alpha (IFNα), interleukin-1 beta (IL-1β)) upon stimulation with toll-like receptor 4 (TLR4), TLR7/8 and retinoic acid–inducible gene I (RIG-I), however an increased basal secretion of pro-inflammatory cytokines is seen with age (28).

1.2.1 (c) Natural Killer cells

Natural killer (NK) cells are large granular lymphocytes crucial in removing virally infected senescent cells and tumours (29). The NK cell compartment is made up of primarily $CD56^{dim}$ cells which possess cytotoxic properties, both natural and antibody-dependent, whilst the remaining $CD56^{bright}$ cells are responsible for producing an assortment of cytokines and chemokines that influence immunomodulation (30). Studies have shown that with age, there is an increase in the number of $CD56^{dim}$ NK cells along with a corresponding decrease in $CD56^{bright}$ NK cells (31, 32). At a single cell level, aged NK cells demonstrate a decrease in cytotoxicity which is a result of reduced localisation of the cytolytic protein perforin towards the immunological synapse with age (32, 33). Production of anti-viral cytokines, in particular interferon-gamma (IFN-γ) and tumour necrosis factor alpha (TNF-α), by aged NK cells is decreased upon target cell stimulation, when compared with NK cells from young subjects (29, 34, 35).

1.2.1 (d) Dendritic cells

Bridging the gap between innate and adaptive immunity, dendritic cells (DCs) are the predominant antigen-presenting cells (APCs) and are comprised of two subsets; conventional DCs (cDCs), alternatively known as myeloid DCs (mDCs), and plasmacytoid DCs (pDCs) (36). Studies have highlighted that in cohorts over 60 years of age, the number of mDCs decreases whilst pDC numbers remain unchanged when compared with the young cohort (37, 38). With age, pDCs demonstrate a reduced ability to release the type I IFN cytokine upon stimulation

with toll-like receptor TLR9 ligand due to defective interferon regulatory factor 7 (IRF7) phosphorylation (39). The capacity of DCs to uptake and present antigens to naïve T cells diminishes with age; resulting in the diminished ability to prime a robust adaptive immune response (40, 41). The expression of specific genes involved in antigen presentation is significantly reduced in $CD1c^+$ mDCs from aged individuals. HLA class II histocompatibility antigen DR beta 5 chain (HLA-DRB5), HLA Class II histocompatibility antigen DQ alpha 2 chain (HLA-DQA2), and Rab-interacting lysosomal protein (RILP) were all downregulated in DCs from older adults compared to young individuals (42).

1.2.2 Adaptive immune ageing

1.2.2 (a) Thymic involution

The thymus, a primary lymphoid organ, is the site of T cell development occurring through a sequence of proliferation and differentiation phases, known as thymopoiesis (43). Haematopoietic stem cells (HSCs) residing in the bone marrow produce T cell progenitors called thymocytes which undergo maturation into single-positive CD4 and CD8 naïve T cells.With age, the thymus undergoes significant structural changes characterised by a diminished thymic mass and altered tissue organisation and microenvironment, termed thymic involution (44). In mice, age-related thymic involution has been shown to reduce total thymic and thymic epithelial cell (TEC) cellularity by 50% when comparing mice at 16 weeks with those 4 weeks of age (45). Alongside TEC decline is an expansion of fibroblasts and adipocytes, disrupting the normally well-defined cortex and medullar zones (46, 47). Age-associated thymic involution considerably affects thymic output, most notably causing a decrease in the numbers of naïve T cells produced (48).

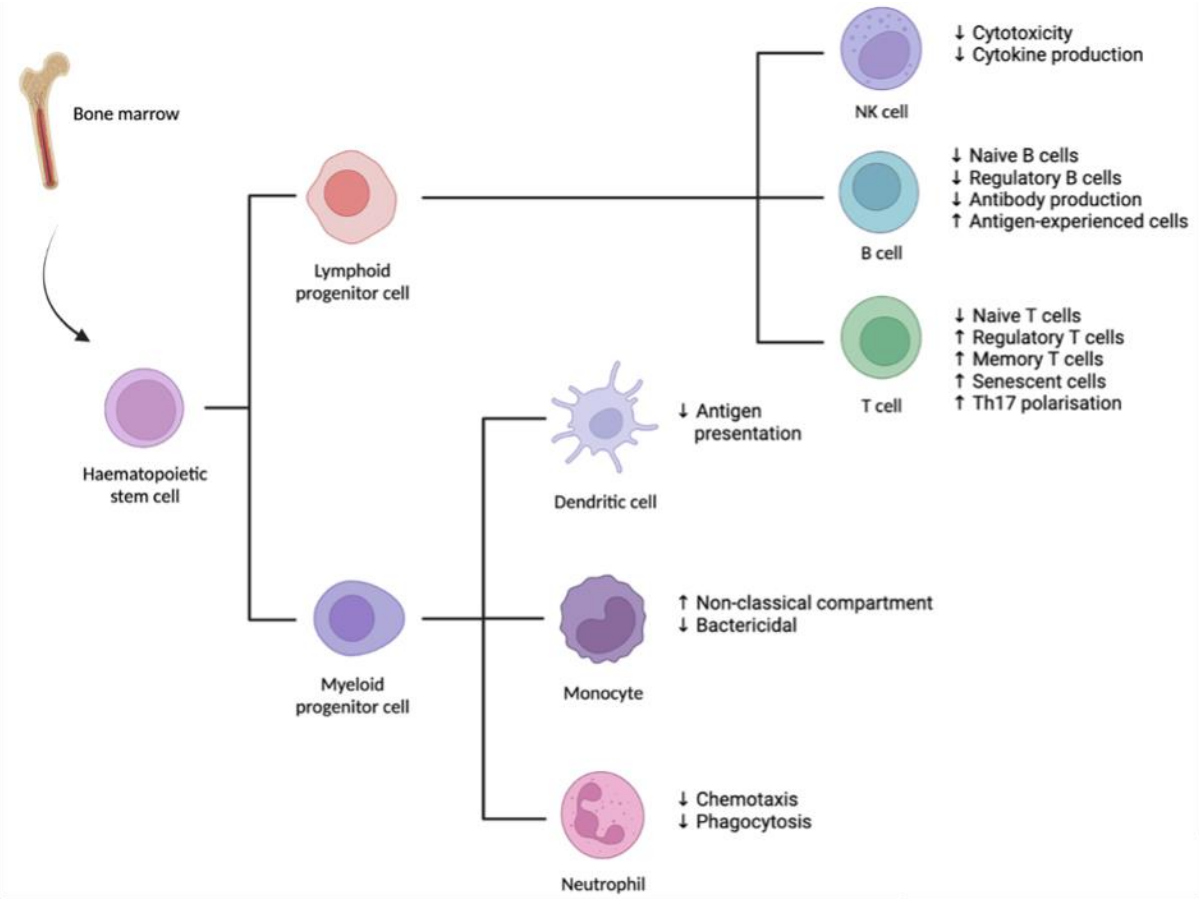

Figure 2. Hallmarks of adaptive and innate immunesenescence.
Ageing is associated with innate and adaptive immune system dysfunction resulting in the inability to respond appropriately to pathogenic challenge leading to dysregulated systemic inflammation. Ineffective pathogen clearance due to defective innate functioning alongside the failure of APCs to properly present antigens to the adaptive arm impairs lymphocyte priming and activation. In combination with intrinsic T and B cell senescence, affecting antibody generation and regulatory capacity, the overall consequence is a higher susceptibility to disease with age.

Recently, a study using T cell receptor excision circles (TRECs) generated during TCR development in maturing T lymphocytes as a method of measuring thymic output, reported an age-dependent decline in TREC expression in human peripheral blood mononuclear cells (PBMCs) (49). This reduction in naïve T cell output subsequently impacts the peripheral T cell pool landscape, leading to reduced cell diversity and diminished immunosurveillance capacity (48). Various underlying mechanisms have been proposed, one of which suggests that age-related defects in the stomal niches of the thymus contributes to thymic involution (43). The structural integrity of the thymus is disrupted due to the aforementioned increase in fibrosis and adiposity with age, affecting the thymic microenvironment leading to a reduction in thymopoiesis. Interleukin 7 (IL-7), produced by TECs, has a key role in thymopoiesis however studies have reported an age-dependent decline in IL-7 production, possibly attributed to the loss of major histocompatibility complex (MHC) class II^+ TECs in the aged thymus (50, 51).

1.2.2 (b) T cell subset redistribution and ageing

As previously mentioned, ageing is associated with a shift in the naïve: memory T cell ratio, a result of an increase in antigen-specific memory T cells that have encountered pathogens and a decrease in antigen-naïve T cells (52, 53). $CD4^+$ and $CD8^+$ memory T cells can be further classified into 3 subsets based on the expression of CD45RA and the chemokine receptor CCR7 cell surface markers; central memory ($CD45RA^-CCR7^+$), effector memory ($CD45RA^-CCR7^-$) and the terminally differentiated effector memory cells re-expressing CD45RA ($CD45RA^+CCR7^-$)(54). With age, a decrease in central memory (CM) T cells is observed whilst the effector memory (EM) compartment increases due to an accumulation of the terminally differentiated effector memory (EMRA) T cells (55, 56). These shifts in memory T cell composition are more pronounced in the cytotoxic $CD8^+$ compared to helper $CD4^+$ T cells (55).

1.2.2 (c) T cell senescence

With chronological ageing due to repeated antigenic stimulation T cells undergo replicative senescence, leading to an accumulation of senescent T cells, especially within the EMRA subset of the memory T cell population (57). Replicative senescence describes the process through which cells enter a condition of irreversible cell cycle arrest after numerous courses of replication, a state characterised by distinct alterations in gene expression and mediated

by initiation of either one or both p53/p21$^{WAF1/CIP1}$ and p16^{INK4A}/pRB tumour suppressor pathways (58).

Key features exhibited by senescent T cells include accumulation of unrepaired DNA damage, primarily in the form of double-strand breaks (DSBs), apoptosis resistance and telomere shortening (Figure 3) (59). Another hallmark is the increased secretion of cytokines, chemokines and proteinases by senescent T cells, known as the senescence-associated secretory phenotype (SASP). Many of the SASP components are pro-inflammatory in nature such as the cytokines interleukin-6 (IL-6), interleukin-8 (IL-8) and IL-1β therefore, as senescent T cells accumulate with age, continuous SASP generates a pro-inflammatory environment contributing to the low-grade, chronic inflammation that occurs with age, termed inflammageing (60, 61). Among the various T cell subsets, human senescent CD8^{+} TEMRA cells present with an extremely inflammatory secretory profile distinctive of the SASP which has been shown to be dependent on p38 mitogen-activated protein kinases (MAPK) signalling (62). Essential for senescence growth arrest due to its capacity to activate p53/p21$^{WAF1/CIP1}$ and p16^{INK4A}/pRB pathways, p38 MAPK has been identified as a key regulator of the SASP and is capable of promoting SASP in genotoxic-induced senescence (63). This occurs primarily via increased transcriptional activity of the nuclear factor kappa-light-chain-enhancer of activated B cells (NF-κB) protein complex. Inhibition of NF-κB using short hairpin RNAs (shRNAs) targeting the p65 subunit of NF-κB prevented induction of IL-6, IL-8 and CXC motif chemokine ligand 1 (CXCL1) SASP factors in senescent fibroblasts (64). In the context of age-associated senescence, reactive oxygen species (ROS) production acts as a trigger for the p38 MAPK pathway, the downstream effects of which stabilise SASP-dependent mRNA (65). Senescent T cells are characterised by increased mitochondrial ROS production due to the accumulation of dysfunctional mitochondria possibly as a result of defective mitophagy (60). It is thought that increased mitochondrial mass may serve as a protective measure against senescence, compensating for the decline in function with age, nevertheless, the persistent ROS production of aged mitochondria drives the senescent phenotype in T cells.

In addition to alterations in signalling pathways as biomarkers of senescence, T cells undergo various morphological changes with age that are indicative of senescent cells. Typically, senescent cells display a larger and irregularly shaped cell body, mediated by mammalian

target of rapamycin complex 1 (mTORC1) protein complex activation in response to senescence-inducing stimuli (65). An age-associated decline in growth factors, such as growth differentiation factor 11 (GDF11) and the growth hormone/insulin like growth factor-I axis, is also observed and possibly contributes to mTORC1 stimulation leading to cell enlargement (66).

1.2.2 (d) Ageing and T cell Functional changes

$CD4^+$ T cells develop into effector cells capable of secreting a wide variety of cytokines depending on the T_h1, T_h2, T_h17 or regulatory T cell (T_{reg}) subset (67). $CD8^+$ cytotoxic T cells function to eliminate damaged cells and cells infected by intracellular pathogens, for example viruses and cytoplasmic bacteria, through secretion of perforins, granulysin and granzymes (68). Activation of T cells requires T cell receptor (TCR) stimulation with peptide antigens via interactions with MHC class I ($CD8^+$) or MHC class II ($CD4^+$) on APCs, forming an immunological synapse (IS) (69). With age, declines in TCR repertoire diversity and signalling intensity have been observed whereby the ability of naïve $CD4^+$ T cells from aged mice to establish immunological synapses was defective when compared with young naïve $CD4^+$ T cells. This was due to impaired ability of aged $CD4^+$ T cells to redistribute the cytoskeletal protein F-actin towards the edge of the cell following incubation with anti-CD3, resulting in an age-related decrease in lamellopodia formation (70). On a transcriptional level, TCR signalling is controlled by microRNAs (miRNAs), specifically the expression of miR-181a in T cells (71). Ageing is associated with a decline in miR-181a expression, seen in both $CD4^+$ and $CD8^+$ T cells, in addition to further reductions in expression upon activation and differentiation (72, 73). Therefore, aged T cells possess diminished TCR sensitivity and require greater antigenic stimulation to trigger activation however, due to deficiencies in T cell-APC interactions, this higher activation threshold is not

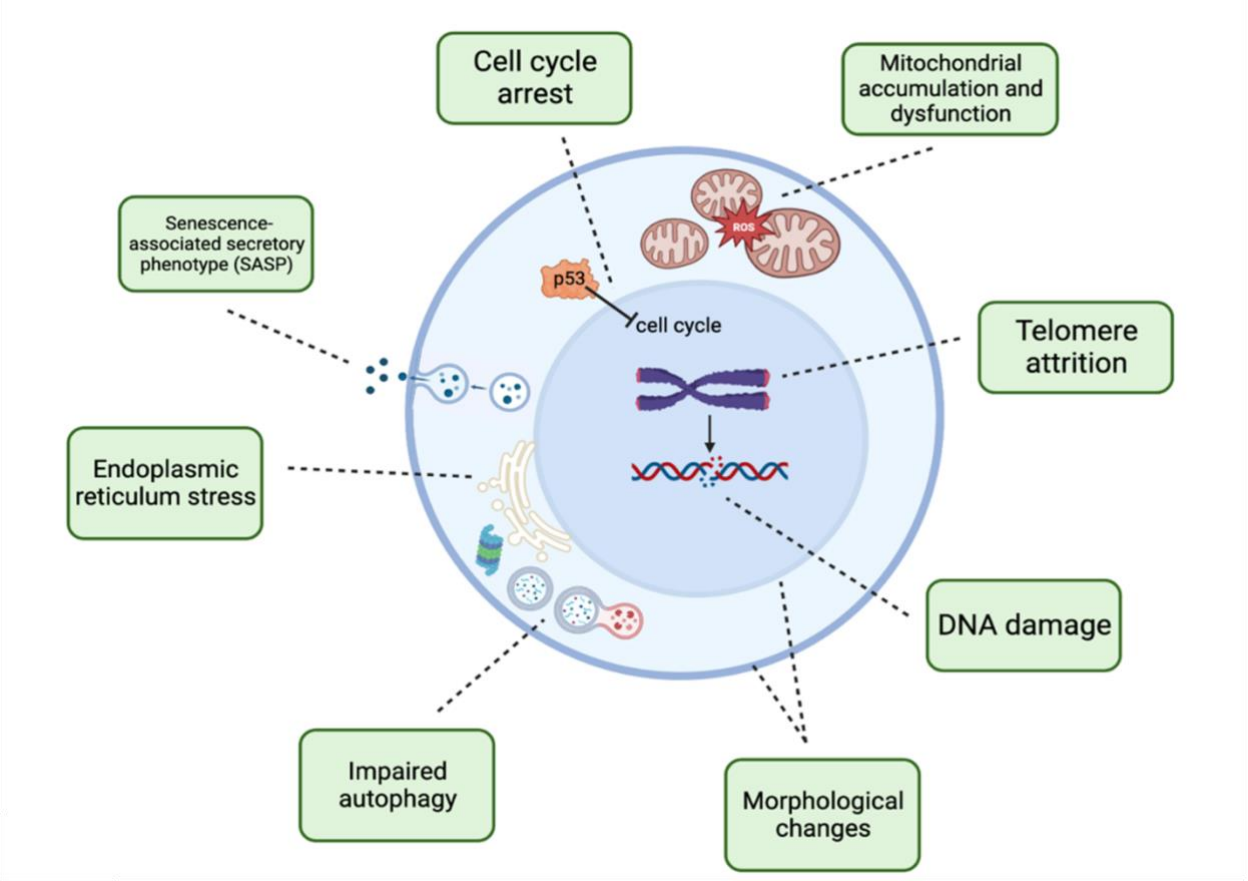

Figure 3. Hallmarks of senescent T cells.
During replicative senescence, the shortening of telomeres and excessive, unrepaired DNA damage in T cells triggers the upregulation of p53, causing irreversible cell cycle arrest. These cells possess dysfunctional mitochondria displaying extreme oxidative stress in the form of increased ROS production which contributes to impaired proteostasis mechanisms. Accumulation of defective mitochondria occurs due to senescent cells being less capable of clearance via mitophagy. Considerable changes to the secretome of senescent cells take place, characterised by a shift towards pro-inflammatory factors, known as the senescence-associated secretory phenotype (SASP) which contributes to inflammageing.

being met. Following activation, T cells from mice demonstrate an age-associated decline in proliferative capacity, with both $CD4^+$ and $CD8^+$ T cells from $\geq$ 22 month-old mice showing no proliferative response to low (low anti-CD3), intermediate (low anti-CD3 + anti-CD28), or high (high anti-CD3 + anti-CD28) stimuli (74). These aged T cells also showed a decline in the production of IL-2, a crucial driver of T cell proliferation, and similarly the T cells from aged mice displayed no proliferation in response to exogenous IL-2 stimulation. Additionally, the age-associated reduction in IL-2 levels impairs the ability of naïve $CD4^+$ T cells to properly polarise into the T_h1 and T_h2 helper subsets, leading to incomplete differentiation and thus poor effector functions (75). Ageing is also accompanied by skewing of helper differentiation towards the T_h17 phenotype and an increase in the T_h1:T_h2 ratio (76). This T_h17 increase with age may in part be due to the aforementioned decline in the cytokine IL-2, which works to suppress T_h17 differentiation. Aged murine T cells cultured with anti-IL-2 demonstrated a blunted increase in the T_h17 population compared with young T cells, indicating that IL-2 was already dampened in the aged mice (77). T_h17 cells are characterised by the production of the pro-inflammatory cytokine IL-17, consequently, increases in T_h17 cells lead to higher levels of circulating IL-17 thus contributing to inflammageing.

1.2.2 (e) Regulatory T cell Ageing

T_{regs} play a vital role in regulating immune responses to self and foreign antigens and play a vital role in protecting against autoimmunity (78). Ageing is accompanied by an increase in circulating T_{reg} numbers, possibly a result of a lifetime of effector cell generation in response to infections, as it has been proposed that effector cells encourage T_{reg}-mediated suppression (79). Elevated T_{reg} numbers may also be a compensatory mechanism for the decline in immunosuppressive function exhibited by aged T_{regs}. Whilst conventional T cell (T_{conv}) proliferation was effectively suppressed by young T_{regs}, the ability of aged T_{regs} to suppress the proliferation of T_{conv} *in vitro* was impaired (80). This expansion of T_{regs} with increasing age is a key contributor to the decline in IL-2 levels due to the ample expression of IL-2 receptor (IL-2R) on the cell surface, emphasising the crucial role of the cytokine in T_{reg} function. Ablation of the IL-2R α-chain in mice, which facilitates the sequestering of IL-2 from effector T cells, led to early onset and greater severity of disease compared to wild-type (WT) mice (81). It has been proposed that T_{regs} may be partially responsible for the age-related preferential

differentiation of T_h17 cells through consumption of IL-2, thus promoting IL-17A production, in addition to being implicated in the induction of T cell senescence (82, 83).

1.2.2 (f) B cell Ageing

B cells operate as APCs, specifically recognising conformational antigen epitopes via the B cell receptor (BCR) consequently priming and activating T cells through the expression of MHC class II (84). B cells also possess the ability to secrete immunomodulatory cytokines, influencing processes such as the maturation of Peyer's patches and isolated lymphoid follicles in the gut, $CD4^+$ T cell immune responses and regulation of inflammatory signals (85).

Whilst total peripheral B cell numbers remain stable throughout adult life, B cell production within the bone marrow declines with advancing age, attributable to cell-specific alterations as well as changes to the microenvironment of lymphoid organs (86). Isolated HSCs from aged individuals displayed significantly reduced capability to produce lymphoid B lineage cells leading to increases in myeloid progenitors developing from single HSCs and thus an increase in the myeloid: lymphoid ratio. This diminished committal to B cell differentiation is indicated by the reduction of early B cell populations, for instance the age-associated decrease in mature naïve B cells (87). Ageing is also accompanied by B cell functional defects, primarily lower levels of antibodies and production of antibodies with low protective function; a contributing factor in the poorer vaccine responses reported in the elderly (88). Another prominent change to B cells with age is the emergence of the novel age-associated B cell (ABC) subset that have been shown to play an important role in viral infections, as well as post infection (89, 90, 91, 92). Additionally, ABCs have been implicated in the reduced B lymphopoiesis seen with age due to the production of TNF-α, disrupting the early stages of B cell development through apoptosis (93). Ageing is associated with an increased prevalence of autoimmune diseases, and in both mouse models of autoimmunity and human disease ABCs are elevated, thought to be promoted by TLR7 and TLR9 signalling (94). Upon TLR stimulation, ABCs have been shown to secrete autoantibodies, recognising self-molecules and proteins such as chromatin and the centromeres of chromosomes (95). The presence of autoantibodies has been associated with various autoimmune disorders, for instance type 1 diabetes mellitus and systemic lupus erythematosus (SLE). Lastly, numerical and functional

loss in immunoregulatory B cells (B_{regs}) is another potential contributor towards the increased risk for autoimmune diseases (96).

1.2.3 Inflammageing

Another universal feature of ageing is prolonged increase in basal levels of proinflammatory markers (TNF-α, C-reactive protein (CRP), IL-6), a state known as inflammageing (59). A recently developed metric for systemic inflammation (iAge) has been recognised as a predictor of the ageing trajectory (97). Expanding evidence highlights inflammageing as a major risk factor in a multitude of age-related diseases (ARDs) such as cancer, cardiovascular diseases, age-related frailty and development of cognitive defects; together resulting in ill health in older adults (98, 99, 100). Thus, there is an increasing drive towards testing anti-inflammageing therapies to promote healthy ageing process. Multiple factors have been recognised as potential contributors towards inflammageing including accumulation of senescent cells with SASP phenotype, impaired autophagy processes resulting in accumulation of cellular debris and damage-associated molecular patterns (DAMPs), immunesenescence and gut microbiome dysbiosis (which will be discussed later).

1.3 Gut Microbiome

1.3.1 Composition and diversity

Within the human gastrointestinal (GI) tract resides around 100 trillion microorganisms, consisting of fungi, viruses, archaea and predominantly bacteria (101). To date, over 1000 different gut bacterial species have been identified and classified taxonomically into 6 major phyla: Bacteroidetes, Firmicutes, Actinobacteria, Proteobacteria, Verrucomicrobia and Fusobacteria, with 90% of gut bacteria belonging to either Firmicutes or Bacteroidetes (102). An ecologically diverse gut microbiota community is considered healthy, in terms of bacterial richness (the number of existing taxa) and evenness (the abundance of said microbial constituents) (103).

1.3.2 Functions

The human gut microbiota retains a symbiotic relationship with the host, providing immunological, metabolic and protective functions to the healthy individual whilst obtaining nutrients from host dietary components (104). Nutrient metabolism is one of the key functions of the gut bacteria as they possess the ability to ferment indigestible oligosaccharides and other carbohydrates which may have missed absorption (105, 106). Fermentation by gut microbes such *Faecalibacterium, Bacteroides* and *Bifidobacterium*, result in the production of metabolites such as short-chain fatty acids (SCFAs), bile acids and certain amino acids (106, 107). SCFAs derived from the gut microbiota, namely butyrate, propionate, valerate and acetate, provide a vital source of energy for the epithelium that make up the intestinal epithelial barrier and are essential to the maintenance of gut barrier integrity (108). Multiple studies have reported on the immunomodulatory function of the microbiome, which is discussed later in section 1.5 (109, 110, 111, 112). The gut microbiota also contributes to antimicrobial protection within the GI tract by prohibiting the overgrowth of inhabiting pathogens (104). This is done via modulation of the intestinal mucus layers and antimicrobial peptide (AMP) synthesis, such as α-defensins, by host Paneth cells (113, 114).

1.4 Ageing of the gut microbiome

1.4.1 Microbiome composition changes

Advancing age is accompanied by alterations to the gut microbial composition, causing an imbalance in beneficial and opportunistic bacteria, referred to as microbial dysbiosis (115). Age-related dysbiosis is characterised by a reduction in beneficial and commensal bacteria such as *Bifidobacterium, Bacteroidetes* and *Coprococcus*, which are key to maintaining a healthy gut homeostasis. Coinciding with this, there is an enrichment of opportunistic pathobionts such as Enterobacteriaceae and *Staphylococcus* which promote a pro-inflammatory gut environment (116, 117). Alongside age, environmental factors such as altered diet and increased antibiotic use also influence the gut bacteria composition and promote microbiome dysbiosis (118, 119).

1.4.2 Microbial metabolite profile shift

Microbial metabolism provides a key method of facilitating the cross-talk between the intestinal microbiota and host via the production of metabolites (120). The gut microbiota assist in the fermentation of indigestible dietary factors thus generating metabolites such as short-chain fatty acids (SCFAs), in addition to converting primary bile acids to secondary bile acids (106, 121).

With age, there is a clear shift in the metabolite profile, primarily characterised by a dramatic decline in the levels of faecal SCFAs, with total SCFA concentrations more than halving from 76.4mM in adults under 50 years, to 32.3mM in faecal samples from the oldest age group (>80 y/o) (122, 123). The decrease in SCFAs is in part due to an age-associated reduction in SCFAs-producing bacteria (*Bifidobacterium*) (2, 124). Coinciding with this decrease in microbiome-derived SCFAs is an increase in the levels of ammonia, branched fatty acids and phenols seen in the aged population (125). Another potential contributor could be age-associated changes to diet, for example a lower fibre consumption, and an increase in antibiotic treatment with age which correlates with reduced colonic SCFAs (126).

Whilst the changes to SCFAs with age and the subsequent effects have been investigated the most to date, there is emerging evidence of the involvement of other microbiome-derived metabolites in certain age-associated diseases. Plasma levels of trimethylamine-*N*-oxide (TMAO), a chlorine product synthesised by gut microbiota, have been shown to increase with age in both humans and mice when compared with a young cohort (127). The same study also reported TMAO-induced neuron senescence along with a down-regulation of the mammalian target of rapamycin (mTOR) signalling pathway and impaired cognitive performance in mice. Despite recent studies suggesting an association between TMAO and Alzheimer's disease, the specific mechanisms of microbiome metabolite regulation of brain function are still yet to be fully defined (128).

1.4.3 Increased Intestinal Barrier permeability

The intestinal epithelial barrier functions as the primary barrier that regulates the transportation of nutrients and microbial components into circulation and acts as an interface

for interactions between commensal bacteria residing in the gut and the host immune system (129, 130). The outermost mucus layer, produced by goblet cells, overlays the one-cell-thick intestinal epithelium layer made up of intestinal epithelial cells (IECs) joined together by junctional complexes such as tight junction proteins (zonulin and occludin) and adherens junctions. Specialised IECs known as Paneth cells secrete AMPs such as defensins in response to particular bacterial products, helping to maintain microbiota homeostasis (131). Below the epithelium layer is the lamina propria (LP), a thin layer of connective tissue that hosts both adaptive and innate immune cells such as T cells, B cells and macrophages (132). Commensal bacteria residing in the gut positively impact the intestinal barrier integrity through the production of metabolites such as SCFAs and secondary bile acids (133). However, the age-associated compositional changes that the gut microbiota undergoes is a potential contributor towards a reduction in intestinal barrier integrity leading to increased intestinal permeability (134).

Other alterations to the intestinal barrier, reported in aged mice, is a reduction in the number of viable goblet cells as well as a thinning of the colonic mucus layer due to a greater number of apoptotic goblet cells (135). Additionally, remodelling of the intestinal barrier with age occurs to the composition of IEC tight junctions as analysis of zonula occludens-1 (ZO-1) and occludin mRNA in old rats showed a downregulation of these tight junction proteins compared with young rats (136). Increases in levels of microbial translocation biomarkers such as lipopolysaccharide-binding protein (LBP) have been observed in aged non-human primates compared to the young, demonstrating a surrogate marker for increased intestinal barrier permeability (137). Importantly, a study done in aged germ-free mice has recently shown that this translocation of gut microbes and microbial products into the blood stream contributes to the persistent, low-grade inflammation occurring with age (61, 138). Intestinal permeability causes these microbe-associated molecular patterns (MAMPs) to be in direct contact with the host immune cells present in the LP and circulation, thus provoking an immune response in the absence of an infection (138, 139). Lipopolysaccharide (LPS) stimulation is known to induce pro-inflammatory cytokine (IL-6) production by monocytes/macrophages; thus, contributing towards inflammageing (138). Furthermore, elevated levels of circulating MAMPs with age have numerous pathological implications such

as increased risk of inflammatory diseases and metabolic disorders in older adults, such as increased susceptibility to CVD (130, 140).

1.4.4 Potential contributors towards age associated microbiome changes

Often, advancing age brings about significant lifestyle changes, such as altered exercise and dietary patterns in older adults resulting in malnutrition (141, 142)(118). It is well known that physical activity levels deteriorate with age, attributable to reductions in upper and lower muscle strength in addition to the predominance of frailty in older adults (143). Exercise has the ability to significantly effect gut bacteria composition as seen in murine studies, for example mice undergoing voluntary exercise displayed increased beta diversity (measure of similarity or dissimilarity between communities) after 12 weeks compared to baseline levels (144). Similar results have been seen in humans, with the gut microbiome of elite athletes displaying greater alpha diversity (measure of distribution of species abundances in a sample) in comparison to that of control groups. Specifically, a decrease in abundance of the phylum Bacteroidetes was noted in the elite athletes, whilst abundances of Firmicutes such as *Ruminococcaceae* and *Succinivibrionaceae* was increased; thus, suggesting that age-associated decline in physical functioning levels is a potential contributor towards microbiome dysbiosis in aged hosts (145). Another possible environmental factor contributing to age-associated microbiome disturbances is recurrent antibiotic usage in the elderly due to increases in bacterial infections with age leading to repeated hospital admissions. Repeated courses of the antibiotic ciprofloxacin resulted in loss of diversity and bacterial community composition shifts occurring 3-4 days post treatment (146). Following completion of the study, the composition of the participants' gut microbiota was altered from its state prior to the initial course of antibiotics, highlighting the global impact of recurring antibiotic consumption on the microbiome.

1.5 Gut microbiome and immune cross talk

1.5.1 Immune system and the microbiome

Due to the exceptionally dense microbial community present in the gut, it is imperative that the intestinal immune system develops immune tolerance towards commensal microbes whilst also remaining responsive to invading pathogens. Maintaining homeostasis requires persistent communication between the gut microbiome and the host immune system, with studies describing considerable bidirectional contact occurring between compartments, mediated by the intestinal epithelial barrier (147, 148). Immunosurveillance within the gut is carried out in part by the large presence of macrophages residing in the LP which, due to the expression of phagocytic receptors specific to bacteria such as triggering receptor expressed on myeloid cells 2 (TREM-2), are effective in the removal of translocating bacteria breaching the epithelial barrier (149). Notably, mucosal macrophages exposed to bacterial products or bacteria themselves are hyporesponsive to such stimuli which usually trigger significant pro-inflammatory responses in other macrophage populations located around the body (150). By efficiently eliminating low-grade microbe infiltration whilst downregulating unnecessary inflammatory responses, resident macrophages work to achieve the preservation of both intestinal tissue integrity and equilibrium of the microbiome-host immunity interface (151). Similarly, DCs interact with commensals or commensal antigens that may have unintentionally migrated across the epithelial barrier through capture and trafficking to the mesenteric lymph node (MLN) whereby presentation to IgA^+ B cells occur (152). Secretory IgA (SIgA) from B cells is transported from the LP into the intestinal lumen via transcytosis and exerts effects on the commensal population, one mechanism of which is immune exclusion, describing the process of crosslinking surface antigenic epitopes thus prohibiting the attachment of microorganisms to epithelium and/or impeding their penetration through the intestinal barrier (153). One study highlighted the ability of gut commensals to influence the amount of bacterial antigen reaching the MLN, as higher titers of non-invasive *Salmonella* were observed in the MLN of antibiotic-treated mice compared to untreated counterparts. It was shown that $CX3CR1^{hi}$ mononuclear phagocytes, displaying both macrophage- and DC-like phenotypes, were responsible for the transportation of *Salmonella* to the MLN under dysbiotic conditions independent of the MyD88 signalling pathway (154).

Immune tolerance is also maintained heavily by a specific subset of FoxP3$^+$ T_{regs} and bacterial species such as *B. fragilis* play a vital role in inducing FoxP3$^+$ T_{regs} to produce IL-10 (155, 156). Thus, the microbiome has become a known intrinsic regulator of intestinal immune responses, achieving a mutualistic existence via numerous signalling mechanisms.

1.5.2 Mechanisms underlying microbiome exerted impact on the immune system

Communication between gut microorganisms and host immunity is primarily accomplished through recognition of microbial signals by PRRs, for instance TLRs, leading to downstream immune activation. One such signal is the capsular carbohydrate polysaccharide A (PSA), produced by *B. fragilis* and highly expressed in the capsule component of the bacteria (157). It is via this immunomodulatory molecule that the gram-negative obligate anaerobe is capable of inducing both pro- and anti-inflammatory effects, such as the aforementioned promotion of IL-10 production by T_{regs}, which have been shown to work in combination with a particular subset of $CD4^+CD45Rb^{low}CD62L^-CD44^+FoxP3^-$ T effector/memory ($Rb^{Lo}T_{em}$) cells, the expansion of which is induced by PSA, to suppress inflammatory reactions (158). $Rb^{Lo}T_{em}$-FoxP3$^+$ T_{reg} interaction is mediated by IL-4 signalling, demonstrated via *in vitro* IL-4 neutralisation which led to complete inhibition of IL-10 production during $Rb^{Lo}T_{em}$ and FoxP3$^+$ T_{reg} co-culture. Only through neutralisation of the IL-4 receptor CD124 on the FoxP3$^+$ T_{regs} was production of IL-10 sufficiently blocked, indicating a communication pathway achieved by IL-4 secretion from $Rb^{Lo}T_{em}$ cells, binding to CD124 expressed on FoxP3$^+$ T_{regs} and subsequent release of IL-10 (159). Prior to contact with T cells, PSA is initially taken up by APCs such as DCs and converted to smaller fragments to then be presented to CD4$^+$ T cells through MHC II (160). Recognition of PSA occurs due to TLR-2 ligation, which forms a heterodimer with TLR-1, working in combination with the C-type lectin PRR Dectin-1. Following this, phosphoinositide 3-kinase (PI3K) pathway activation takes place and is crucial for downstream inactivation of glycogen synthase kinase 3β (GSK3β) via phosphorylation leading to expression of anti-inflammatory genes in a cAMP response element-binding protein (CREB)-dependent manner (161).

Gut microbial metabolites are another example of symbiosis factors facilitating microbiome-immune crosstalk, the most well studied of which are SCFAs. Providing a range of beneficial

effects to both gut commensals and host cells, SCFAs are an energy source for colonocytes, regulators of host immune responses and key moderators of gut homeostasis (Figure 4) (162, 163). SCFAs possess the ability to stimulate both innate and adaptive immune cells directly, assisting in the development of gut immune tolerance. Within the colon of GF mice, T_{reg} numbers are significantly reduced however, supplementation of individual or a combination of SCFAs led to an expansion of colonic T_{reg} (cT_{reg}) frequency and numbers. Treatment of isolated GF mouse cT_{regs} *in vitro* with propionate specifically stimulated IL-10 secreting $FoxP3^+$ cT_{regs}, a process dependent on G-protein coupled receptor (GPR) 43 expression and subsequent downstream signalling, leading to suppression of pro-inflammatory factors such as IL-6, IFNγ and IL-1β (164). SCFAs are also able to stimulate $CD4^+$ effector T cells via GPR43 ligation, explicitly regulating $CD4^+$ T_h1 functionality by increasing the expression of B lymphocyte-induced maturation protein 1 (Blimp-1) and inducing production of IL-10 (165). Whilst SCFAs are known histone deacetylase (HDAC) inhibitors, the effects seen in IL-10 producing T_h1 cells occurred independently of HDAC inhibition, as shown by the inability of a known HDAC inhibitor Trichostatin A (TSA) to affect IL-10 secretion in WT or $GPR43^{-/-}$ KO T_h1 cells. Treatment with butyrate however lead to elevated levels of IL-10 in WT but not $GPR43^{-/-}$ T_h1 cells, demonstrating that these effects are GPR43-mediated. In particular, butyrate heightens the memory capability of activated antigen-primed $CD8^+$ T cells, as memory $CD8^+$ T cells derived from *in vitro*-activated transgenic (gBT-I) cells transferred to specific-pathogen-free (SPF) mice on a high-fibre diet were able to produce greater numbers of secondary effector cells compared to memory gBT-I cells in control mice (166). Another GPR of which butyrate is a ligand is GPR109a, typically expressed by APCs such as macrophages and DCs (167, 168). Interaction with this receptor promotes both APCs to display anti-inflammatory phenotypes, another mechanism through which SCFAs regulate gut inflammation. KO *Niacr1*$^{-/-}$ (encoding for GPR109a) mice were immensely affected by DSS-induced colitis, characterised by loss of the tight junction claudin-3 and increased serum levels of IL-6, IL-1β and CXCL1, whilst in the WT mice colonic inflammation did not occur (169). The presence of SCFAs alters IgA and IgG antibody production by B cells, as shown in mice fed a high fibre diet (HFD) which had higher levels of IgA in the caecal lumen and increased serum IgG levels compared with low fibre diet (LFD) counterparts (170). Increases in antibody production are in part attributable to the ability of SCFAs to promote B cell differentiation into plasma cells (PCs) by upregulation of genes associated with PC differentiation such as *Prdm1*, *Aicda* and *Xbp1*.

Treatment with butyrate or propionate significantly decreased TNF-α production in LPS-stimulated murine neutrophils *in vitro* via deactivation of NF-κB, thus inducing an overall anti-inflammatory response (171). Peripheral recruitment of neutrophils to sites of inflammation is attenuated by SCFAs upon interaction with GPR41, particularly their influx into the airways, due to a dampening in the macrophage production of CXCL1, a principal neutrophil-recruiting chemokine (172).

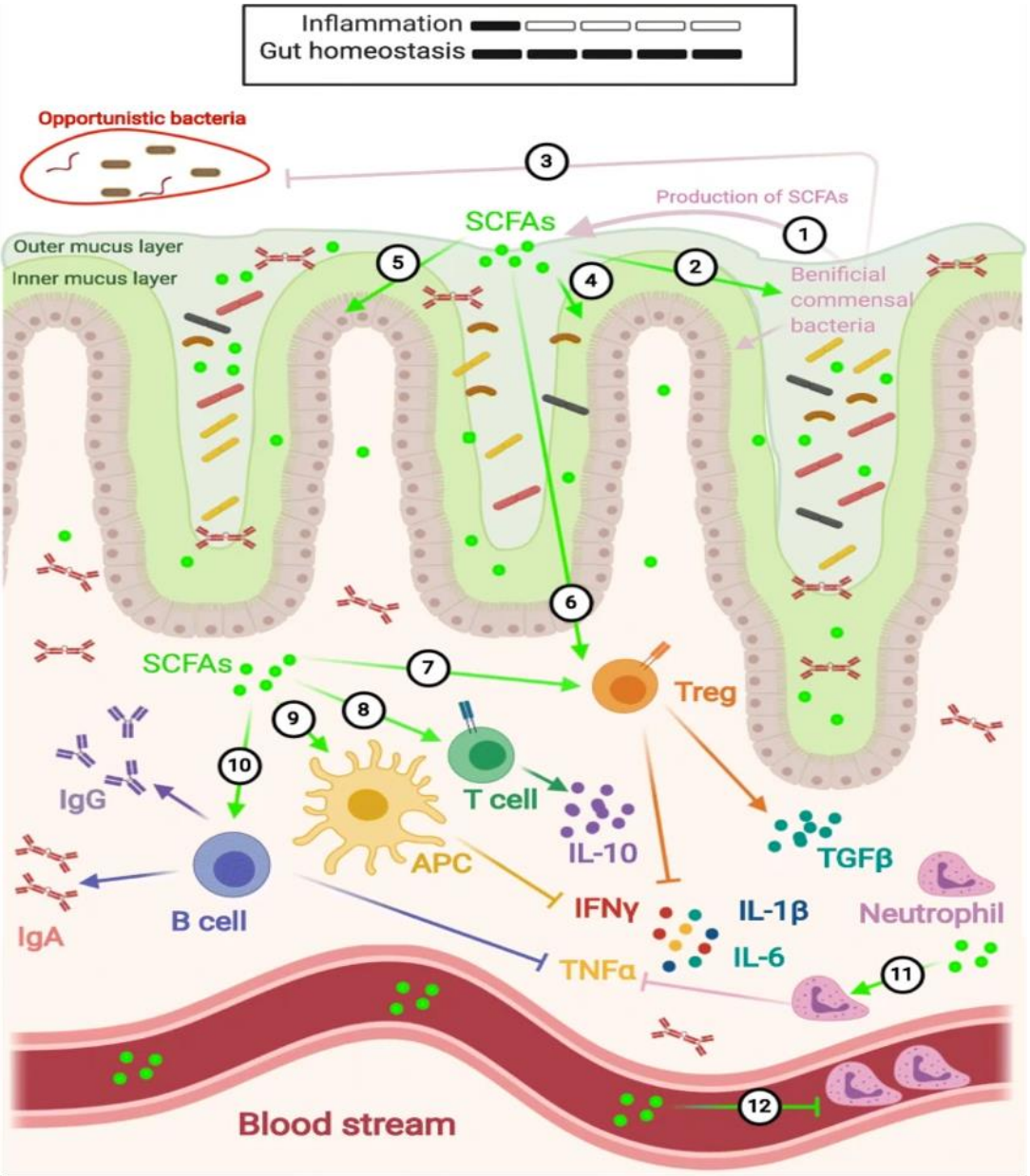

Figure 4. Immunomodulatory mechanisms of SCFAs.
(1) SCFAs are exclusively generated by commensal bacteria, predominantly belonging to the Firmicutes phylum. **(2)** Working as part of a positive feedback loop, SCFAs promote beneficial bacteria growth and thus **(3)** preventing establishment of opportunistic bacteria assisted by **(4)** the encouragement of defensive mucus production. SCFAs provide a source of energy for both **(5)** absorptive IECs and **(6)** immune cells. Able to traverse the intestinal epithelial barrier, they facilitate the development of gut immune tolerance by inducing anti-inflammatory responses in **(7)** FoxP3^{+} T_{regs} ; **(8)** T cells; **(9)** APCs in particular macrophages and DCs; **(10)** B cells which are also stimulated by SCFAs to secrete antibodies; **(11)** neutrophils whose recruitment from the periphery is likewise influenced by SCFAs (2).

1.6 Potential links between immunesenescence, inflammageing and microbial dysbiosis

With the growing amount of research into the impact of ageing on the microbiome, immune system and inflammation, evidence pointing towards possible associations between gut dysbiosis, immunesenescence and inflammageing has emerged. The first evidence supporting this hypothesis comes from a study in aged germ-free mice, that are protected from microbiome dysbiosis and intestinal barrier dysfunction and also do not display features of inflammaging and are protected from features of macrophage ageing (133, 138). Further evidence of this causal relationship between microbial dysbiosis and immunesenescence in humans comes from a recent study by the group reporting that a faecal microbiota transplant (FMT) from a young donor, alongside restoring microbiome homeostasis and increasing faecal levels of SCFAs, particularly butyrate, also possess anti-immunosenescent properties and results in a decline in senescent T cell and an expansion of regulatory T and B cells in aged *C. difficile* infection patients (173).

1.7 Preliminary data supporting this study

Advancing age is accompanied by an accumulation of senescent $CD28^{-ve}$ $CD57^{+ve}$ T cells, displaying a state of replicative arrest (174). We hypothesized that age-associated microbiome dysbiosis and the resulting loss of SCFAs contributed towards an aged T cell phenotype. To test this hypothesis, Jessica Conway in the Duggal group collected paired stool and blood samples from healthy young and aged participants (Figure 5A). Similar to previous reports (123), we have observed a decline in stool SCFA levels of butyrate ($p < 0.001$), in aged older adults (Figure 5B). Peripheral blood T cell subsets, particularly senescent $CD28^{-ve}$ $CD57^{+ve}$ CD4 and CD8 T cell frequency were enumerated, and we have reported a negative association with stool butyrate levels (Figure 5C, D).

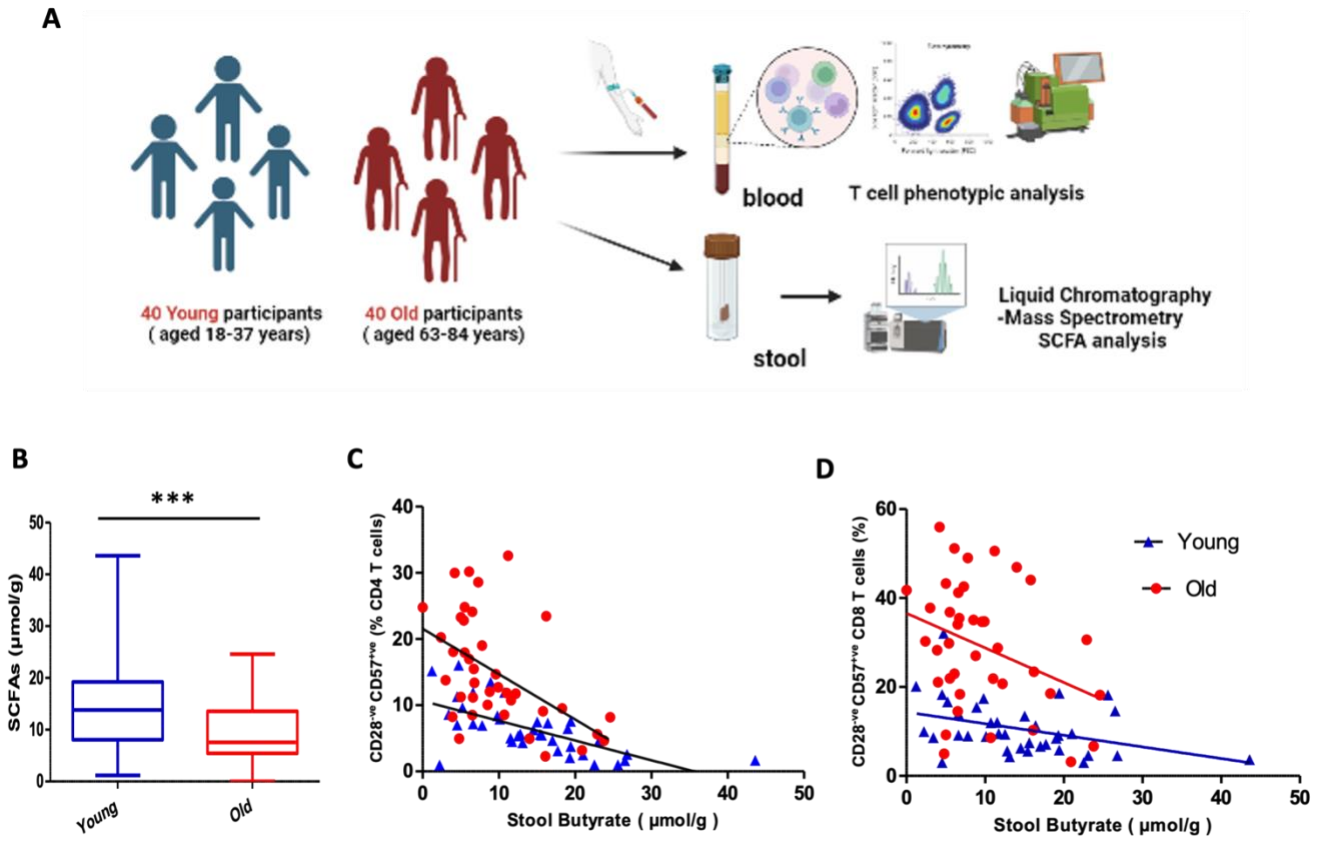

Figure 5. Stool butyrate levels correlate with peripheral accumulation of senescent T cells in older adults.
(A) Schematic study design. **(B)** Representative histograms show stool butyrate levels in healthy young individuals (blue; n = 36) and healthy aged participants (n = 39) as measured by high-performance liquid chromatography. Scatterplots show correlation between stool butyrate levels and senescent **(C)** CD4 T cell **(D)** CD8 T cell frequency in the peripheral blood of healthy young individuals (blue; n = 36) and healthy aged participants (n = 39).

1.8 Aims and hypothesis

Despite the data only being correlative, it brought to light butyrate as an attractive target with potential senomorphic properties that needs to be tested. This project aims at dissecting the exact mechanisms by which butyrate contributes towards slowing the development of senescence features in aged T cells. If we dissect how and if butyrate modulates senescence in T cells this may help develop novel therapies to boost immune health in older adults to promote healthy ageing.

This hypothesis will be tested via five key objectives:

1. To establish an in-vitro model for proliferation-induced senescence in T cells
2. To investigate the anti-SASP properties of butyrate on aged T cells
3. To investigate the protective effect of butyrate on T cells by reducing development of a senescent phenotype
4. To determine the mechanisms underlying senomorphic properties of butyrate on T cell subsets
5. To investigate the impact of faecal metabolites derived from young mice on senescence within the aged murine spleen

2.0 Materials and Methods

2.1 Materials

2.1.1 Reagents and chemicals

- Complete RPMI media: RPMI1640 medium (Sigma-Aldrich, UK) supplemented with 10% Heat inactivated faecal calf serum and 100U/ml penicillin, 100ug/ml streptomycin and 2mM glutamine (Sigma-Aldrich, UK)
- Ficoll-Paque™ Plus (GE Healthcare, USA)
- autoMACS® Running buffer: 0.5% (w/v) bovine serum albumi (BSA), 2mM ethylenediaminetetraacetic acid (EDTA), phosphate-buffered saline (PBS), 0.09% (v/v) azide (Miltenyi Biotec, Germany)
- Phosphate buffer saline (PBS): one PBS tablet (Sigma-Aldrich, UK) dissolved in 500ml deionised water (ddH_2O)
- Sodium butyrate (Sigma-Aldrich, UK)
- Freezing medium: 10% dimethyl sulfoxide (DMSO; Sigma-Aldrich, UK) in heat-inactivated FCS (HiFCS; Gibco®, Invitrogen, UK)
- Foxp3 Transcription factor staining kit: fixation/permeabilization concentrate, fixation/perm diluent, permeabilization buffer (eBioscience™, Thermo Fischer, UK)
- Phorbol myristate acetate (PMA; Sigma-Aldrich, UK)
- Ionomycin from Streptomyces conglobatus (Sigma-Aldrich, UK)
- Anti-CD3 monoclonal antibody (mAb; Thermo Fischer, UK)
- 4% paraformaldehyde (Thermo Fischer, UK)
- 100% methanol (VWR Chemicals, USA)
- MitoTracker™ Red/MitoTracker™ Green/MitoSOX™ Red dyes (Thermo Fischer, UK)
- EasySep™ Human T cell isolation kit (Stemcell™ Technologies)
- Human IL-6/IL-8 (CXCL8)/IL-1β/CCL3 (MIP-1 α) DuoSet ELISA kits (R&D Systems, USA)
- ELISA wash buffer: 0.05% Tween® 20 (Sigma-Aldrich, UK) in PBS
- Stop solution for ELISAs: sulfuric acid (H_2SO_4)

- RNeasy® Mini RNA isolation kit (Qiagen, Germany)
- nCounter® Master Kit, Prep Plates and Cartridges (NanoString Technologies)
- Guava® Autophagy LC3 antibody-based assay kit (Luminex, USA)

Antibody	Clone	Isotype	Dilution	Source
Cell surface markers				
Anti-human CD3 PEcy7	UCHT1	Mouse IgG1κ	1:50	Thermo Fischer, UK
Anti-human CD4 BV421	RPA-T4	Mouse IgG1κ	1:50	BD Biosciences, USA
Anti-human CD8 PE	MEM-31	Mouse IgG2a	1:50	ImmunoTools, Germany
Anti-human CD45RA APC	HI100	Mouse IgG2bκ	1.5:50	BioLegend, USA
Anti-human CD45RA PerCPcy5.5	HI100	Mouse IgG2bκ	1.5:50	BioLegend, USA
Anti-human CD45RA PEcy5	HI100	Mouse IgG2bκ	1.5:50	BioLegend, USA
Anti-human CCR7 FITC	150503	Mouse IgG2a	1:25	R&D Systems, USA
Anti-human CCR7 APC	REA546	Recombinant human IgG1	1:25	Miltenyi Biotec, Germany
Anti-human GPR109A APC	245106	Rat IgG2b	1:50	R&D Systems, USA
Anti-human GPR43/FFAR2 APC	1000624	Mouse IgG2b	1:50	R&D Systems, USA
Anti-human CD57 PerCPcy5.5	QA17A04	Mouse IgG1κ	1:50	BioLegend, USA
Transcription factors				
Anti-human Foxp3 PE	PCH101	Rat IgG2aκ	1:25	eBioscience, UK
Anti-human p-p53 APC	184727	Mouse IgG2b	1:25	R&D Systems, USA
Anti-human NFκB PE	B33B4WP	Mouse IgG2aκ	1:25	eBioscience, UK
Other intracellular markers				
Anti-human H2AX PE	CR55T33	Mouse IgG1κ	1:25	Thermo Fischer, UK
Anti-human Phospho S6 PE	cupk43k	Mouse IgG1κ	1:25	Thermo Fischer, UK
Anti-human Ki-67 PE	Ki-67	Mouse IgG1κ	1:25	BioLegend, UK
Anti-human p38 MAPK PE	36/p38 (pT180/pY182)	Mouse IgG1κ	1:25	BD Biosciences, USA
Isotype controls	**Clone**	**Dilution**		**Source**
Mouse IgG1κ PEcy7	MOPC-21	1:50		BioLegend, UK

Mouse IgG1κ BV421	X40 (RUO)	1:50	BD Biosciences, UK
Mouse IgG1κ PerCPcy5.5	MOPC-21	1:50	BioLegend, UK
Mouse IgG1κ PE	MOPC-21	1:25	BioLegend, UK
Mouse IgG2a PE	FAB3744P	1:50	R&D Systems, UK
Mouse IgG2bκ APC	27-35	1.5:50	BioLegend, UK
Mouse IgG2bκ PEcy5	MPC-11	1.5:50	BioLegend, UK
Mouse IgG2a FITC	20102	1:25	R&D Systems, UK
Rat IgG2b APC	141945	1:50	R&D Systems, UK
Mouse IgG2b APC	133303	1:50	R&D Systems, UK
Rat IgG2aκ PE	eBR2a	1:25	eBioscience, UK
Mouse IgG2aκ PE	eBM2a	1:25	eBioscience, UK

Table 1*. Anti-human antibodies and isotype controls used for cell surface and intracellular immunofluorescent staining.*

2.2 Methods

2.2.1 Study design and blood letting

In total, 10 healthy young (20-35 years, mean age 28 years) and 7 healthy old (63-75 years, mean age 72 years) participants were recruited for this study. All participants were bled in the morning between (9 – 11 am) under sterile conditions by a qualified healthcare professional using a standard venepuncture technique. Three green heparin vacutainers (18 ml) of blood was collected for the experiments done on PBMCs and Eight vacutainers (48 ml) was collected for T cell isolation experiments. All participants were healthy and did not suffer from any chronic immune related diseases (e.g. autoimmune disorders) or on any medications that impact the immune system and one of the patients had an infection at the time of blood sampling. The study was approved by the HRA and Health and Care Research Wales (HRCW) Approval (IRAS 301974) and all participants provided written informed consent).

2.2.2 Stool sample preparation and LC-MS analysis

To each stool sample (1 gm) a few (5-10) ceramic microbeads were added, and the vial was shaken at 2500 rpm for 10 minutes. Samples were then centrifuged at 13,000 rpm for 10 minutes and collected supernatant was passed through a Whatman Uniprep filter vial (0.45µ). Samples were analysed by LC-MS using Waters Acquity UPLC coupled to a Waters TQS-µ mass spectrometer operated in positive multiple reaction mode (MRM). Samples were quantified to a limit of quantification of 25 µg/ml in the final solution alongside butyric acid standards (50 – 1000 µg/ml). For quantification, D2-propionic acid was used as internal standard for butyrate. The mass spectrometer was operated in negative electrospray selected ion monitoring mode for parent ion (89.12), fragment ion (43), cone voltage (20), collision energy (10).

2.2.3 PBMC isolation

PBMCs from venous blood samples were isolated utilising Ficoll-Paque density gradient centrifugation. Whole blood was diluted with complete RPMI-1640 medium supplemented with 10% HiFCS and GPS at a 1:1 ratio. In order to create a Ficoll-Paque density gradient, 10-15 ml of blood was carefully layered onto 6 ml of Ficoll-Paque™ Plus. The blood gradients

were centrifuged at 420 x *g* for 30 minutes at room temperature (22 °C) with no break. Post centrifugation, PBMCs residing at the plasma-Ficoll-Paque interface were transferred to 25 ml universals (Stardsted, UK) containing 5 ml of autoMACS® Running buffer. Washing steps with autoMACS® Running buffer were carried out twice at 300 x *g* for 10 minutes at room temperature. Post-wash, supernatants were discarded and the cell pellets re-suspended in 10 ml of autoMACS® Running buffer. Using a haemocytometer, PBMCs were counted and suspended in complete pre-warmed RPMI-1640 at a concentration of 1 million cells / ml.

2.2.4 *In vitro* culture model for induction of replicative senescence in PBMCs

Prior to cell culture, a sterile 96-well U bottom plate (Corning™ Costar™, USA) was incubated for 1 hour with a 2μg/ml solution of anti-CD3 mAb (Thermo Fisher, UK) was prepared, 50μl of this solution was added into each well of a 96 well round bottom microtitre plates 37 °C. Post incubation, freshly isolated PBMCs were then plated at 150 μl per well, in the presence of butyrate (1mM) or in the absence of the SCFA (control). The 96-well U bottom plate was then incubated at 37 °C for 72 hr in a humidified atmosphere of 5% CO_2. Post culturing, the PBMCs were transferred to Eppendorfs which were then spun in the mini centrifuge at 3000 rpm for 3 minutes at room temperature. Supernatants from the pelleted cells were removed and stored in separate labelled Eppendorfs at -80 °C for future use. Following this, cell pellets were re-suspended in 50 μl of PBS ready for antibody staining.

2.2.5 Cell surface immunostaining for T cell phenotyping via multi-colour flow cytometry

Isolated PBMCs re-suspended in 50 μl of non-sterile PBS were transferred to 5ml polypropylene round-bottom tubes (BD Falcon™) and stained with a combination of antibodies: PEcyanine7-conjugated anti-human CD3 antibody, Brilliant Violet™ 421-conjugated anti-human CD4 antibody, PEcyanine 5.5/APC/PerCP-conjugated anti-human CD45RA antibody and FITC/APC-conjugated anti-human CCR7 antibody for 20 minutes on ice in the dark. Post incubation, cells were washed with 500 μl of non-sterile PBS and centrifuged at 250 x *g* for 5 minutes at 4 °C. Following this, supernatants were discarded and PBMCs were re-suspended in 300 μl of non-sterile PBS for flow cytometric analysis on a MACSQuant flow cytometer (Miltenyi Biotech, Germany). To ascertain lymphocyte numbers, lymphocytes were gated depending on forward scatter (FSC) / side scatter (SSC) characteristics and subsequently

the 10,000 $CD3^+$ population of lymphocytes was gated on. From these, the $CD4^+$ and $CD4^-$ populations were identified which were then further classified based on CD45RA and CCR7 expression into four subsets: naïve ($CD45RA^+CCR7^+$), central memory (CM: $CD45RA^-CCR7^+$), effector memory (EM: $CD45RA^-CCR7^-$) and the terminally differentiated effector memory cells re-expressing CD45RA (EMRA: $CD45RA^+CCR7^-$) (Figure 6A-D). The frequencies of these four subsets withing the T cell pool were calculated. The gates for different populations were set using appropriate isotype controls. Multicolour immunostaining compensation was performed to ensure that the spectral emission of different fluorochrome conjugated-antibodies did not overlap by staining cells individually with each antibody. Flow cytometry data was analysed using Flow Jo™ v10.8 software (BD Biosciences, USA).

2.2.6 Intracellular staining for transcription factors

Staining of intracellular markers and transcription factors was done using the FoxP3 transcription factor staining kit (eBioscience™, Thermo Fischer). Following cell surface staining, cells were resuspended in 1 ml of fix medium (fixation/permeabilization concentrate diluted 1:3 in fixation/perm diluent) and incubated for 30 minutes on ice in the dark. Following incubation, cells were washed with 500 μl of perm medium (permeabilization buffer diluted 1:10 with ddH_2O) and centrifuged at 250 x *g* for 5 minutes at 4 °C. Post centrifugation, the cells were resuspended in 50 μl of perm medium and stained intracellularly for transcription factors and intracellular senescence markers for 30 minutes in the dark at room temperature (Table 1). Following this, cells were washed with 500 μl of perm medium and centrifuged at 250 x *g* for 5 minutes at 4 °C after which the supernatants were discarded, and the cells resuspended in 300 μl of non-sterile PBS for flow cytometric analysis (Figure 6E).

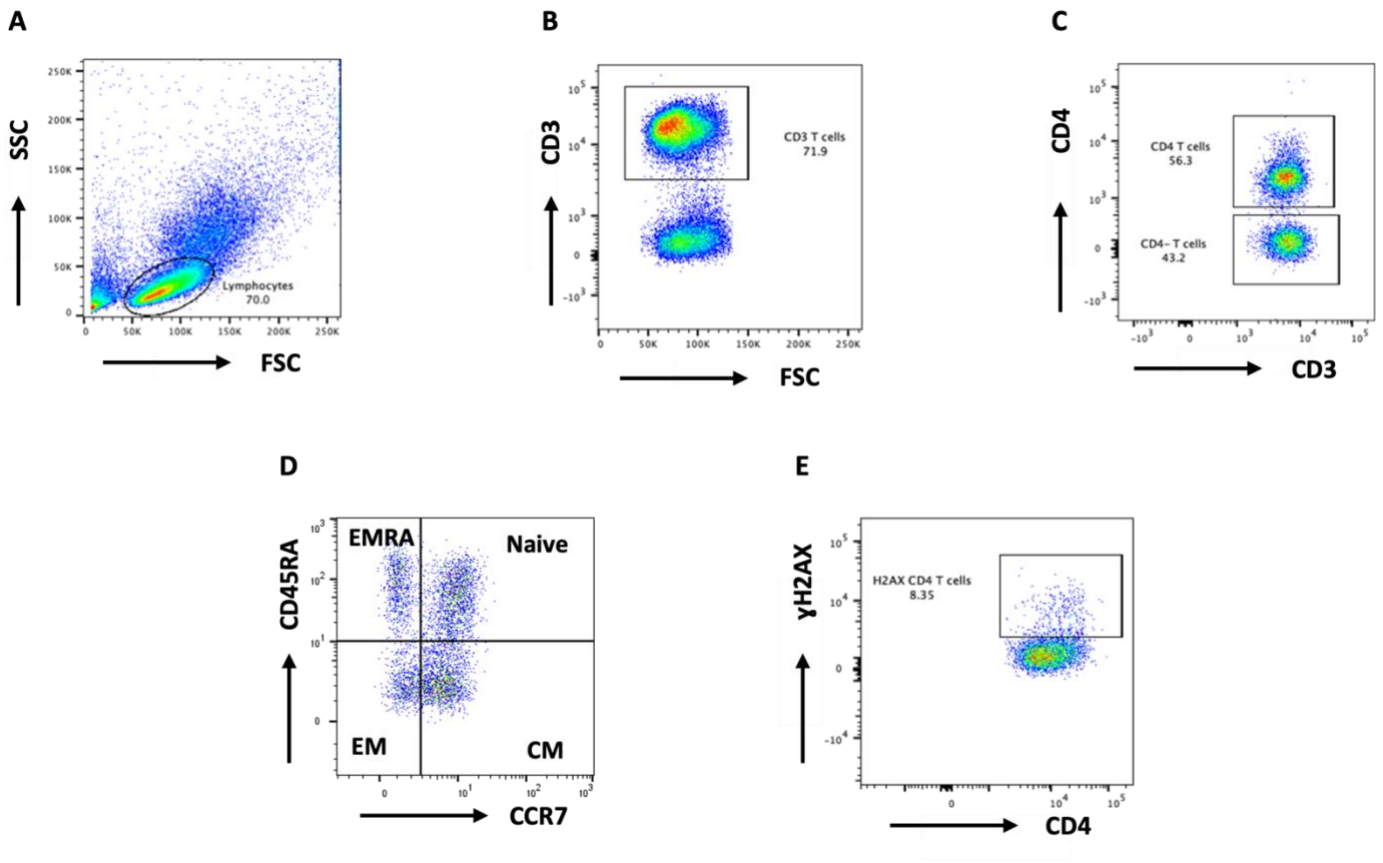

Figure 6. Gating strategy for phenotyping T cell subsets from PBMCs and the expression of intracellular markers/transcription factors.

(A) Cells were gated on a FSC/SSC flow cytometry plot in order to evaluate the circulating lymphocyte pool composition. **(B)** From these, the $CD3^+$ lymphocyte population was identified and gated on and subsequently, the lymphocytes were categorised further into the **(C)** $CD4^+$ and $CD4^-$ T cell subpopulations. **(D)** Following this, $CD4^+$ and $CD4^-$ T cells were analysed for CD45RA and CCR7 expression which allowed for the identification of 4 subsets: naïve ($CD45RA^+CCR7^+$), CM ($CD45RA^-CCR7^+$), EM ($CD45RA^-CCR7^-$) and EMRA ($CD45RA^+CCR7^-$). **(E)** The frequency of T cell subsets expressing various intracellular markers (e.g. H2AX) and transcription factors (see Table 1), and the expression levels of these markers was quantified via intracellular staining.

2.2.7 Stimulation and staining for p38 MAPK activation

PBMCs were stimulated with Ionomycin (500ng/ml; Sigma Aldrich, UK) and phorbol myristate acetate (PMA) (50 ng/ml; Sigma Aldrich, UK) for 30 minutes at 37°C. Post stimulation, PBMCs were washed with 300 μl of non-sterile PBS and centrifuged at 250 x g for 5 minutes at 4°C. Post centrifugation, cells were stained with a combination of anti-human CD3, CD4, CD45RA and CCR7 cell surface antibodies for 20 minutes in the dark on ice. Post incubation, the PBMCs were washed with 500 μl of PBS and spun at 250 x g for 5 minutes at 4°C. Cell supernatants were discarded and the cell pellets were resuspended in 100 μl of 4% paraformaldehyde (PFA), vortexed, and incubated for 30 minutes at room temperature in the dark. Post incubation, 1 ml of ice-cold methanol (100%) was added to the cells which were then incubated for 10 minutes on ice. Subsequently, cells were washed in 300 μl of non-sterile PBS at 250 x g for 5 minutes at 4°C to remove the methanol, the supernatants were discarded, and the washing step was repeated. Post second wash, supernatants were discarded, the PBMCs were resuspended in 50 μl of non-sterile PBS, and then incubated for 30 minutes in the dark at room temperature with anti-human p38 MAPK. Post incubation, cells were washed in 300 μl of non-sterile PBS at 250 x g for 5 minutes at 4°C, after which the supernatants were discarded and the cell pellets resuspended in 300 μl of non-sterile PBS for flow cytometric analysis. The frequencies of $p38^{+ve}$ cells within T cell subsets were recorded.

2.2.8 MitoTracker™ and MitoSOX™ staining of PBMCs

Freshly isolated PBMCs were stained with either MitoTracker™ green/red or MitoSOX™ red (Thermo Fisher) mitochondrial dyes for 30 minutes at 37°C. Post incubation, cells were washed with 300 μl of non-sterile PBS at 250 x g for 5 minutes at 4°C and subsequently stained with a combination of anti-human CD3, CD4, CD45RA and CCR7 cell surface antibodies for 20 minutes in the dark on ice. Following this, cells were washed again in 300 μl of non-sterile PBS at 250 x g for 5 minutes at 4°C, the supernatants were discarded, and cells were then resuspended in 300 μl of non-sterile PBS for flow cytometric and Image Stream analysis. The MFI values within T cell subsets were recorded.

2.2.9 Autophagy assay

Autophagy in cultured PBMCs was assessed using the Guava® Autophagy LC3 antibody-based assay kit (Luminex). Following 3-day culture in the presence or absence (control) of butyrate (section 2.2.4), PBMCs were stimulated with 10 μl diluted Autophagy Reagent A (1:50 in pre-warmed complete RPMI medium) for 2 hours. Post stimulation, cells were washed with 300 μl of non-sterile PBS and centrifuged at 250 x g for 5 minutes at 4°C. PBMCs were then stained with a combination of anti-human CD3, CD4, CD45RA and CCR7 cell surface antibodies for 20 minutes in the dark on ice. Post incubation, cells were washed in 100 μl 1X diluted Autophagy Assay Buffer (5X Assay Buffer diluted 1:5 with ddH_2O) and centrifuged at 300 x g for 5 minutes at 4°C. Following this, PBMCs were resuspended in 100 μl of 1X diluted Autophagy Reagent B (10X Reagent B diluted 1:10 with ddH_2O) and centrifuged immediately at 300 x g for 5 minutes at 4°C. Post spin, cells were resuspended in diluted anti-LC3 FITC antibody (20X anti-LC3 diluted 1:20 in 1X Assay Buffer) and incubated for 30 minutes on ice. Following incubation, PBMCs were washed in 150 μl 1X Assay Buffer and centrifuged at 300 x g for 5 minutes at 4°C. Finally, cells were resuspended in 300 μl of non-sterile PBS for flow cytometric analysis. The frequencies of $LC3^{+ve}$ cells within T cell subsets and LC3 expression were recorded.

2.2.10 Stimulation and staining for phosphorylated S6

PBMCs were stimulated with Ionomycin (500ng/ml; Sigma Aldrich) and phorbol myristate acetate (PMA) (50 ng/ml; Sigma Aldrich) for 30 minutes at 37°C. Post stimulation, PBMCs were washed with 300 μl of non-sterile PBS and centrifuged at 250 x g for 5 minutes at 4°C. Post centrifugation, cells were stained with a combination of anti-human CD3, CD4, CD45RA and CCR7 cell surface antibodies for 20 minutes in the dark on ice. Post incubation, the PBMCs were washed with 500 μl of PBS and spun at 250 x g for 5 minutes at 4°C. Cell supernatants were discarded and the cell pellets were resuspended in 1 ml of fix medium (fixation/permeabilization concentrate diluted 1:3 in fixation/perm diluent) and incubated for 30 minutes on ice in the dark. Following incubation, cells were washed with 500 μl of perm medium (permeabilization buffer diluted 1:10 with ddH_2O) and centrifuged at 250 x *g* for 5 minutes at 4 °C. Post centrifugation, the cells were resuspended in 50 μl of perm medium and then incubated for 30 minutes in the dark at room temperature with anti-human phospho S6. Post incubation, cells were washed in 300 μl of non-sterile PBS for 250 x g for 5 minutes at

4°C, after which the supernatants were discarded and the cell pellets resuspended in 300 μl of non-sterile PBS for flow cytometric analysis. The frequencies of phospho $S6^{+ve}$ cells within T cell subsets and phospho S6 expression were recorded.

2.2.11 ImageStream analysis

Post-culture, the fluorescence of single-colour stained PBMCs was initially measured (to optimize the laser strength) followed by experimental samples which were run on the calibrated ImageStream IS100 (Amnis) for simultaneous acquisition of bright field and scatter. Six fluorescent images were collected for each cell and the data files were stored as .rif files followed by analysis using IDEAS 4.0.735 software. The doublets and debris were gated out using bright field area vs. aspect ratio feature and in-focus single cells and to locate the distribution of signals within cells.

2.2.12 ELISA on cell culture supernatants

IL-6, IL-8 (CXCL8), IL-1β and CCL3 (MIP-1α) concentrations were measured in supernatants collected from cell cultures using commercially available kits from R&D Systems® DuoSet human ELISA kits as per manufacturer's instructions. To summarise, cell culture supernatant samples were diluted 1:50 (IL-6, IL-1β), 1:100 (CCL3) or 1:200 (IL-8) in reagent diluent (0.2 μm filtered, 1% BSA in PBS) and added to the wells of a pre-coated and blocked 96-well microplate. Following incubation for 2 hours at room temperature, wells were aspirated and washed 3X with wash buffer (0.05% Tween® 20 in PBS), after which 100 μl of the detection antibody (diluted with reagent diluent to working concentration from stock) was added to each well. Post 2 hours incubation at room temperature, wells were aspirated and washed again 3X in wash buffer before incubation with 100 μl of streptavidin-HRP (diluted 40-fold with reagent diluent to working concentration) for 20 minutes at room temperature in the dark. Post incubation, wells were aspirated and washed 3 times in 200 μl wash buffer prior to being incubated in 100 μl of tetramethylbenzidine (TMB) substrate solution for 20 minutes at room temperature in the dark. Once incubated, 50 μl of stop solution was distributed into the wells and the optical density was determined on a spectrophotometer with a primary wavelength of 450 nm and a wavelength correction set to 540 nm, using Gen5 software.

Cytokine concentrations were determined via standard curve created from values acquired from standards of known cytokine concentrations generated on Prism® v7 (GraphPad).

2.2.13 T cell isolations from PBMCs

Following on from the PBMC isolation (section 2.2.3) and the plating of cells (section 2.2.4), the remaining PBMCs were centrifuged at 300 x g for 10 minutes at room temperature, counted on the Sysmex XN-1000 and made up to 5 x 10^7 / ml in PBS with 2% FBS (Sigma-Aldrich, UK) and 1mM EDTA. The cell suspension was then transferred to a 5ml polypropylene round-bottom tube and 50 µl isolation cocktail/ml of sample was added to the PBMCs and gently pipetted up and down to mix. The tube was then incubated for 5 minutes at room temperature. Post incubation, the RapidSpheres™ were vortexed for 30 seconds and 40 µl RapidSpheres™/ml of sample was added to the tube, pipetting up and down to mix. Following this, the tube was placed in an EasyEights™ 5 ml tube magnet and incubated for 5 minutes at room temperature. Once incubated, the enriched cell suspension was transferred into a new 5 ml tube which was then placed in the magnet and incubated at room temperature for 5 minutes. The isolated T cells were pipetted into a new 5 ml tube, counted and resuspended in complete pre-warmed RPMI-1640 at a concentration of 1 million cells / ml. Following this, 150 µl of the isolated T cell suspension was plated per well in an anti-CD3 mAb coated 96-well U bottom plate and butyrate (1mM) was added to the appropriate wells. The plate was then incubated at 37 °C for 72 hr in a humidified atmosphere of 5% CO_2. Post-culturing, the T cells were transferred to labelled Eppendorfs and spun in the mini centrifuge at 3000 rpm for 3 minutes at room temperature. Supernatants from the pelleted cells were removed and stored in separate labelled Eppendorfs at -80 °C for future use whilst the cell pellets were resuspended in a freezing medium and stored in labelled cryovials at -80 °C prior to RNA isolations.

2.2.14 RNA isolations from T cells

RNA was isolated from frozen T cells, using the RNeasy® Mini Kit (Qiagen, Germany), that were thawed in a water bath and washed. Briefly, cryovials were thawed on ice, resuspended dropwise in 10 ml of ice-cold sterile PBS and centrifuged at 300 x g for 10 minutes at room temperature. Cells were then resuspended in 1 ml of ice-cold sterile PBS, transferred to a 1.5

ml RNase-free Eppendorf and centrifuged at 3000 rpm for 3 minutes using a mini centrifuge. Following this, 350 μl of RLT buffer with β-mercaptoethanol (10 μl β-ME per 1 ml of RLT buffer) was used to resuspend the cells, which were then incubated at room temperature for 10 minutes. Post incubation, 350 μl of 70% ethanol was added to the cells and the Eppendorf was vortexed for 30 seconds before 700 μl of the cell suspension was added to a RNeasy® mini column which was spun for 15 seconds at 8000 x g, discarding the flow-through after each spin. Post centrifugation, 350 μl of buffer RW1 was added to the RNeasy® column and the cells were centrifuged for 15 seconds at 8000 x g. Afterwards, 80 μl of DNase I mix (10 μl DNase I stock solution in 70 μl of RDD buffer) was added directly to the RNeasy® column membrane. Following a 15-minute incubation at room temperature, 350 μl of buffer RW1 was added and the column spun for 15 seconds at 8000 x g. Subsequently, cells were spun with 500 μl of buffer RPE for 15 seconds at 8000 x g after which the flow-through was discarded and another 500 μl of buffer RPE was added to the RNeasy® column which was spun for 2 minutes at 8000 x g. The RNeasy® column was then placed in a new 2 ml collection tube and centrifuged at full speed for 1 minute to dry the column membrane. Post centrifugation, 12 μl of RNase-free water was added directly to the column membrane and left to rest for 5 minutes at room temperature before centrifuging for 3 minutes at 8000 x g. Isolated RNA concentrations and purity values (A260/A280 and A260/A230) were determined via NanoDrop™ (Thermo Fisher).

2.2.15 NanoString nCounter gene expression analysis

Isolated RNA was thawed on ice and diluted with RNase-free water to 100 ng / μl. The thermal cycler was preheated to 65°C and the lid to 70°C, during which time the nCounter® Reporter CodeSet and Capture ProbeSet tubes were thawed at room temperature in the dark. The hybridization master mix was prepared by pipetting 70 μl of the hybridization buffer into the Reporter CodeSet tube and repeatedly inverting the tube to mix. Next, 8 μl of the hybridization master mix was added to each tube of the 12-well notched strip tubes followed by 5 μl of diluted sample RNA. The Capture ProbeSet tube was mixed by inverting and 2 μl was added to each tube which was then flicked to ensure complete mixing and spun briefly before being placed in the preheated 65 °C thermal cycler and incubated for 16 hours. Hybridized RNA samples were then purified using the nCounter® Prep Station. Prior to

purification, nCounter® Prep Plates and Cartridge were thawed at room temperature for 20-30 minutes. Once thawed, the Prep Plates were spun at 2000 x g for 2 minutes at room temperature, the lids removed, and loaded on to the Prep Station. Following this, the tips and foil piercers, tip sheaths, Cartridge and empty 12-well notched stip tubes were all loaded on to the Prep Station. Finally, the hybridized sample RNA was removed from the thermal cycler and loaded on to the Prep Station which was then run on high sensitivity (3 hours 5 minutes). Post run, the nCounter® Cartridge was removed and sealed immediately with an adhesive cover in preparation for analysis on the nCounter® Digital Analyzer. Gene counts/expression was analysed using the nSolver™ v4.0 analysis software (NanoString® Technologies).

2.2.16 Sectioning of murine spleen tissue samples

In brief, at the University of East Anglia (UEA) Disease Modelling Unit Facility, groups of six young (6 months) and aged (24 months) male C57BL/6J mice were housed in ventilated cages. Mice were maintained under a 12-hour light:12-hour dark cycle and fed a standard chow diet. At baseline, stool pellets were collected from young mice. Following this, to diminish the existing gut microbiome, mice received a 3-day broad-spectrum antibiotic treatment. Post-antibiotic treatment, aged mice received oral gavage of young faecal supernatant (from heterochronic young donor pool) at two separate time points, 72 hours apart. Young and aged control mice received PBS gavage at these time points. At the end of the experiment, spleen samples were obtained to determine the impact of the young gut microbiome and its components on the aged spleen. All experiments involving mice were given approval from the UEA Animal Welfare and Ethical Review Body. Upon receiving the samples, the spleen tissues were immediately stored at -80°C. In preparation for sectioning, the spleen samples were thawed and placed into a Tissue-Tek® Cryomold® (Sakura Finetek) on a layer of Tissue-Tek® optimal cutting temperature (OCT) compound (Sakura Finetek). The remainder of the cryomold was filled with OCT compound and placed on dry ice until solid. Cryomolds containing one spleen in OCT per mould were stored at -80°C until sectioning. The frozen tissue sample was placed directly into the cryochamber of the Leica CM1950 cryostat and left for 30 minutes to equilibrate. Following this, the frozen tissue sample was removed from the cryomold and secured on to a pre-cooled specimen disk which was then placed in the freeze shelf of the cryochamber and left for 10 minutes to allow for additional cooling. Post cooling,

the disk was inserted into the specimen head and the tissue orientated perpendicular to the blade. The initial surface of OCT was trimmed away at a setting of 6 μm which was then increased to 10 μm. Tissue sections were cut randomly throughout the sample at a thickness of 7 μm in the cryostat at -20°C and transferred to a labelled pre-cooled positively charged microscope slide (Leica Biosystems). Three sections were placed per slide with a total of 4 slides per tissue sample. Once sectioned, the remaining tissue sample was placed back in the original cryomold, covered with a layer of OCT compound and stored at -80°C. The microscope slides were left to air dry overnight at room temperature and wrapped in foil the following day then stored at -80°C in a labelled microscope box.

2.2.17 Lamin B1 and DAPI staining of spleen sections

The microscope slide containing tissue sections was thawed at room temperature for 30 minutes. Tissue was fixed in ice-cold neat acetone for 10 minutes at -20°C and then washed twice with non-sterile PBS in a staining jar for 4 minutes. The lamin B1 monoclonal rabbit antibody (Abcam, UK) was diluted 1:1000 with 10% normal goat serum (NGS) and 0.2% triton (Sigma-Aldrich, UK) in non-sterile PBS. Post washes, the microscope slide was removed from the staining jar and dried on a paper towel and using a hydrophobic barrier PAP pen (Cosmo Bio Ltd, UK), a circle was drawn around the tissue sample. Following this, the slide was incubated with 150 μl of the primary antibody mixture overnight at 4°C in a humidity chamber in the dark. The next day, the microscope slide was washed three times with non-sterile PBS in a staining jar for 4 minutes. The anti-rabbit alexa-fluor 555 secondary antibody (Cell Signalling Technology, USA) was diluted 1:300 with 0.2% triton in non-sterile PBS. Post wash, 150 μl of secondary antibody mixture was pipetted onto the tissue which was then incubated for 1 hour in the dark at room temperature. Post incubation, the slide was washed three times with non-sterile PBS for 3 minutes. The DAPI stain was diluted 1:1000 with non-sterile PBS and post-wash, 150 μl of diluted DAPI was pipetted onto the tissue. The slide was then incubated for 10 minutes in the dark at room temperature. Following this, the slide was washed twice with non-sterile PBS for 3 minutes and then dried. One drop of ImmunoSelect® antifading mounting medium (Dianova, Germany) was placed onto each tissue sample and a coverslip was carefully applied on top. Clear nail varnish was spread around the edges of the

coverslip and then left to air dry prior to fluorescent imaging on the Olympus IX71 fluorescent microscope.

2.2.18 Statistical analysis

Statistical analysis was achieved using GraphPad Prism® software. For normally distributed data, a paired student t-test, or a one-way ANOVA with Bonferroni multiple comparison post hoc tests were performed where appropriate. Statistical significance was accepted at $P \leq 0.05$.

3.0 Results

3.1 Setting up an *in vitro* model of proliferation-induced T cell senescence

Replicative senescence induction was originally recognized as a method for establishing a cellular model of senescence (175) and thus to evaluate the contribution of butyrate in controlling the development of T cell senescence we took advantage of a cellular model of proliferation-induced senescence in which, we cultured PBMCs in CD3-coated wells for 3 days and have confirmed that continuous proliferation (Figure 7A; upregulation of Ki-67, a cellular marker for proliferation) can induce DNA DSBs by inhibiting the activity of DNA topoisomerase II-induced robust phosphorylation of histone H2AX at serine 139, indicated by the appearance of DNA-damage foci and confirmed by increased expression of a marker of DNA damage (γ-H2AX) (Figure 7B), which activates p53 to elicit cell-cycle arrest and induce senescence (Figure 7C) (176, 177). Furthermore, we have also confirmed an upregulation in the SASP phenotype, pro-inflammatory cytokines (IL-6) in cell culture-supernatant 72hr post-culture (Figure 7D).

3.2 Senomorphic properties of butyrate: dampening of senescence-associated secretory phenotype in aged T cells

After validating the *in vitro* model of proliferation-induced T cell senescence, we sought to determine the optimal concentration of butyrate to add to the 3 day PBMC culture. Following incubation for 3 days, we observed a dose-dependent effect of butyrate on IL-6 levels present in cell culture supernatants and, compared with untreated control cells, we observed a significant decline in the levels of the SASP component IL-6 in supernatants in CD3-treated cells incubated with butyrate at 1mM concentration ($p = 0.002$) (Figure 8A). We therefore cultured T cells for 3 days in CD3-coated wells with or without 1mM of butyrate followed by collection of supernatants, RNA isolations and evaluation of senescence markers via flow cytometry (Figure 8B). Importantly, we have observed a significant reduction in the secretion of pro-inflammatory

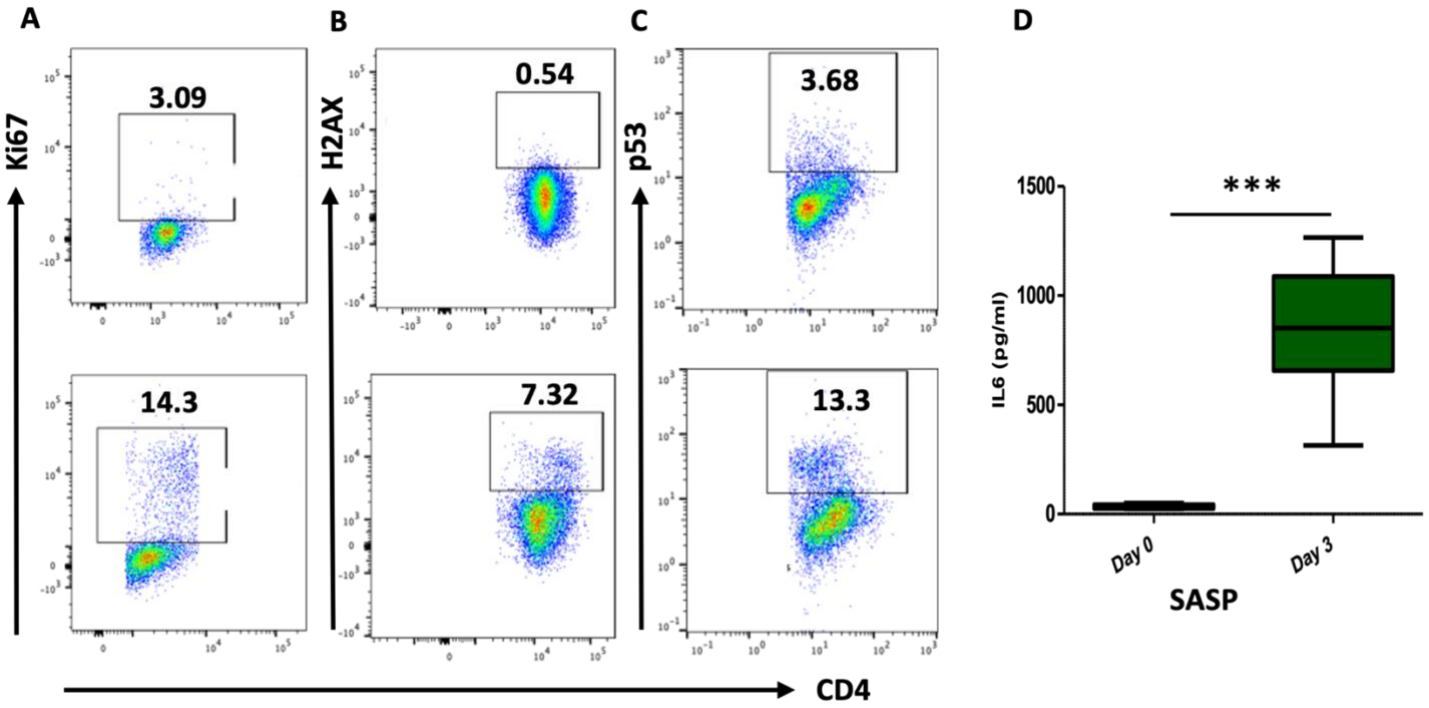

Figure 7. A cellular model of proliferation-induced T cell senescence.

In-vitro culture of PBMCs in CD3-coated wells for 3 days representative flow cytometry images for **(A)** proliferation marker Ki67 **(B)** DNA damage (H2AX) marker **(C)** replicative arrest mediated by upregulation of tumour-suppressor pathway p53. **(D)** Senescent cells secrete products (SASP) that are important contributors to aging and an upregulation of SASP factor IL-6 has been observed in cell-culture supernatant at day3 indicative of three independent experiments. Statistical analysis was performed by two-tailed paired Student's t-test. Data are shown as the mean ± SD ***p < 0.001

SASP features, including IL-6, p = 0.003 (Figure 8C), IL-8, p = 0.008 (Figure 8D), IL-1β p = 0.04 (Figure 8E) by aged PBMCs cultured in the presence of SCFA butyrate. To confirm that the sodium component of the sodium butyrate treatment was not contributing to the senomorphic effects observed, we cultured aged cells for 3 days in CD3-coated wells incubated with either 1mM sodium butyrate or 1mM sodium bicarbonate and measured IL-6 production compared to that of untreated controls. Supernatant levels of IL-6 were significantly decreased following butyrate treatment (p = 0.006) compared to control, whilst sodium bicarbonate treatment did not affect IL-6 production with levels remaining similar to those of the control (Figure 8F).

3.3 Regulation of senescence phenotype by butyrate in aged T cells

The process of cellular senescence induces a stable cell cycle arrest in response to stresses/damage such as reactive oxygen species, and chromatin perturbation that induces activation of stress pathways such as p53 in response to DNA damage (178). To determine whether butyrate impacts the exhibition of a senescent phenotype in T cell subsets, we compared the protein expression of p53 in naïve ($CD45RA^{+ve}$ $CCR7^{+ve}$), central memory ($CD45RA^{-ve}$ $CCR7^{+ve}$), effector memory ($CD45RA^{-ve}$ $CCR7^{-ve}$) and terminally differentiated EMRA ($CD45RA^{+ve}$ $CCR7^{-ve}$) CD4 and CD8 T cell subsets. A significant decrease in the frequency of phosphorylated p53 expressing EMRA CD4 T cells (p = 0.02) [Supplementary Figure 1A], naïve CD8 T cells (p = 0.01) and EMRA CD8 T cells (p = 0.03) (Figure 9A, B) has been observed in butyrate-cultured PBMCs compared to untreated controls. Next, on investigating p53 expression levels a similar decline in EMRA CD4 T cells (p = 0.02), and Naïve CD8 T cells (p = 0.004) cultured in the presence of butyrate [Supplementary Figure 1B and Figure 9C respectively] Additionally, we examined expression of the DNA damage marker γ-H2AX in the 4 subsets within aged CD4 and CD8 T cells. Naïve CD4 (p = 0.03) and CD8 (p = 0.04) T cells displayed a significant reduction in frequency of γ-H2AX expression [Supplementary Figure 1C and Figure 9D respectively]. The expression level of γ-H2AX was significantly decreased in both naïve (p = 0.04) and EMRA (p = 0.04) CD8 T cells (Figure 9E) however no significant changes were observed in the CD4 T cells [Supplementary Figure 1D]. The results seen in the CD8 T cells were also confirmed via ImageStream analysis (Figure 9F)

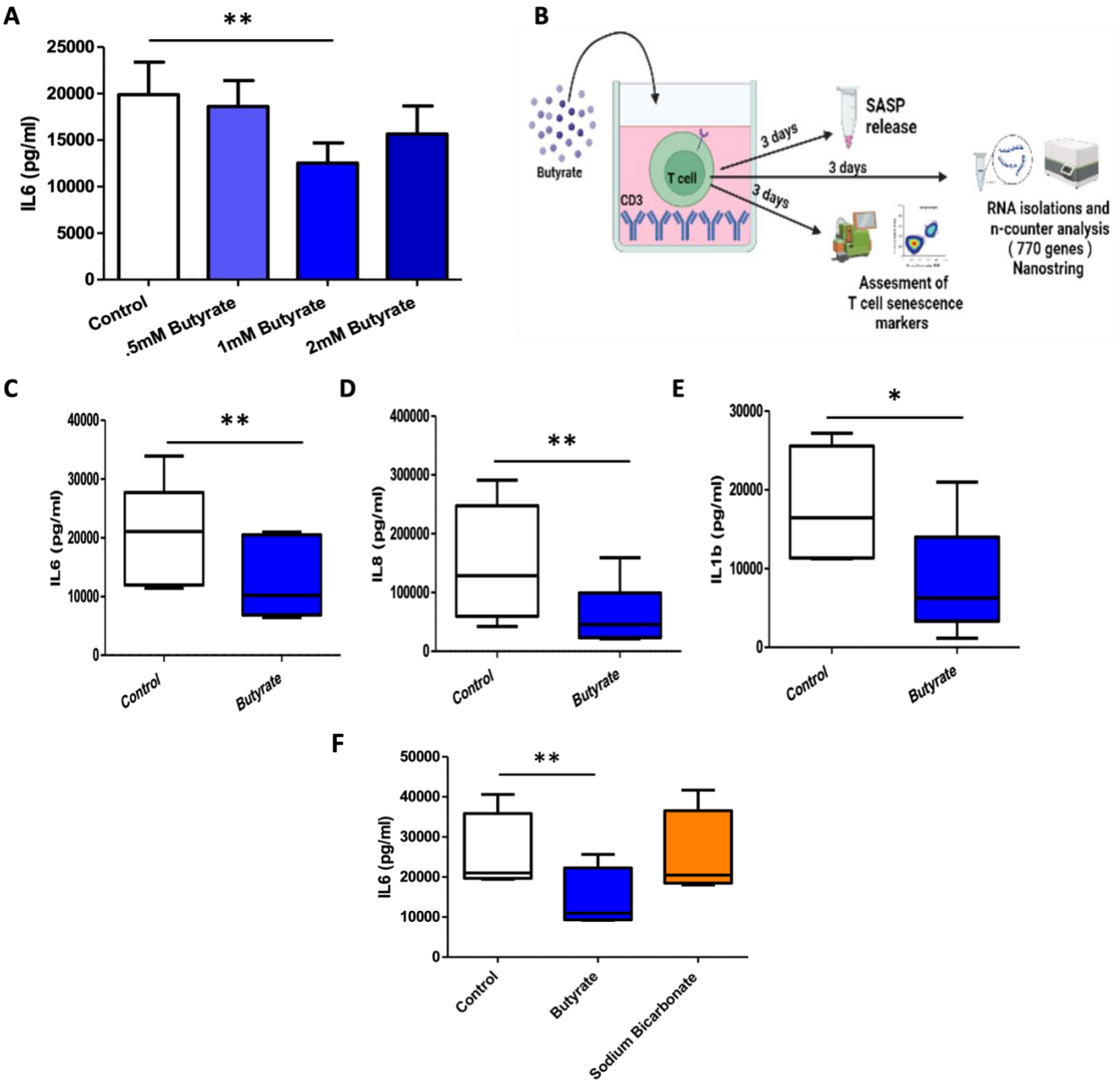

Figure 10. Characterisation of the senomorphic properties of butyrate and attenuation of SASP phenotype.
(A) CD3 treated PBMC cells were incubated with different concentrations of butyrate (0.5-2 mM) for 72 hours. At the end of treatment, IL6 concentration in cell-culture supernatant was measured by ELISA (n = 3). **(B)** Schematic of experimental design indicating culturing of T cells in CD3 coated plates with SCFA butyrate for 72 hr (n = 6) and collection of cell-culture supernatants for determining SASP features by ELISA and assessment of features of senescence via flow cytometry. The secretion of **(C)** IL-6 **(D)** IL-8 **(E)** IL-1β from CD3 treated T cells in presence of butyrate. **(F)** The secretion of IL-6 from CD3 treated T cells in the presence of butyrate or sodium bicarbonate compare with untreated control. Data are mean ± SEM of six independent experiments. Statistical analysis was performed by two-tailed paired Student's t-test *p <0.05, **p < 0.01.

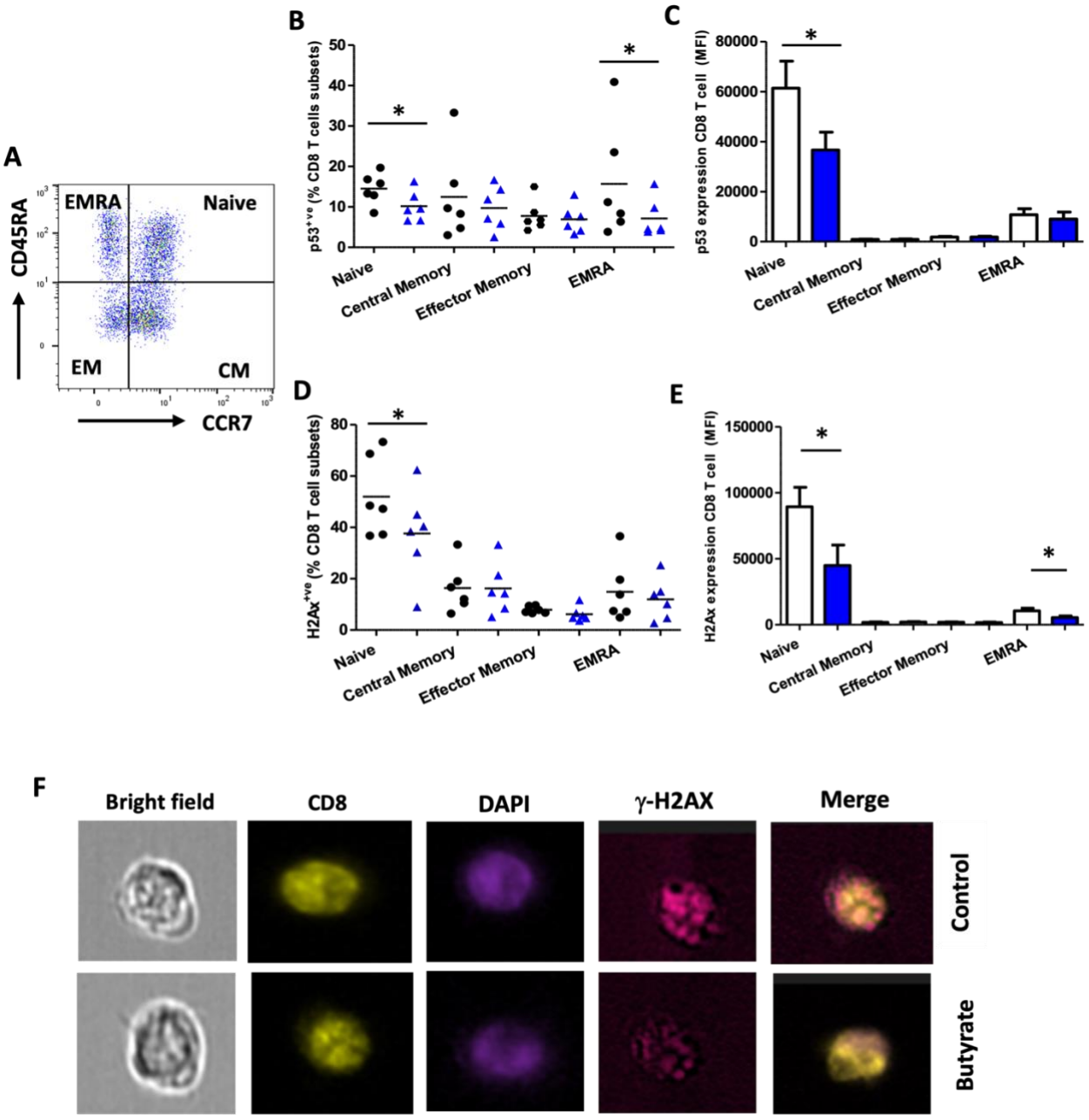

Figure 13. Characterisation of anti-senescence properties of butyrate.

(A) Representative flow cytometry showing gating strategy for T cell subsets based on phenotypic expression of CD45RA/CCR7 staining. In-vitro culture of PBMCs in CD3-coated wells for 3 days in the presence (blue)/absence of SCFA butyrate. On day 3 **(B)** frequency of phosphorylated p53 expressing CD8 T cell subsets, **(C)** p53 expression levels in CD8 T cell subsets, **(D)** frequency of γ-H2AX expressing CD8 T cell subsets and **(E)** γ-H2AX expression levels (MFI) in CD8 T cell subsets were measured. Statistical analysis was performed using a two-tailed paired Student's t-test. The bar charts show expression data as the mean ± SEM of six different experiments * $p = 0.05$ **(F)** Representative Image stream images of cells stained with cell surface marker CD8, nuclear DAPI stain and DNA damage marker γ-H2AX and merged image when PBMCs were cultured in CD3-coated wells for 3 days in the presence/absence of SCFA butyrate.

3.4 Impact of butyrate on nuclear translocation of phosphorylated nuclear factor kappa B (NF-κB) in aged T cells

The nuclear translocation of NF-κB plays a central role in regulation of inflammatory responses via induction of transcriptional regulation of the expression of pro-inflammatory cytokine genes by binding to specific promoter elements (179). To elucidate the mechanisms by which butyrate may influence the secretion of pro-inflammatory cytokines by T cells we investigated its impact on NF-kB inhibition. A significant decrease in the frequency of phosphorylated NF-kB expressing EM and EMRA CD4 T cells ($p = 0.05$ and $p = 0.03$ respectively) (Figure 10A) and EMRA CD8 T cells ($p = 0.04$) (Figure 10C) has been observed in butyrate-cultured PBMCs compared to untreated controls. Next, on investigating NF-kB expression levels a similar decline in EM and EMRA CD4 T cells ($p = 0.01$ and $p = 0.02$), and Naïve CD8 T cells ($p = 0.02$) cultured in the presence of butyrate was observed (Figure 10B and D).

3.5 Investigating effect of butyrate on p38 signalling in aged T cells

Terminally differentiated human effector memory T cells that re-express CD45RA (EMRA) are known to possess senescence features, such as SASP secretion that are maintained in part by activation of p38MAPK signalling (180). We investigated whether inhibition of phosphorylation status of p38 by butyrate was a potential mechanism underlying its senomorphic properties, but did not detect any significant differences between frequency of p-p38 expressing CD4 and CD8 T cells subsets in control vs butyrate (Figure 11A and C respectively) or its expression levels (Figure 11B and D respectively).

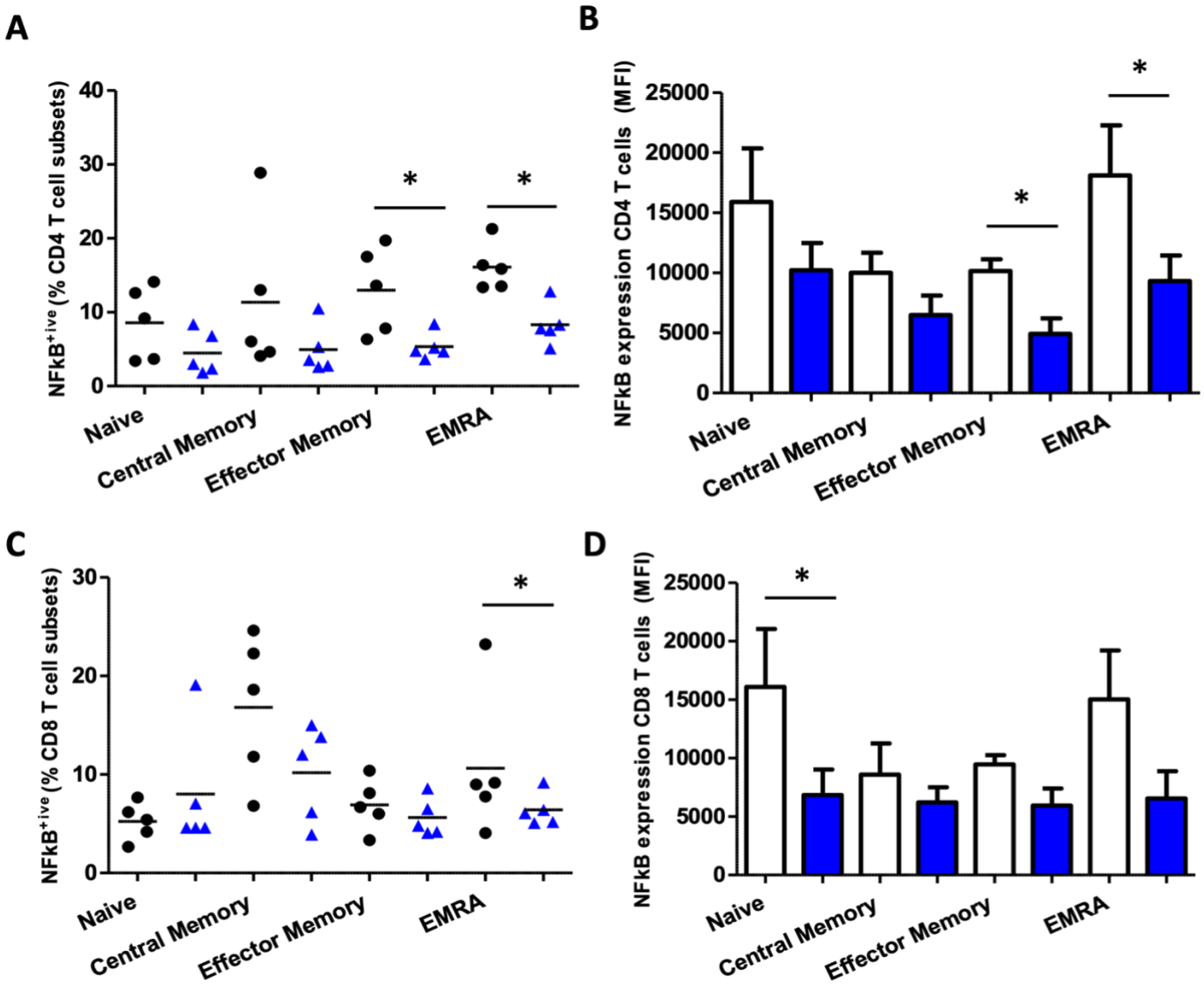

Figure 16. Effect of butyrate on nuclear translocation of nuclear factor kappa B (NF-kB) in aged T cells.
In vitro culture of PBMCs in CD3-coated wells for 3 days in the presence (blue)/absence of SCFA butyrate for **(A)** frequency of phosphorylated NF-kB expressing CD4 T cell subsets and **(C)** CD8 T cell subsets. NF-kB expression levels in **(B)** CD4 and **(D)** CD8 T cell subsets. Statistical analysis was performed by a two-tailed paired Student's t-test. Data are shown as the mean ± SD *$p < 0.05$.

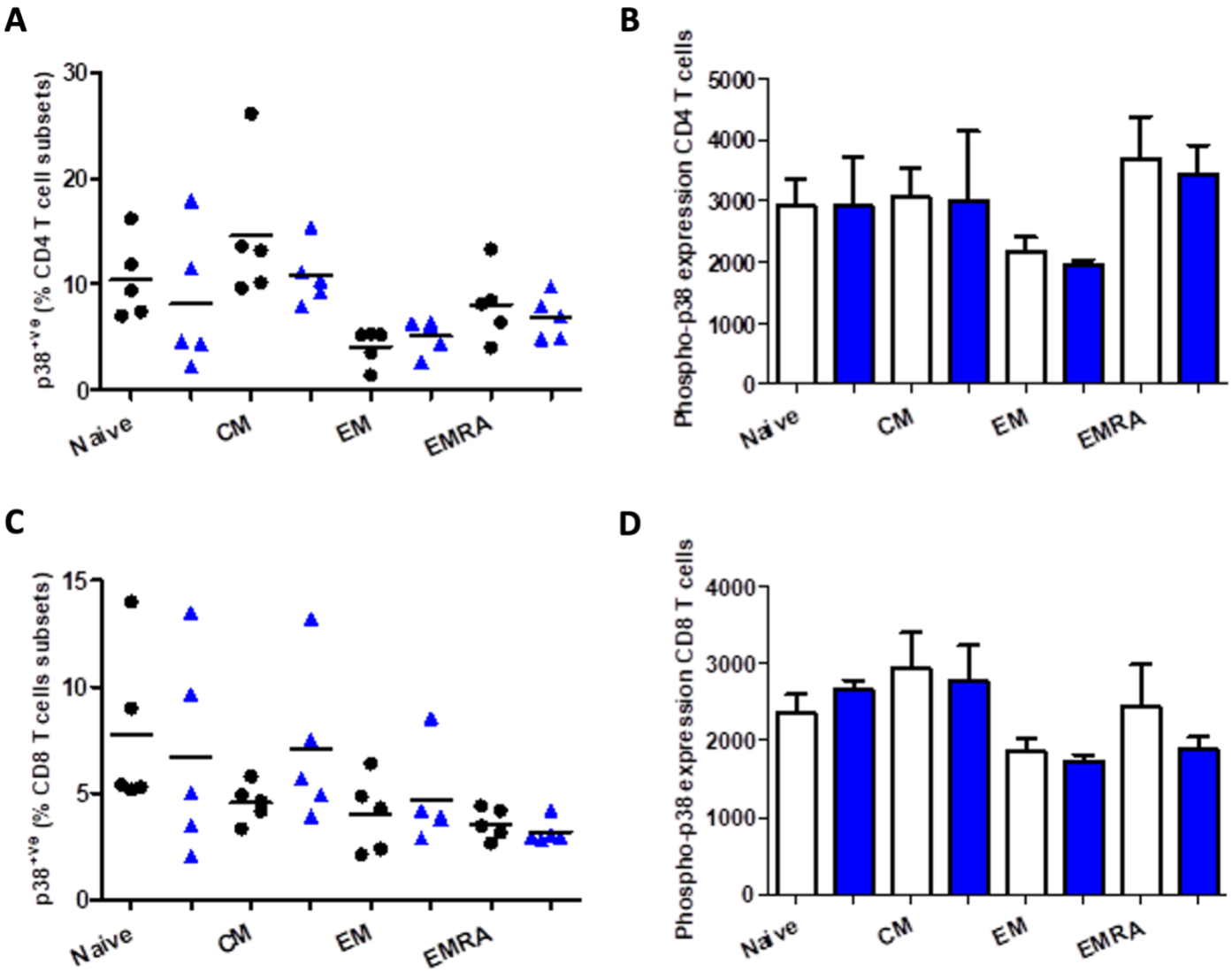

Figure 17. Effect of butyrate on phosphorylated p38 MAPK in aged T cells.
In vitro culture of PBMCs in CD3-coated wells for 3 days in the presence (blue)/absence of SCFA butyrate and stimulation with PMA/ionomycin for **(A)** frequency of phosphorylated p38 MAPK expressing CD4 T cells subsets and **(C)** CD8 T cell subsets. Phosphorylated p38 MAPK levels in **(B)** CD4 T cell subsets and **(D)** CD8 T cell subsets. Statistical analysis was performed by a two-tailed paired Student's t-test. Data are shown as the mean ± SD.

3.6 Mitochondrial mass and ROS production regulation by butyrate

With age, it is known that various moderators of cellular preservation decline and processes involved in mitochondrial biogenesis are impaired (181). Increased mitochondrial mass is a feature of senescent cells, with the accumulation of dysfunctional mitochondria contributing to inflammageing and the exacerbation of the senescent phenotype (182, 183). We made use of the mitochondria-specific MitoTracker™ green dye, which binds mitochondrial membranes in a mitochondrial membrane potential (MMP) independent manner, to determine changes in mitochondrial mass in young and aged T cells. We observed a significant decline in MitoTracker™ green expression levels in aged EMRA CD4 T cells ($p = 0.02$) cultured with butyrate (Figure 12B), as seen by a downward shift in MFI (Figure 12A), whilst no significant difference in expression levels was seen in the aged CD8 T cells (Figure 12C). These results were confirmed via ImageStream analysis (Figure 12E). Mitochondrial ageing is also characterised by an increase in ROS production which we evaluated in aged T cells incubated with butyrate using the MitoSOX™ Red mitochondrial superoxide indicator. In aged EMRA CD8 T cells exposed to butyrate, we reported a significant decrease in MitoSOX™ expression ($p = 0.001$) (Figure 12D).

3.7 Evaluating the influence of butyrate on autophagy

One of the key hallmarks of senescence is the loss of effective proteostasis, resulting in defective protein degradation and, crucially, impaired removal of dysfunctional cell components via

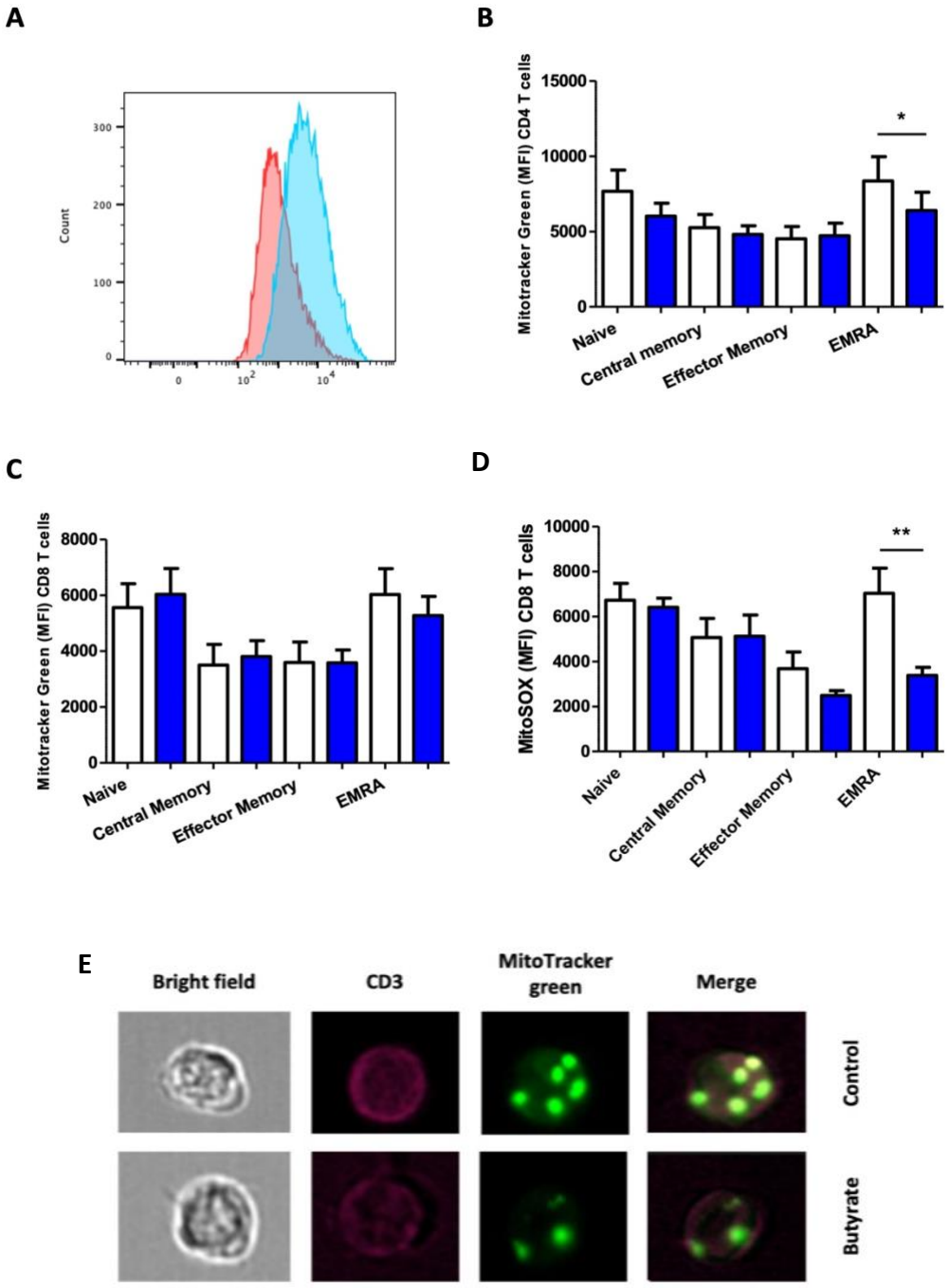

Figure 20. Effect of butyrate on mitochondrial mass and ROS production in T cells.
In vitro culture of PBMCs in CD3-coated wells for 3 days in the presence (blue)/absence of SCFA butyrate and stimulation. **(A)** Representative histogram of the shift in MitoTracker™ green MFI between control (blue) and butyrate (red). MitoTracker™ green expression levels in **(B)** aged CD4 T cell subsets and **(C)** aged CD8 T cell subsets. **(D)** MitoSOX™ red expression levels in young CD4 T cell subsets. **(E)** Representative ImageStream images of cells stained with cell surface marker CD3 and mitochondrial mass indicator MitoTracker™ green and subsequent merged images. Statistical analysis was performed by a two-tailed paired Student's t-test. Data are shown as the mean ± SD *p <0.05, **p < 0.01.

autophagy (184, 185). During formation of the autophagosome, cytosolic microtubule associated protein 1 light-chain 3 (LC3) is cleaved and sequestered to the autophagosome membrane thus making it a useful marker of autophagosome number, and therefore induction of autophagy (186). We sought to determine whether upregulation of autophagy processes by butyrate was a possible underlying mechanism for its ability to regulate mitochondrial mass, however there was no significant difference in the frequency of CD4 and CD8 T cells subsets expressing LC3 in control vs butyrate (Figure 13A and C respectively) or in LC3 expression levels (Figure 13B and D respectively). Additionally, gene expression analysis found no alteration in Atg7 and Atg10 autophagy gene expression between control T cells and those incubated with butyrate (Figure 13E). Regulation of autophagy occurs via the mTOR signalling pathway, the activation of which inhibits autophagy in favour of cell growth through anabolic metabolism (187). A crucial downstream effector of mTOR signalling, ribosomal protein S6 kinase (S6K) activation leads to phosphorylation of the ribosomal protein S6 (phospho S6) which in turn promotes protein synthesis (188). We utilised phospho-S6 as a readout of mTOR activity in order to establish any effect on the pathway by butyrate stimulation. A significant decrease in phospho S6 expression was observed in naïve CD4 T cells ($p = 0.04$) (Figure 14B) in control vs butyrate however, there were no significant changes seen in the frequency of phospho S6 expressing CD4 or CD8 T cells (Figure 14A and C respectively) or in the phospho S6 expression in CD8 T cells (Figure 14D).

3.8 Butyrate alters gene expression in aged T cells

Mechanistically, butyrate is known to act as a HDAC inhibitor, capable of regulating the expression of genes involved in immune system pathways (189, 190, 191, 192). We analysed the gene expression in aged T cells and found 34 genes where the expression was modified following butyrate treatment (Figure 15). In total, 33 of these genes were downregulated including those

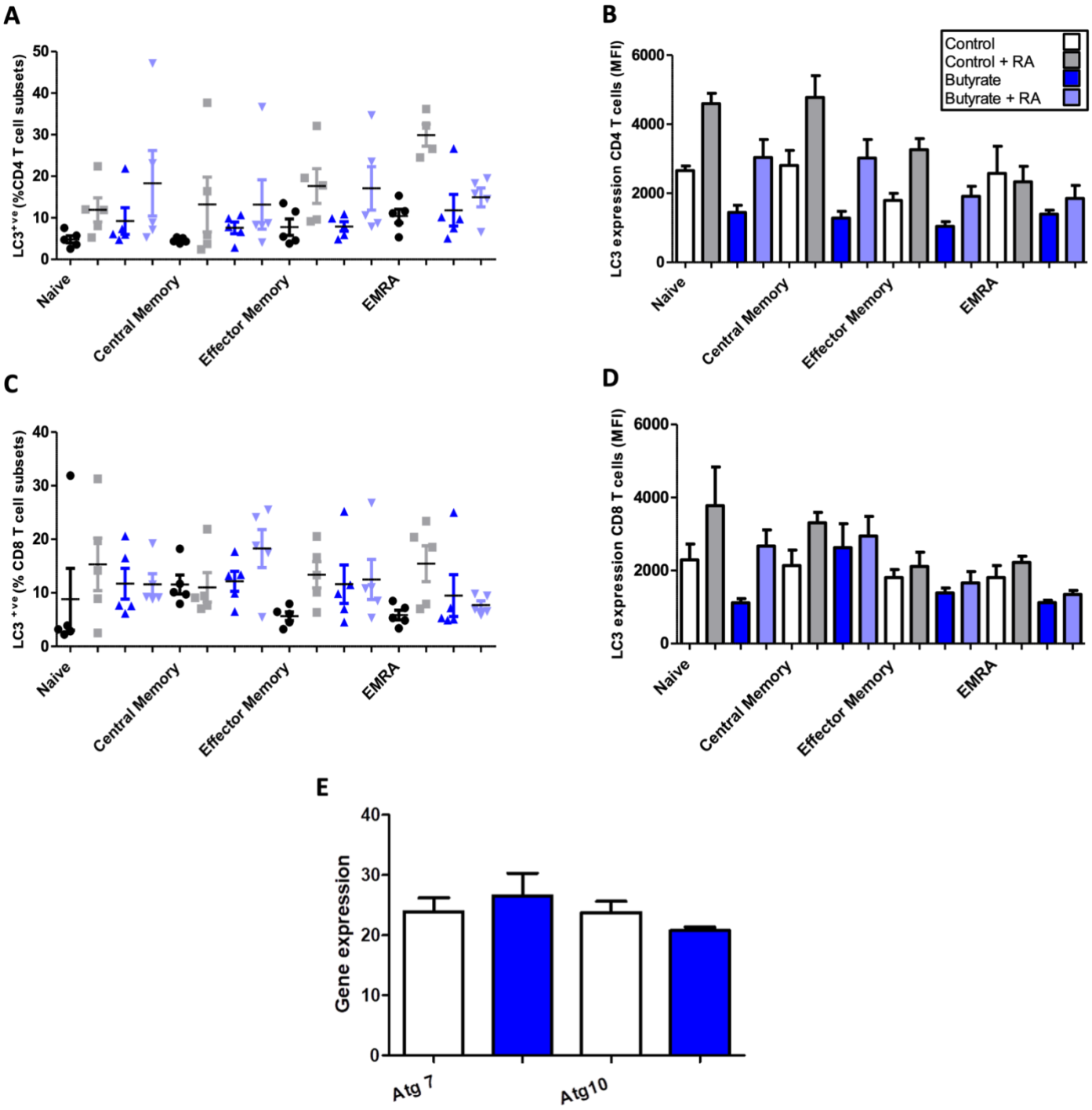

Figure 21. Effect of butyrate on autophagy in T cells.

In vitro culture of PBMCs in CD3-coated wells for 3 days in the presence/absence of SCFA butyrate and with/without Autophagy Reagent A stimulation for **(A)** frequency of LC3 expressing young CD4 T cells subsets and **(C)** CD8 T cell subsets. LC3 expression levels in **(B)** young CD4 T cell subsets and **(D)** CD8 T cell subsets. **(E)** Gene expression of the autophagy genes Atg7 and Atg 10 in aged T cells following *in vitro* culture of isolated T cells in CD3-coated wells for 3 days in the presence (blue)/absence of SCFA butyrate. Statistical analysis was performed by a two-tailed paired Student's t-test. Data are shown as the mean ± SD.

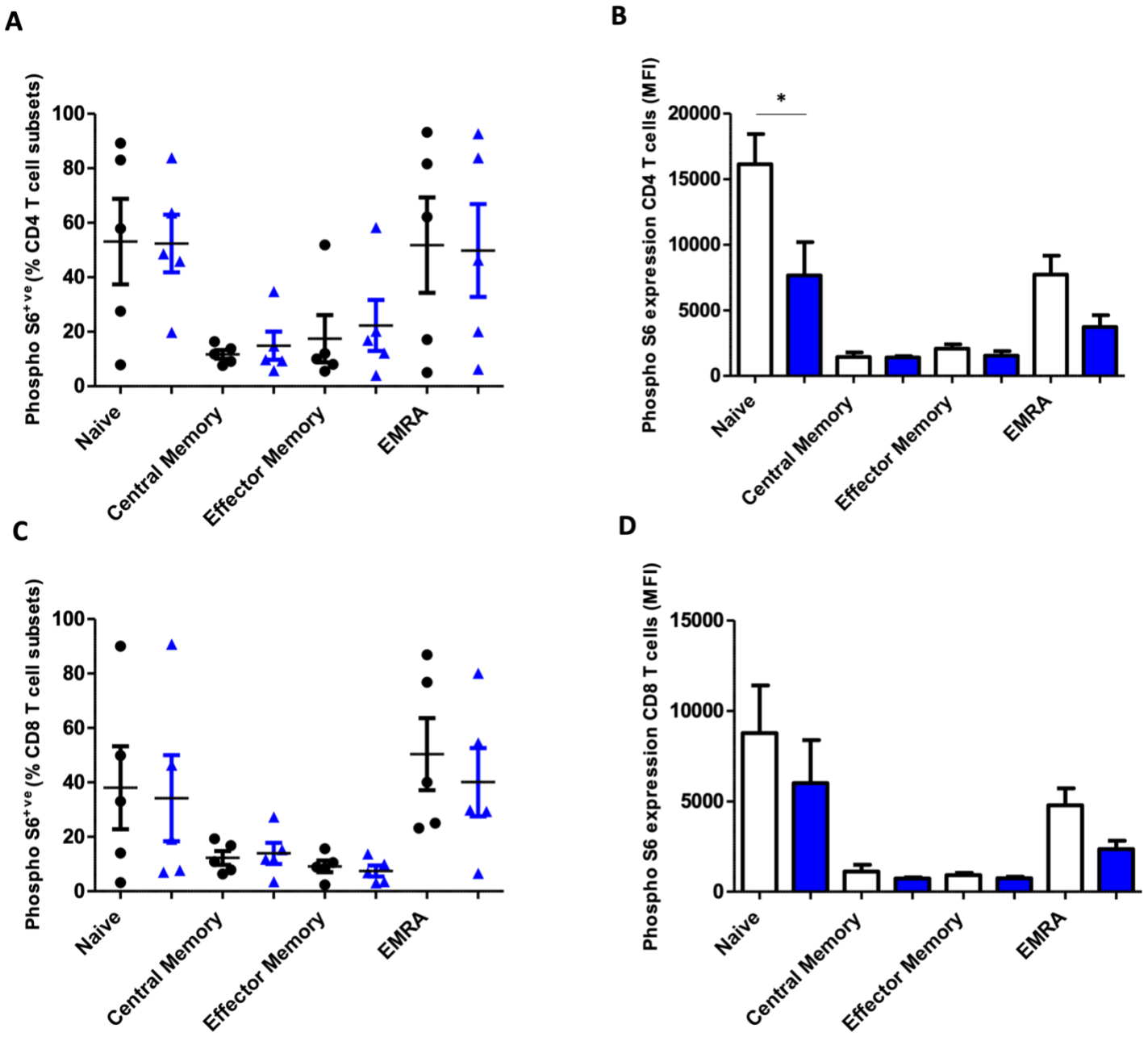

Figure 24. Effect of butyrate on mTOR activity in T cells.

In vitro culture of PBMCs in CD3-coated wells for 3 days in the presence (blue)/absence of SCFA butyrate and with PMA/Ionomycin stimulation for **(A)** frequency of phosphorylated S6 expressing young CD4 T cells subsets and **(C)** CD8 T cell subsets. Phosphorylated S6 expression levels in **(B)** young CD4 T cell subsets and **(D)** CD8 T cell subsets. Statistical analysis was performed by a two-tailed paired Student's t-test. Data are shown as the mean ± SD *p <0.05

associated with apoptosis such as BAX (p = 0.01) and RPS6 (p = 0.05), cell exhaustion genes such as LAG3 (p = 0.02) and ZAP70 (p = 0.02), and cellular senescence associated such as KLRG1 (p = 0.05) and CDKN1A (p = 0.04). Only one gene was upregulated by butyrate, glucose-6-phosphate isomerase (GPI) which encodes a protein involved in glycolysis and also acts extracellularly as an autocrine motility factor (p = 0.03).

3.9 Anti-senescent properties of butyrate *in vivo*

With age, senescent cells display a loss of the nuclear structural protein lamin B1 leading to destabilisation of the nuclear integrity (193, 194). Downregulation of lamin B1 leads to further nuclear changes such as the emergence of cytoplasmic chromatin fragments (CCFs) that are secreted extracellularly with the ability to stimulate DDR in other cells (195). We conducted immunohistochemical staining for lamin B1 on murine spleen sections in order to elucidate the effect of butyrate on cellular senescence, using lamin B1 expression as a biomarker of senescent cells (196). Compared to young control mice, the aged control mice displayed a distinct decrease in cells expressing lamin B1, the loss of which was recovered in the aged mice supplemented with the faecal filtrate of young mice (Figure 16A). Quantification of lamin B1 mean fluorescence intensity (MFI) confirmed these findings, with the lamin B1 MFI value significantly reduced in aged controls compared with the young counterparts (p = 0.025). In aged mice supplemented with faecal filtrate, expression of lamin B1 was restored to levels seen in the young controls, indicated by the significant increase in MFI in the aged + faecal filtrate group compared with aged controls (p = <0.001) (Figure 16B).

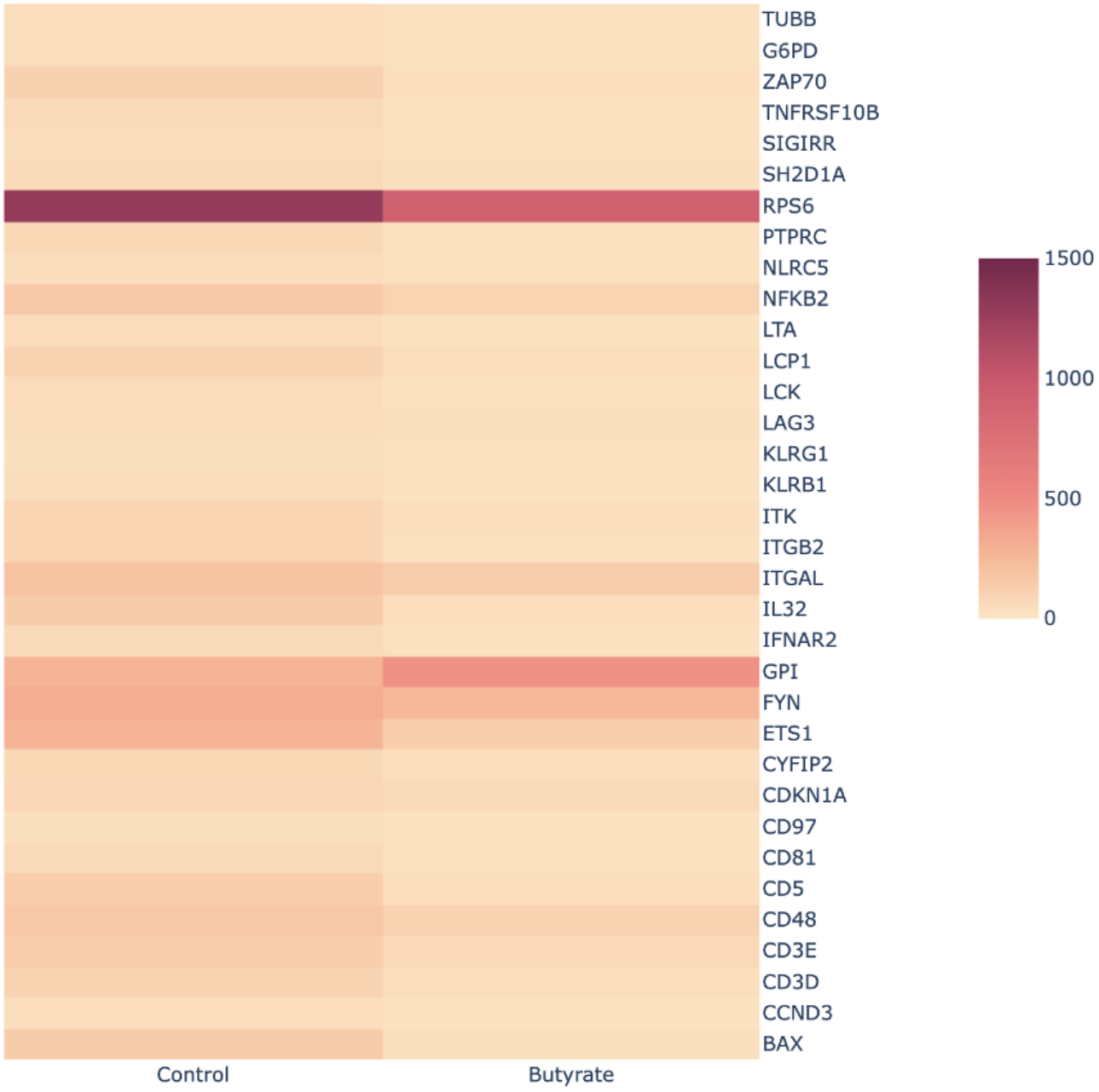

Figure 27. Changes in gene expression in aged T cells cultured with butyrate.
Heatmap of the 34 differentially expressed genes from *in vitro* culture of aged T cells in CD3-coated wells for 3 days in the presence/absence of SCFA butyrate.

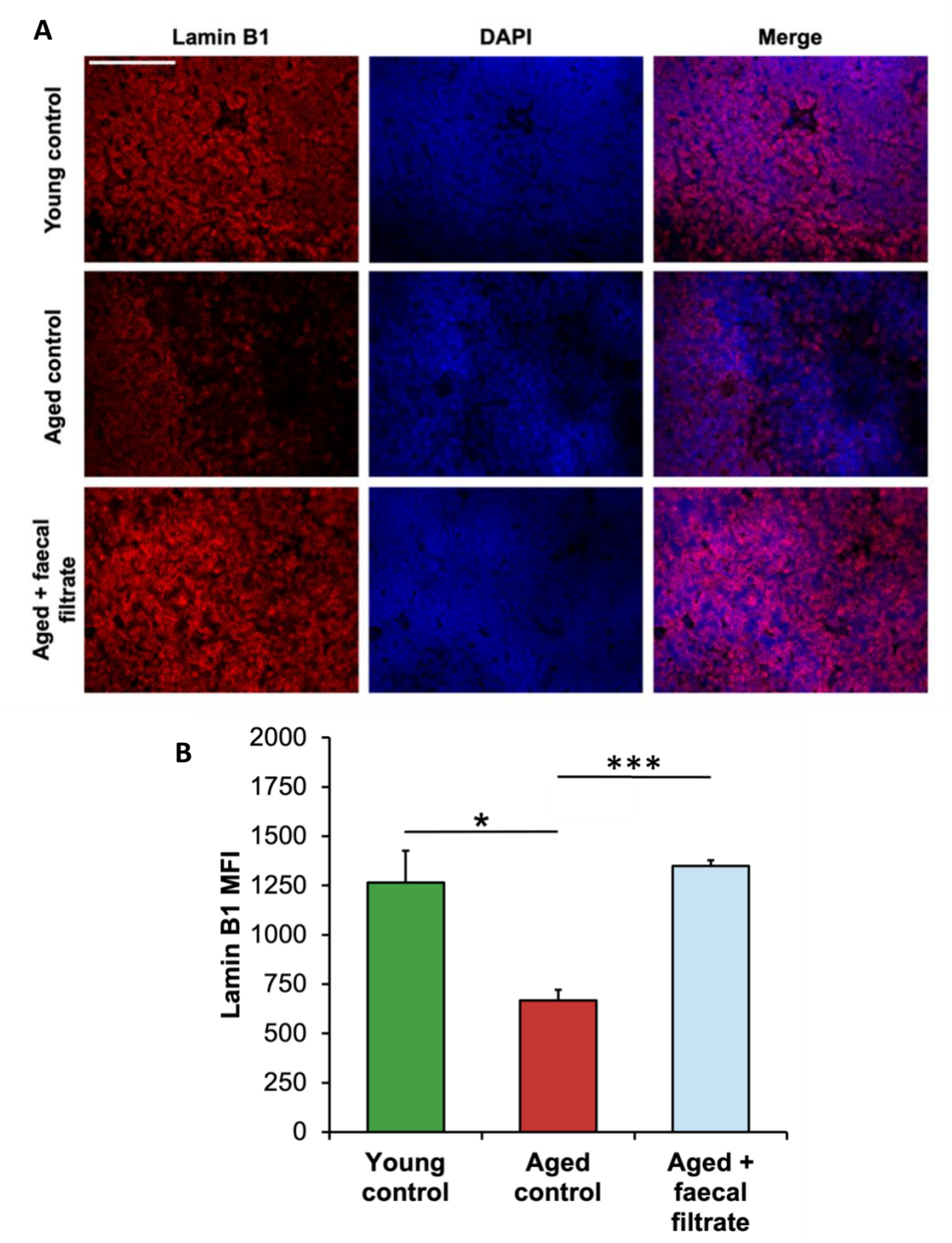

Figure 29. Immunostaining of murine spleen tissue for DAPI and Lamin B1.
(A) Representative fluorescence microscope images (40X) of splenic sections from young and aged control mice, and aged mice that received supplementation with faecal filtrate from young mice, which were stained for lamin B1 (red) and DAPI (blue) markers (young = 6 months, aged = 24 months). Scale bar = 10 μm. **(B)** Lamin B1 mean fluorescence intensity (MFI) values were quantified from 40x images and groups were compared using a two-tailed paired Student's t-test. Data are shown as the mean ± SD *p <0.05, ***p <0.001

4.0 Discussion

Older adults possess a diminished ability to combat antigenic challenges due to defective immune responses, known as immunesenescence (197). Recent studies have highlighted the capacity for immunomodulation by the SCFA butyrate via direct interaction with GPR41, GPR43 and GPR109A receptors on the surface of both innate and adaptive immune cells (198, 199). Differentiation in the presence of butyrate produces macrophages with preserved enhanced antimicrobial functioning *in vitro* in comparison to control macrophages (190). The authors also observed these effects *in vivo*, with oral butyrate supplementation boosting the bacterial killing ability of murine colonic macrophages. Butyrate-stimulated DCs significantly encourage the induction of IL-10-producing T_{regs} (Tr1) with potent immunosuppressive capacity (168, 200). Studies also demonstrate direct interactions between butyrate and T cells, as enhanced cytotoxic capability of $CD8^+$ T cells alongside the increased establishment of $CD8^+$ T cell memory in the presence of butyrate (166, 201). Given the established ability of butyrate to modulate T cell phenotype and functioning, the aim of this thesis was to investigate immunomodulation by butyrate in the context of T cell senescence, examining the potential anti-senescence features of butyrate via its regulation of DNA damage, SASP, gene expression and mitochondrial activity in aged T cells.

4.1 Senomorphic and anti-senescence properties of butyrate

Having identified cellular senescence as a key driver of the ageing process, it has become a major target for deferring organismal ageing and the onset of ARDs (202). Approaches so far have primarily focused on molecules capable of inducing senescent cell death (senolytics), or those which prevent the development of the senescent phenotype (senostatics). We examined the ability of butyrate, as a senomorphic compound, in altering the phenotype of senescent T cells to more closely resemble those of healthy young cells. Our results demonstrated that stimulation with butyrate significantly decreased expression of the DNA damage marker γH2AX in aged T cells, similar to results observed in senescent primary human

umbilical vein endothelial cells (HUVECs) and senescent human aortic smooth muscle cells (hASMCs) treated with the butyrate analogue β-hydroxybutyrate (β-HB) (203). Additionally, we showed that in aged T cells, butyrate treatment led to reductions in phosphorylated p53 expression. Therefore, not only is butyrate capable of mitigating DNA damage, but also possesses anti-senescent features by altering downstream signalling responses responsible for cell cycle arrest. This contrasts with the study by Han *et al.* in which β-HB had no effect on the phosphorylation of p53 in HUVECs or hASMCs however, differences in cell models could potentially contribute to this discrepancy (203).

As previously mentioned, with age, one of the most notable phenotypic changes observed in senescent cells is the emergence of SASP, promoting a pro-inflammatory microenvironment capable of damaging neighbouring cells and organs (62, 64). We assessed whether incubation with butyrate would have an anti-inflammatory effect on aged T cells by measuring secretion of various inflammatory mediators. In agreement with earlier studies on lymphocytes (204) and other immune cells (205, 206), our results demonstrate a significant decrease in the levels of pro-inflammatory cytokines, such as IL-6 and IL-1β, present in the supernatants of butyrate-stimulated T cells. Similarly, Goldberg *et al.* noted that production of IL-1β by neutrophils from elderly humans was inhibited by β-HB via prevention of NLRP3 inflammasome priming and assembly (207). Butyrate also downregulated the NLRP3 inflammasome in macrophages where the gene expression of both IL-1β and IL-6 was significantly reduced, indicating one potential method through which butyrate exerts senomorphic activity by attenuating the SASP phenotype (208).

Key regulators of the SASP, transcription factors NF-κB and p38 MAPK, are activated in response to stress and damage signals in senescent T cells (209, 210). Coinciding with other literature, we noted that butyrate downregulated the protein expression of NF-κB in T cells isolated from elderly humans (208, 211, 212). The mammalian NF-κB family contains 5 subunits that regulate pro-inflammatory cytokine production via binding as either homodimers or heterodimers to promoter regions of cytokine genes in the nucleus (213). The most common dimer formed is the p50/p65 heterodimer, and studies suggest that regulation of NFκB activity by butyrate occurs through its modulation of the heterodimer p50/p65

subunits. Both Usami *et al.* and Jiang *et al.* observed reductions in p65 phosphorylation, and thus its activation, in butyrate-treated PBMCs and macrophages respectively (208, 212). Similarly, Aguilar *et al.* found that p65 concentration was lower in human endothelial cells following incubation with butyrate (211). In addition to this, the authors assessed p50/p65 translocation to the nucleus from the cytoplasm and detected a reduction in nuclear p65 and increase in cytoplasmic p50 in endothelial cells stimulated with butyrate. Higher levels of p50 in the cytoplasm is thought to facilitate formation of the p50/p50 homodimer, the activity of which is inhibitory of NF-κB activation. Our gene expression analysis results revealed that butyrate significantly downregulated the expression of NFKB2, the gene responsible for encoding the NF-κB p52 subunit, demonstrating that butyrate is capable of regulating NF-κB on both the gene and protein level. Post incubation with butyrate, our results show that expression levels of p38 MAPK were unchanged in aged T cells. Currently there are no studies reporting p38 MAPK inhibition by butyrate in immune cells or any other cell type, implying that downregulation of p38 MAPK signalling is not an underlying mechanism of the anti-inflammatory effects of butyrate.

Gene expression analysis from old T cells cultured in the presence of butyrate revealed a downregulation in cyclin dependent kinase inhibitor 1a (CDKN1A ($p21^{Cip1/Waf1}$)), a controller of cell cycle progression at the G1 phase that is shown to be induced in cellular senescence (214). In aged T cells, butyrate stimulation also led to a reduction in gene expression of p53, which closely regulates CDKN1A expression, thus providing further justification for the inhibition of senescent markers by butyrate. Despite this, our results also showed that butyrate caused a downregulation of the CCND3 gene, encoding for cyclin-D3 which functions as a driver of cell cycle progression (215). This finding suggests that whilst butyrate is senomorphic, it does not necessarily promote the proliferation of T cells. In support of butyrate functioning as a senomorphic rather than a senolytic, the pro-apoptotic regulator BAX was also downregulated in aged T cells treated with butyrate indicating that it does not promote the apoptosis of senescent cells. Interestingly, the only gene we found to be upregulated by butyrate was GPI, which encodes the enzyme glucose-6-phosphate isomerase responsible for catalysing the conversion of glucose-6-phosphate to fructose-6-phsophate in the second step of glycolysis (216). GPI downregulation has been linked to the induction of cellular senescence in fibrosarcoma cells via activation of p21, implying that upregulation of

this gene may be another mechanism through which butyrate exerts anti-senescent effects, however direct connections cannot be made without further investigation.

Altogether, these findings suggest that butyrate possesses anti-inflammatory, senomorphic properties and is capable of exerting anti-senescent effects through attenuation of DNA damage and cell cycle arrest, alongside inhibiting activation of SASP regulators thus mitigating pro-inflammatory cytokine secretion.

4.2 Impact of butyrate on mitochondrial mass and ROS generation in aged T cells

With age, mitochondrial function gradually declines as a result of mitochondrial DNA (mtDNA) damage, impaired mitophagy processes leading to inefficient organelle turnover and overall alterations in mitochondrial dynamics (197). Both $CD4^+$ and $CD8^+$ EMRA T cells produce more mitochondrial ROS compared to the other less differentiated subsets. This is in part due to EMRA T cells exhibiting various senescence attributes however, impairing mitochondrial function accelerates senescence, as observed by increased p53 levels and decreased population doublings in $CD4^+$ EMRA T cells following mitochondrial damage (183). We sought to elucidate the effects of butyrate on the accumulation of dysfunctional mitochondria in aged human T cells. Our results show that stimulation with butyrate could potentially promote the clearance of damaged mitochondria due to a reduction in the mitochondrial mass of old EMRA CD4 T cells. Despite these observations, we did not detect any significant changes in the level of autophagy occurring in young T cells treated with butyrate compared with control, suggesting that butyrate does not decrease mitochondrial mass via promotion of autophagic processes. Instead, butyrate may exert its effects though the influence of mitochondrial dynamics, comprising of fission and fusion machineries (217). Tailor *et al.* reported a decline in the mitochondrial mass of colorectal cancer cells post incubation with butyrate in addition to a reduction in the protein level of dynamin-related protein 1 (DRP1) gene, a key regulator of mitochondrial fission (218). The authors proposed a mechanism through which butyrate inhibits the formation of the cyclin B1-CDK1 complex, responsible for

the activation of DRP1, and thus supresses DRP1 phosphorylation leading to mitochondrial fusion.

4.3 In-vivo characterisation of anti-senescent properties of microbiome metabolites

We have demonstrated that butyrate is capable of modulating the senescent phenotype of aged T cells *in vitro* therefore, given these findings, we next sought to identify whether these anti-senescent effects occurred *in vivo*. With age, lamin B1 expression is reduced upon induction of cellular senescence and triggers SASP via CCF formation (219, 220). We examined the splenic lamin B1 expression in young control, old control, and old mice that received the faecal filtrate from young mice, and found that mice given faecal filtrate, containing microbe-derived metabolites, possessed greater levels of lamin B1 compared with old control counterparts. Han *et al.* reported similar *in vivo* effects in response to upregulation of circulating β-HB levels in mice induced by fasting, in which thoracic aorta tissue protein levels of lamin B1 were significantly increased (203). The authors suggest that β-HB promotes cellular quiescence by upregulation of lamin B1, thus preventing senescence induced by oxidative stress. Our results demonstrate the efficacy of supplementation with microbial metabolites in reducing markers of senescence *in vivo*, providing interesting insight into the potential of therapeutically utilising metabolites, in particular the SCFA butyrate, to delay the onset of senescence and the senescence phenotype in the ageing population.

4.4. Study limitations

In accordance with other literature, and following preliminary experiments ascertaining the dose effects of butyrate concentrations (see Figure 8A), a treatment of 1mM butyrate was decided upon and used in all subsequent immune assays (190, 221, 222). Although present in high concentrations within the colon (10 – 20mM), systemic butyrate levels are significantly lower (1 – 15 μM) therefore, it must be considered that the 1mM concentration of butyrate used far exceeds the physiological levels that PBMCs would be exposed to (223). Additionally, cell viability was not measured in combination with the evaluation of IL-6, IL-8 and IL-1β

supernatant levels following butyrate treatment. Consequently, the lack of normalisation of cytokine and chemokine levels to cell densities means the observed decrease in levels of these signalling molecules cannot reliably be attributed to the effects of butyrate, rather than cell death. The absence of energy-matched controls in the experiments means we cannot say with certainty that these senomorphic and anti-senescent affects are not owing to the presence of other energy sources being utilised by the cells.

4.5 Future direction and impact on the life of older adults

Correlations between stool butyrate levels and accretion of senescent T cells in older adults provided the basis for this study in which we demonstrated the anti-senescent effects of microbial metabolites (butyrate) on aged humans and rodents both *in vitro* and *in vivo* respectively. The proposed next step in continuing this work is to carry out a microbiome-based intervention trial in elderly adults receiving sodium butyrate supplements and analysing the differences in immunesenescence parameters between baseline and post-intervention (Figure 8). Up until recently, human intervention studies based around SCFAs were met with difficulty largely due to the issue of selectively controlling the production of SCFAs in the human gut. Development of a novel method for delivering SCFAs directly to the colon by utilising the polymer inulin as a metabolite transporter molecule has opened up the possibility of targeted SCFA delivery in humans (224, 225). Supplementation with synthesised inulin-propionate ester was shown to significantly decreased pro-inflammatory cytokine (IL-8) levels in overweight adults along with a trend of increasing the proportion of T_{regs} within the peripheral $CD4^+$ T cell pool (226). Given the ability of butyrate to modulate T cell immunesenescence, applying these inulin esters to administer butyrate to the colon of healthy old adults would be an ideal method to observe its senomorphic effects in humans.

Currently, healthspan and lifespan are not aligned due to the prevalence of age-associated diseases that occur as a result of immunesenescence. Inflammageing is a consistent underlying factor of these pathologies, implicated in not only their development, but also exacerbation of the diseased state. Butyrate supplementation presents a conceivable postbiotic therapy capable of improving immune function in the context of ageing via

downregulation of senescence markers (227). A recent study demonstrated the beneficial use of sodium butyrate as an add-on therapy for maintenance of remission in ulcerative colitis patients, a disease characterised by inflammation and microbiome dysbiosis in the colon, highlighting the clinical relevancy of butyrate treatment in inflammatory conditions (228). In addition to the possibility of delaying the onset of ARDs via butyrate supplement as a means of improving healthspan, correlations between dysbiosis and impaired vaccine responses in the elderly have sparked interest in prebiotic and probiotic treatment prior to vaccination. Thus far, there is conflicting evidence for whether prebiotics and probiotics provide beneficial effects on vaccine responses in the elderly (229, 230, 231, 232). Despite this, there are no existing intervention studies which examine the effects of postbiotics on vaccine efficacy in the older population therefore, given the findings of this study and the advancements in SCFA delivery, this may provide another avenue to decrease the healthspan-lifespan gap.

4.5 Conclusions

In summary, this study has shown that the metabolite sodium butyrate possesses anti-senescent and senomorphic properties and is capable of downregulating various senescence markers such as those involved in DNA damage and cell cycle arrest, inflammation, mitochondrial ROS production and nuclear stability. Taken together, we propose that the SCFA butyrate be utilised to dampen the emergence of the senescence phenotype in ageing immune cells which in turn, could provide a novel strategy for combating unhealthy ageing and increasing healthspan.

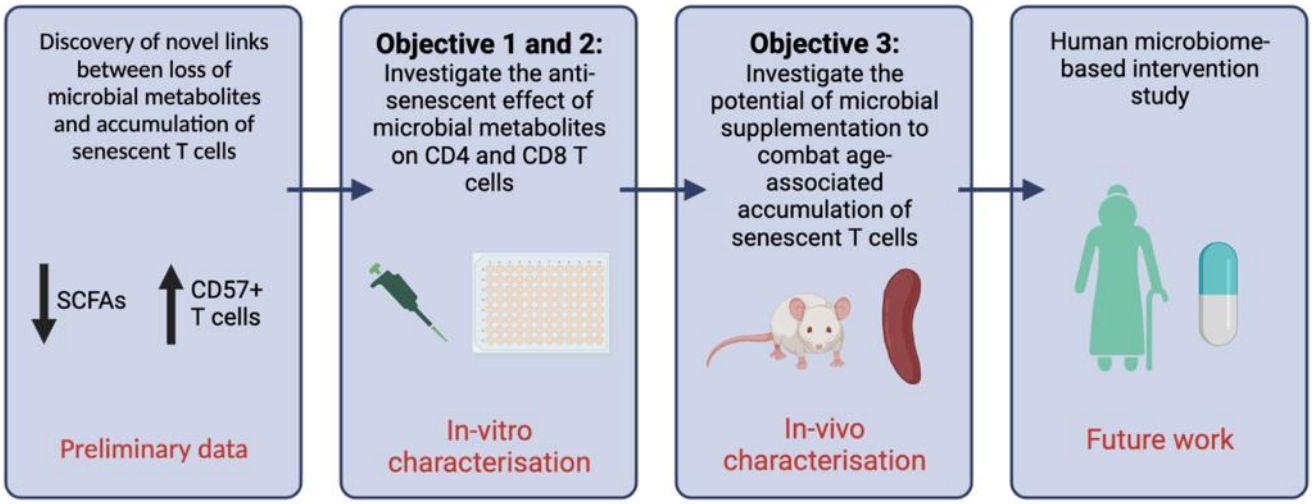

Figure 32. Study objectives and future directions.

References

1. Garmany A, Yamada S, Terzic A. Longevity leap: mind the healthspan gap. NPJ Regen Med. 2021;6(1):57.
2. Ragonnaud E, Biragyn A. Gut microbiota as the key controllers of "healthy" aging of elderly people. Immun Ageing. 2021;18(1):2.
3. United Nations DoEaSA, Population Division. World Population Prospects Highlights. 2019.
4. Maresova P, Javanmardi E, Barakovic S, Barakovic Husic J, Tomsone S, Krejcar O, et al. Consequences of chronic diseases and other limitations associated with old age - a scoping review. BMC Public Health. 2019;19(1):1431.
5. Bennett JE, Stevens GA, Mathers CD, Bonita R, Rehm J, Kruk ME, et al. NCD Countdown 2030: worldwide trends in non-communicable disease mortality and progress towards Sustainable Development Goal target 3.4. The Lancet. 2018;392(10152):1072-88.
6. MacNee W, Rabinovich RA, Choudhury G. Ageing and the border between health and disease. Eur Respir J. 2014;44(5):1332-52.
7. Dato S, Rose G, Crocco P, Monti D, Garagnani P, Franceschi C, et al. The genetics of human longevity: an intricacy of genes, environment, culture and microbiome. Mech Ageing Dev. 2017;165(Pt B):147-55.
8. Dong X, Milholland B, Vijg J. Evidence for a limit to human lifespan. Nature. 2016;538(7624):257-9.
9. Olshansky SJ. Measuring our narrow strip of life. Nature. 2016.
10. Queen NJ, Hassan QN, 2nd, Cao L. Improvements to Healthspan Through Environmental Enrichment and Lifestyle Interventions: Where Are We Now? Front Neurosci. 2020;14:605.
11. Committee HoLSaTS. HoF Ageing Report - Ageing; Science, Technology and Healthy Living. 2021.
12. Aiello A, Farzaneh F, Candore G, Caruso C, Davinelli S, Gambino CM, et al. Immunosenescence and Its Hallmarks: How to Oppose Aging Strategically? A Review of Potential Options for Therapeutic Intervention. Front Immunol. 2019;10:2247.
13. Zheng Y, Liu X, Le W, Xie L, Li H, Wen W, et al. A human circulating immune cell landscape in aging and COVID-19. Protein Cell. 2020;11(10):740-70.
14. Crooke SN, Ovsyannikova IG, Poland GA, Kennedy RB. Immunosenescence and human vaccine immune responses. Immun Ageing. 2019;16:25.
15. Goronzy JJ, Weyand CM. Immune aging and autoimmunity. Cell Mol Life Sci. 2012;69(10):1615-23.
16. Lian J, Yue Y, Yu W, Zhang Y. Immunosenescence: a key player in cancer development. J Hematol Oncol. 2020;13(1):151.
17. Yousefzadeh MJ, Flores RR, Zhu Y, Schmiechen ZC, Brooks RW, Trussoni CE, et al. An aged immune system drives senescence and ageing of solid organs. Nature. 2021;594(7861):100-5.
18. Brubaker AL, Rendon JL, Ramirez L, Choudhry MA, Kovacs EJ. Reduced neutrophil chemotaxis and infiltration contributes to delayed resolution of cutaneous wound infection with advanced age. J Immunol. 2013;190(4):1746-57.
19. Shaw AC, Goldstein DR, Montgomery RR. Age-dependent dysregulation of innate immunity. Nat Rev Immunol. 2013;13(12):875-87.
20. Simell B, Vuorela A, Ekstrom N, Palmu A, Reunanen A, Meri S, et al. Aging reduces the functionality of anti-pneumococcal antibodies and the killing of Streptococcus pneumoniae by neutrophil phagocytosis. Vaccine. 2011;29(10):1929-34.
21. Nauseef WM, Borregaard N. Neutrophils at work. Nat Immunol. 2014;15(7):602-11.
22. Simmons SR, Tchalla EYI, Bhalla M, Bou Ghanem EN. The Age-Driven Decline in Neutrophil Function Contributes to the Reduced Efficacy of the Pneumococcal Conjugate Vaccine in Old Hosts. Front Cell Infect Microbiol. 2022;12:849224.

23. Duong L, Radley HG, Lee B, Dye DE, Pixley FJ, Grounds MD, et al. Macrophage function in the elderly and impact on injury repair and cancer. Immun Ageing. 2021;18(1):4.
24. Hearps AC, Martin GE, Angelovich TA, Cheng WJ, Maisa A, Landay AL, et al. Aging is associated with chronic innate immune activation and dysregulation of monocyte phenotype and function. Aging Cell. 2012;11(5):867-75.
25. De Maeyer RPH, Chambers ES. The impact of ageing on monocytes and macrophages. Immunol Lett. 2021;230:1-10.
26. Wong CK, Smith CA, Sakamoto K, Kaminski N, Koff JL, Goldstein DR. Aging Impairs Alveolar Macrophage Phagocytosis and Increases Influenza-Induced Mortality in Mice. J Immunol. 2017;199(3):1060-8.
27. De Maeyer RPH, van de Merwe RC, Louie R, Bracken OV, Devine OP, Goldstein DR, et al. Blocking elevated p38 MAPK restores efferocytosis and inflammatory resolution in the elderly. Nat Immunol. 2020;21(6):615-25.
28. Metcalf TU, Wilkinson PA, Cameron MJ, Ghneim K, Chiang C, Wertheimer AM, et al. Human Monocyte Subsets Are Transcriptionally and Functionally Altered in Aging in Response to Pattern Recognition Receptor Agonists. J Immunol. 2017;199(4):1405-17.
29. Hazeldine J, Lord JM. The impact of ageing on natural killer cell function and potential consequences for health in older adults. Ageing Res Rev. 2013;12(4):1069-78.
30. Gounder SS, Abdullah BJJ, Radzuanb N, Zain F, Sait NBM, Chua C, et al. Effect of Aging on NK Cell Population and Their Proliferation at Ex Vivo Culture Condition. Anal Cell Pathol (Amst). 2018;2018:7871814.
31. Przemska-Kosicka A, Childs CE, Maidens C, Dong H, Todd S, Gosney MA, et al. Age-Related Changes in the Natural Killer Cell Response to Seasonal Influenza Vaccination Are Not Influenced by a Synbiotic: a Randomised Controlled Trial. Front Immunol. 2018;9:591.
32. Hazeldine J, Hampson P, Lord JM. Reduced release and binding of perforin at the immunological synapse underlies the age-related decline in natural killer cell cytotoxicity. Aging Cell. 2012;11(5):751-9.
33. Rukavina DL, G.; Rubesa,G.; Strbo,N.; Bedenicki,I.; Manestar,D.; Glavas,M.; Christmas,S.E.; Podack,E.R. Age-Related Decline of Perforin Expression in Human Cytotoxic T Lymphocytes and Natural Killer Cells. Blood. 1998.
34. Krishnaraj RB, T. Cytokine sensitivity of human NK cells during immunosenescence, 2. IL2-induced interferon gamma secretion. Immunology Letters. 1996.
35. Judge SJ, Murphy WJ, Canter RJ. Characterizing the Dysfunctional NK Cell: Assessing the Clinical Relevance of Exhaustion, Anergy, and Senescence. Front Cell Infect Microbiol. 2020;10:49.
36. Bulut O, Kilic G, Dominguez-Andres J, Netea MG. Overcoming immune dysfunction in the elderly: trained immunity as a novel approach. Int Immunol. 2020;32(12):741-53.
37. Della Bella S, Bierti L, Presicce P, Arienti R, Valenti M, Saresella M, et al. Peripheral blood dendritic cells and monocytes are differently regulated in the elderly. Clin Immunol. 2007;122(2):220-8.
38. Clements SJ, Maijo M, Ivory K, Nicoletti C, Carding SR. Age-Associated Decline in Dendritic Cell Function and the Impact of Mediterranean Diet Intervention in Elderly Subjects. Front Nutr. 2017;4:65.
39. Sridharan A, Esposo M, Kaushal K, Tay J, Osann K, Agrawal S, et al. Age-associated impaired plasmacytoid dendritic cell functions lead to decreased CD4 and CD8 T cell immunity. Age (Dordr). 2011;33(3):363-76.
40. Wong C, Goldstein DR. Impact of aging on antigen presentation cell function of dendritic cells. Curr Opin Immunol. 2013;25(4):535-41.
41. Agrawal A, Agrawal S, Cao JN, Su H, Osann K, Gupta S. Altered innate immune functioning of dendritic cells in elderly humans: a role of phosphoinositide 3-kinase-signaling pathway. J Immunol. 2007;178(11):6912-22.

42. Rahmatpanah F, Agrawal S, Scarfone VM, Kapadia S, Mercola D, Agrawal A. Transcriptional Profiling of Age-Associated Gene Expression Changes in Human Circulatory CD1c+ Myeloid Dendritic Cell Subset. J Gerontol A Biol Sci Med Sci. 2019;74(1):9-15.
43. Palmer DB. The effect of age on thymic function. Front Immunol. 2013;4:316.
44. Elyahu Y, Monsonego A. Thymus involution sets the clock of the aging T-cell landscape: Implications for declined immunity and tissue repair. Ageing Res Rev. 2021;65:101231.
45. Baran-Gale J, Morgan MD, Maio S, Dhalla F, Calvo-Asensio I, Deadman ME, et al. Ageing compromises mouse thymus function and remodels epithelial cell differentiation. Elife. 2020;9.
46. Lamas A, Lopez E, Carrio R, Lopez DM. Adipocyte and leptin accumulation in tumor-induced thymic involution. Int J Mol Med. 2016;37(1):133-8.
47. Gray DH, Seach N, Ueno T, Milton MK, Liston A, Lew AM, et al. Developmental kinetics, turnover, and stimulatory capacity of thymic epithelial cells. Blood. 2006;108(12):3777-85.
48. Cowan JE, Takahama Y, Bhandoola A, Ohigashi I. Postnatal Involution and Counter-Involution of the Thymus. Front Immunol. 2020;11:897.
49. Tong QY, Zhang JC, Guo JL, Li Y, Yao LY, Wang X, et al. Human Thymic Involution and Aging in Humanized Mice. Front Immunol. 2020;11:1399.
50. Aw D, Silva AB, Maddick M, von Zglinicki T, Palmer DB. Architectural changes in the thymus of aging mice. Aging Cell. 2008;7(2):158-67.
51. Andrew DA, R. Age-associated thymic atrophy is linked to a decline in IL-7 production. Experimental Gerontology. 2002.
52. Zhang H, Weyand CM, Goronzy JJ. Hallmarks of the aging T-cell system. FEBS J. 2021;288(24):7123-42.
53. Goronzy JJ, Fang F, Cavanagh MM, Qi Q, Weyand CM. Naive T cell maintenance and function in human aging. J Immunol. 2015;194(9):4073-80.
54. Larbi A, Fulop T. From "truly naive" to "exhausted senescent" T cells: when markers predict functionality. Cytometry A. 2014;85(1):25-35.
55. Czesnikiewicz-Guzik ML, W.; Cui, D.; Hiruma, Y.; Lamar, D. L.; Yang, Z.; Ouslander, J. G.; Weyand, C. M.; Goronzy, J. J. T cell subset-specific susceptibility to aging. Clin Immunol. 2008.
56. Herndler-Brandstetter D, Landgraf K, Tzankov A, Jenewein B, Brunauer R, Laschober GT, et al. The impact of aging on memory T cell phenotype and function in the human bone marrow. J Leukoc Biol. 2012;91(2):197-205.
57. Chou JPE, R. B. T cell replicative senescence in human ageing. Curr Pharm Des. 2013.
58. Kobashigawa S, M. Sakaguchi Y, Masunaga S, Mori E. Stress-induced Cellular Senescence Contributes to Chronic Inflammation and Cancer Progression. Thermal Medicine. 2019;35(4):41-58.
59. Zhu X, Chen Z, Shen W, Huang G, Sedivy JM, Wang H, et al. Inflammation, epigenetics, and metabolism converge to cell senescence and ageing: the regulation and intervention. Signal Transduct Target Ther. 2021;6(1):245.
60. Hernandez-Segura A, Nehme J, Demaria M. Hallmarks of Cellular Senescence. Trends Cell Biol. 2018;28(6):436-53.
61. C. Franceschi MB, S. Valensin, F. Olivieri, M. De Luca, E. Ottaviani, and G. De Benedictis. Inflamm-aging: An Evolutionary Perspective on Immunosenescence. 2000.
62. Callender LA, Carroll EC, Beal RWJ, Chambers ES, Nourshargh S, Akbar AN, et al. Human CD8(+) EMRA T cells display a senescence-associated secretory phenotype regulated by p38 MAPK. Aging Cell. 2018;17(1).
63. Freund A, Patil CK, Campisi J. p38MAPK is a novel DNA damage response-independent regulator of the senescence-associated secretory phenotype. EMBO J. 2011;30(8):1536-48.
64. Chien Y, Scuoppo C, Wang X, Fang X, Balgley B, Bolden JE, et al. Control of the senescence-associated secretory phenotype by NF-kappaB promotes senescence and enhances chemosensitivity. Genes Dev. 2011;25(20):2125-36.

65. Bent EH, Gilbert LA, Hemann MT. A senescence secretory switch mediated by PI3K/AKT/mTOR activation controls chemoprotective endothelial secretory responses. Genes Dev. 2016;30(16):1811-21.
66. Añón-Hidalgo JC, V.; Rodríguez, A.; Ramírez, B.; Silva, C.; Galofré, J.C.; Salvador, J.; Frühbeck, G.; Gómez-Ambrosi, J. Circulating GDF11 levels are decreased with age but are unchanged with obesity and type 2 diabetes. Impact Journals: Aging. 2019.
67. Golubovskaya V, Wu L. Different Subsets of T Cells, Memory, Effector Functions, and CAR-T Immunotherapy. Cancers (Basel). 2016;8(3).
68. Zhang N, Bevan MJ. CD8(+) T cells: foot soldiers of the immune system. Immunity. 2011;35(2):161-8.
69. Szeto C, Zareie P, Wirasinha RC, Zhang JB, Nguyen AT, Riboldi-Tunnicliffe A, et al. Covalent TCR-peptide-MHC interactions induce T cell activation and redirect T cell fate in the thymus. Nat Commun. 2022;13(1):4951.
70. Garcia GG, Miller RA. Age-dependent defects in TCR-triggered cytoskeletal rearrangement in CD4+ T cells. J Immunol. 2002;169(9):5021-7.
71. Kim C, Ye Z, Weyand CM, Goronzy JJ. miR-181a-regulated pathways in T-cell differentiation and aging. Immun Ageing. 2021;18(1):28.
72. Li G, Yu M, Lee WW, Tsang M, Krishnan E, Weyand CM, et al. Decline in miR-181a expression with age impairs T cell receptor sensitivity by increasing DUSP6 activity. Nat Med. 2012;18(10):1518-24.
73. Kim C, Jadhav RR, Gustafson CE, Smithey MJ, Hirsch AJ, Uhrlaub JL, et al. Defects in Antiviral T Cell Responses Inflicted by Aging-Associated miR-181a Deficiency. Cell Rep. 2019;29(8):2202-16 e5.
74. Pieren DKJ, Smits NAM, van de Garde MDB, Guichelaar T. Response kinetics reveal novel features of ageing in murine T cells. Sci Rep. 2019;9(1):5587.
75. Haynes L, Eaton SM, Burns EM, Randall TD, Swain SL. CD4 T cell memory derived from young naive cells functions well into old age, but memory generated from aged naive cells functions poorly. Proc Natl Acad Sci U S A. 2003;100(25):15053-8.
76. Lee JS, Lee WW, Kim SH, Kang Y, Lee N, Shin MS, et al. Age-associated alteration in naive and memory Th17 cell response in humans. Clin Immunol. 2011;140(1):84-91.
77. Lim MA, Lee J, Park JS, Jhun JY, Moon YM, Cho ML, et al. Increased Th17 differentiation in aged mice is significantly associated with high IL-1beta level and low IL-2 expression. Exp Gerontol. 2014;49:55-62.
78. Rocamora-Reverte L, Melzer FL, Wurzner R, Weinberger B. The Complex Role of Regulatory T Cells in Immunity and Aging. Front Immunol. 2020;11:616949.
79. Lages CSS, I.; Velilla, P. A.; Huang, B.; Warshaw, G.; Hildeman, D. A.; Belkaid, Y.; Chougnet, C. Functional Regulatory T Cells Accumulate in Aged Hosts and Promote Chronic Infectious Disease Reactivation. J Immunol. 2008.
80. Guo Z, Wang G, Wu B, Chou WC, Cheng L, Zhou C, et al. DCAF1 regulates Treg senescence via the ROS axis during immunological aging. J Clin Invest. 2020;130(11):5893-908.
81. Chinen T, Kannan AK, Levine AG, Fan X, Klein U, Zheng Y, et al. An essential role for the IL-2 receptor in Treg cell function. Nat Immunol. 2016;17(11):1322-33.
82. Pandiyan P, Conti HR, Zheng L, Peterson AC, Mathern DR, Hernandez-Santos N, et al. CD4(+)CD25(+)Foxp3(+) regulatory T cells promote Th17 cells in vitro and enhance host resistance in mouse Candida albicans Th17 cell infection model. Immunity. 2011;34(3):422-34.
83. Liu X, Mo W, Ye J, Li L, Zhang Y, Hsueh EC, et al. Regulatory T cells trigger effector T cell DNA damage and senescence caused by metabolic competition. Nat Commun. 2018;9(1):249.
84. Adler LN, Jiang W, Bhamidipati K, Millican M, Macaubas C, Hung SC, et al. The Other Function: Class II-Restricted Antigen Presentation by B Cells. Front Immunol. 2017;8:319.
85. Shen P, Fillatreau S. Antibody-independent functions of B cells: a focus on cytokines. Nat Rev Immunol. 2015;15(7):441-51.

86. Miller JP, Allman D. The decline in B lymphopoiesis in aged mice reflects loss of very early B-lineage precursors. J Immunol. 2003;171(5):2326-30.
87. Pang WW, Price EA, Sahoo D, Beerman I, Maloney WJ, Rossi DJ, et al. Human bone marrow hematopoietic stem cells are increased in frequency and myeloid-biased with age. Proc Natl Acad Sci U S A. 2011;108(50):20012-7.
88. Lee JL, Linterman MA. Mechanisms underpinning poor antibody responses to vaccines in ageing. Immunol Lett. 2022;241:1-14.
89. Hao Y, O'Neill P, Naradikian MS, Scholz JL, Cancro MP. A B-cell subset uniquely responsive to innate stimuli accumulates in aged mice. Blood. 2011;118(5):1294-304.
90. Rubtsov AV, Rubtsova K, Fischer A, Meehan RT, Gillis JZ, Kappler JW, et al. Toll-like receptor 7 (TLR7)-driven accumulation of a novel CD11c(+) B-cell population is important for the development of autoimmunity. Blood. 2011;118(5):1305-15.
91. Eccles JD, Turner RB, Kirk NA, Muehling LM, Borish L, Steinke JW, et al. T-bet+ Memory B Cells Link to Local Cross-Reactive IgG upon Human Rhinovirus Infection. Cell Rep. 2020;30(2):351-66 e7.
92. Johnson JL, Rosenthal RL, Knox JJ, Myles A, Naradikian MS, Madej J, et al. The Transcription Factor T-bet Resolves Memory B Cell Subsets with Distinct Tissue Distributions and Antibody Specificities in Mice and Humans. Immunity. 2020;52(5):842-55 e6.
93. Ratliff M, Alter S, Frasca D, Blomberg BB, Riley RL. In senescence, age-associated B cells secrete TNFalpha and inhibit survival of B-cell precursors. Aging Cell. 2013;12(2):303-11.
94. Naradikian MS, Myles A, Beiting DP, Roberts KJ, Dawson L, Herati RS, et al. Cutting Edge: IL-4, IL-21, and IFN-gamma Interact To Govern T-bet and CD11c Expression in TLR-Activated B Cells. J Immunol. 2016;197(4):1023-8.
95. Elkon K, Casali P. Nature and functions of autoantibodies. Nat Clin Pract Rheumatol. 2008;4(9):491-8.
96. Duggal NA, Upton J, Phillips AC, Sapey E, Lord JM. An age-related numerical and functional deficit in CD19(+) CD24(hi) CD38(hi) B cells is associated with an increase in systemic autoimmunity. Aging Cell. 2013;12(5):873-81.
97. Sayed N, Huang Y, Nguyen K, Krejciova-Rajaniemi Z, Grawe AP, Gao T, et al. An inflammatory aging clock (iAge) based on deep learning tracks multimorbidity, immunosenescence, frailty and cardiovascular aging. Nat Aging. 2021;1:598-615.
98. Verschoor CP, Johnstone J, Millar J, Dorrington MG, Habibagahi M, Lelic A, et al. Blood CD33(+)HLA-DR(-) myeloid-derived suppressor cells are increased with age and a history of cancer. J Leukoc Biol. 2013;93(4):633-7.
99. Husain K, Hernandez W, Ansari RA, Ferder L. Inflammation, oxidative stress and renin angiotensin system in atherosclerosis. World J Biol Chem. 2015;6(3):209-17.
100. Nie K, Zhang Y, Gan R, Wang L, Zhao J, Huang Z, et al. Polymorphisms in immune/inflammatory cytokine genes are related to Parkinson's disease with cognitive impairment in the Han Chinese population. Neurosci Lett. 2013;541:111-5.
101. Valdes AMW, J.; Segal, E.; Spector, T. D. Role of the gut microbiota in nutrition and health. BMJ. 2018.
102. Rinninella E, Raoul P, Cintoni M, Franceschi F, Miggiano GAD, Gasbarrini A, et al. What is the Healthy Gut Microbiota Composition? A Changing Ecosystem across Age, Environment, Diet, and Diseases. Microorganisms. 2019;7(1).
103. Lloyd-Price J, Abu-Ali G, Huttenhower C. The healthy human microbiome. Genome Med. 2016;8(1):51.
104. Jandhyala SM, Talukdar R, Subramanyam C, Vuyyuru H, Sasikala M, Nageshwar Reddy D. Role of the normal gut microbiota. World J Gastroenterol. 2015;21(29):8787-803.
105. Kho ZY, Lal SK. The Human Gut Microbiome - A Potential Controller of Wellness and Disease. Front Microbiol. 2018;9:1835.

106. Agus A, Clement K, Sokol H. Gut microbiota-derived metabolites as central regulators in metabolic disorders. Gut. 2021;70(6):1174-82.
107. Zhou Y, Xu H, Xu J, Guo X, Zhao H, Chen Y, et al. F. prausnitzii and its supernatant increase SCFAs-producing bacteria to restore gut dysbiosis in TNBS-induced colitis. AMB Express. 2021;11(1):33.
108. Kelly CJ, Zheng L, Campbell EL, Saeedi B, Scholz CC, Bayless AJ, et al. Crosstalk between Microbiota-Derived Short-Chain Fatty Acids and Intestinal Epithelial HIF Augments Tissue Barrier Function. Cell Host Microbe. 2015;17(5):662-71.
109. Bansal T, Alaniz RC, Wood TK, Jayaraman A. The bacterial signal indole increases epithelial-cell tight-junction resistance and attenuates indicators of inflammation. Proc Natl Acad Sci U S A. 2010;107(1):228-33.
110. Geuking MB, Cahenzli J, Lawson MA, Ng DC, Slack E, Hapfelmeier S, et al. Intestinal bacterial colonization induces mutualistic regulatory T cell responses. Immunity. 2011;34(5):794-806.
111. Zelante T, Iannitti RG, Cunha C, De Luca A, Giovannini G, Pieraccini G, et al. Tryptophan catabolites from microbiota engage aryl hydrocarbon receptor and balance mucosal reactivity via interleukin-22. Immunity. 2013;39(2):372-85.
112. Castleman MJ, Dillon SM, Purba CM, Cogswell AC, Kibbie JJ, McCarter MD, et al. Commensal and Pathogenic Bacteria Indirectly Induce IL-22 but Not IFNgamma Production From Human Colonic ILC3s via Multiple Mechanisms. Front Immunol. 2019;10:649.
113. Cardoso MH, Meneguetti BT, Oliveira-Junior NG, Macedo MLR, Franco OL. Antimicrobial peptide production in response to gut microbiota imbalance. Peptides. 2022;157:170865.
114. Cornick S, Tawiah A, Chadee K. Roles and regulation of the mucus barrier in the gut. Tissue Barriers. 2015;3(1-2):e982426.
115. Bosco N, Noti M. The aging gut microbiome and its impact on host immunity. Genes Immun. 2021;22(5-6):289-303.
116. Odamaki T, Kato K, Sugahara H, Hashikura N, Takahashi S, Xiao JZ, et al. Age-related changes in gut microbiota composition from newborn to centenarian: a cross-sectional study. BMC Microbiol. 2016;16:90.
117. Biagi E, Candela M, Turroni S, Garagnani P, Franceschi C, Brigidi P. Ageing and gut microbes: perspectives for health maintenance and longevity. Pharmacol Res. 2013;69(1):11-20.
118. David LA, Maurice CF, Carmody RN, Gootenberg DB, Button JE, Wolfe BE, et al. Diet rapidly and reproducibly alters the human gut microbiome. Nature. 2014;505(7484):559-63.
119. Ge X, Ding C, Zhao W, Xu L, Tian H, Gong J, et al. Antibiotics-induced depletion of mice microbiota induces changes in host serotonin biosynthesis and intestinal motility. J Transl Med. 2017;15(1):13.
120. Silva YP, Bernardi A, Frozza RL. The Role of Short-Chain Fatty Acids From Gut Microbiota in Gut-Brain Communication. Front Endocrinol (Lausanne). 2020;11:25.
121. Duboc H, Rajca S, Rainteau D, Benarous D, Maubert MA, Quervain E, et al. Connecting dysbiosis, bile-acid dysmetabolism and gut inflammation in inflammatory bowel diseases. Gut. 2013;62(4):531-9.
122. Rios-Covian D, Gonzalez S, Nogacka AM, Arboleya S, Salazar N, Gueimonde M, et al. An Overview on Fecal Branched Short-Chain Fatty Acids Along Human Life and as Related With Body Mass Index: Associated Dietary and Anthropometric Factors. Front Microbiol. 2020;11:973.
123. Salazar N, Arboleya S, Fernandez-Navarro T, de Los Reyes-Gavilan CG, Gonzalez S, Gueimonde M. Age-Associated Changes in Gut Microbiota and Dietary Components Related with the Immune System in Adulthood and Old Age: A Cross-Sectional Study. Nutrients. 2019;11(8).
124. Biagi E, Nylund L, Candela M, Ostan R, Bucci L, Pini E, et al. Through ageing, and beyond: gut microbiota and inflammatory status in seniors and centenarians. PLoS One. 2010;5(5):e10667.
125. Woodmansey EJ. Intestinal bacteria and ageing. J Appl Microbiol. 2007;102(5):1178-86.
126. Tiihonen K, Ouwehand AC, Rautonen N. Human intestinal microbiota and healthy ageing. Ageing Res Rev. 2010;9(2):107-16.

127. Li D, Ke Y, Zhan R, Liu C, Zhao M, Zeng A, et al. Trimethylamine-N-oxide promotes brain aging and cognitive impairment in mice. Aging Cell. 2018;17(4):e12768.
128. Xu R, Wang Q. Towards understanding brain-gut-microbiome connections in Alzheimer's disease. BMC Syst Biol. 2016;10 Suppl 3:63.
129. Vancamelbeke M, Vermeire S. The intestinal barrier: a fundamental role in health and disease. Expert Rev Gastroenterol Hepatol. 2017;11(9):821-34.
130. Chelakkot C, Ghim J, Ryu SH. Mechanisms regulating intestinal barrier integrity and its pathological implications. Exp Mol Med. 2018;50(8):1-9.
131. Lueschow SR, McElroy SJ. The Paneth Cell: The Curator and Defender of the Immature Small Intestine. Front Immunol. 2020;11:587.
132. Camilleri M. Leaky gut: mechanisms, measurement and clinical implications in humans. Gut. 2019;68(8):1516-26.
133. Conway J, N AD. Ageing of the gut microbiome: Potential influences on immune senescence and inflammageing. Ageing Res Rev. 2021;68:101323.
134. Kim M, Benayoun BA. The microbiome: An emerging key player in aging and longevity. Translational Medicine of Aging. 2020;4:103-16.
135. Sovran B, Hugenholtz F, Elderman M, Van Beek AA, Graversen K, Huijskes M, et al. Age-associated Impairment of the Mucus Barrier Function is Associated with Profound Changes in Microbiota and Immunity. Sci Rep. 2019;9(1):1437.
136. Ren WY, Wu KF, Li X, Luo M, Liu HC, Zhang SC, et al. Age-related changes in small intestinal mucosa epithelium architecture and epithelial tight junction in rat models. Aging Clin Exp Res. 2014;26(2):183-91.
137. E.L. Mitchell ATD, K. Brass, M. Dendinger, R. Barner, R. Gharaibeh, A.A. Fodor, K. Kavanagh. Reduced motility, mucosal barrier function, and inflammation in aged monkeys. J Nutr Health Aging. 2017.
138. Thevaranjan N, Puchta A, Schulz C, Naidoo A, Szamosi JC, Verschoor CP, et al. Age-Associated Microbial Dysbiosis Promotes Intestinal Permeability, Systemic Inflammation, and Macrophage Dysfunction. Cell Host Microbe. 2017;21(4):455-66 e4.
139. Edelblum KL, Sharon G, Singh G, Odenwald MA, Sailer A, Cao S, et al. The Microbiome Activates CD4 T-cell-mediated Immunity to Compensate for Increased Intestinal Permeability. Cell Mol Gastroenterol Hepatol. 2017;4(2):285-97.
140. Dinakaran V. Microbial Translocation in the Pathogenesis of Cardiovascular Diseases: A Microbiome Perspective. Journal of Cardiology & Current Research. 2017;8(6).
141. Van Den Broeke C, De Burghgraeve T, Ummels M, Gescher N, Deckx L, Tjan-Heijnen V, et al. Occurrence of Malnutrition and Associated Factors in Community-Dwelling Older Adults: Those with a Recent Diagnosis of Cancer Are at Higher Risk. J Nutr Health Aging. 2018;22(2):191-8.
142. Agus A, Denizot J, Thevenot J, Martinez-Medina M, Massier S, Sauvanet P, et al. Western diet induces a shift in microbiota composition enhancing susceptibility to Adherent-Invasive E. coli infection and intestinal inflammation. Sci Rep. 2016;6:19032.
143. Milanovic Z, Pantelic S, Trajkovic N, Sporis G, Kostic R, James N. Age-related decrease in physical activity and functional fitness among elderly men and women. Clin Interv Aging. 2013;8:549-56.
144. Evans CC, LePard KJ, Kwak JW, Stancukas MC, Laskowski S, Dougherty J, et al. Exercise prevents weight gain and alters the gut microbiota in a mouse model of high fat diet-induced obesity. PLoS One. 2014;9(3):e92193.
145. Clarke SF, Murphy EF, O'Sullivan O, Lucey AJ, Humphreys M, Hogan A, et al. Exercise and associated dietary extremes impact on gut microbial diversity. Gut. 2014;63(12):1913-20.
146. Dethlefsen L, Relman DA. Incomplete recovery and individualized responses of the human distal gut microbiota to repeated antibiotic perturbation. Proc Natl Acad Sci U S A. 2011;108 Suppl 1(Suppl 1):4554-61.

147. Atarashi K, Tanoue T, Ando M, Kamada N, Nagano Y, Narushima S, et al. Th17 Cell Induction by Adhesion of Microbes to Intestinal Epithelial Cells. Cell. 2015;163(2):367-80.
148. Ohnmacht CP, J.; Cording, S.; Wing, J. B.; Atarashi, K.; Obata, Y.; Gaboriau-Routhiau, V.; Marques, R.; Dulauroy, S.; Fedoseeva, M.; Busslinger, M.; Cerf-Bensussan, N.; Boneca, I. G.; Voehringer, D.; Hase, K.; Honda, K.; Sakaguchi, S.; Eberl, G. . The microbiota regulates type 2 immunity through RORγt+ T cells. Science. 2015.
149. N'Diaye EN, Branda CS, Branda SS, Nevarez L, Colonna M, Lowell C, et al. TREM-2 (triggering receptor expressed on myeloid cells 2) is a phagocytic receptor for bacteria. J Cell Biol. 2009;184(2):215-23.
150. Smythies LE, Sellers M, Clements RH, Mosteller-Barnum M, Meng G, Benjamin WH, et al. Human intestinal macrophages display profound inflammatory anergy despite avid phagocytic and bacteriocidal activity. J Clin Invest. 2005;115(1):66-75.
151. Scharen OP, Hapfelmeier S. Robust microbe immune recognition in the intestinal mucosa. Genes Immun. 2021;22(5-6):268-75.
152. Reboldi A, Arnon TI, Rodda LB, Atakilit A, Sheppard D, Cyster JG. IgA production requires B cell interaction with subepithelial dendritic cells in Peyer's patches. Science. 2016;352(6287):aaf4822.
153. Wei M, Shinkura R, Doi Y, Maruya M, Fagarasan S, Honjo T. Mice carrying a knock-in mutation of Aicda resulting in a defect in somatic hypermutation have impaired gut homeostasis and compromised mucosal defense. Nat Immunol. 2011;12(3):264-70.
154. Diehl GE, Longman RS, Zhang JX, Breart B, Galan C, Cuesta A, et al. Microbiota restricts trafficking of bacteria to mesenteric lymph nodes by CX(3)CR1(hi) cells. Nature. 2013;494(7435):116-20.
155. Round JL, Lee SM, Li J, Tran G, Jabri B, Chatila TA, et al. The Toll-like receptor 2 pathway establishes colonization by a commensal of the human microbiota. Science. 2011;332(6032):974-7.
156. Rubtsov YP, Rasmussen JP, Chi EY, Fontenot J, Castelli L, Ye X, et al. Regulatory T cell-derived interleukin-10 limits inflammation at environmental interfaces. Immunity. 2008;28(4):546-58.
157. Alvarez CA, Jones MB, Hambor J, Cobb BA. Characterization of Polysaccharide A Response Reveals Interferon Responsive Gene Signature and Immunomodulatory Marker Expression. Front Immunol. 2020;11:556813.
158. Johnson JL, Jones MB, Cobb BA. Polysaccharide-experienced effector T cells induce IL-10 in FoxP3+ regulatory T cells to prevent pulmonary inflammation. Glycobiology. 2018;28(1):50-8.
159. Jones MB, Alvarez CA, Johnson JL, Zhou JY, Morris N, Cobb BA. CD45Rb-low effector T cells require IL-4 to induce IL-10 in FoxP3 Tregs and to protect mice from inflammation. PLoS One. 2019;14(5):e0216893.
160. Johnson JL, Jones MB, Cobb BA. Polysaccharide A from the capsule of Bacteroides fragilis induces clonal CD4+ T cell expansion. J Biol Chem. 2015;290(8):5007-14.
161. Erturk-Hasdemir D, Oh SF, Okan NA, Stefanetti G, Gazzaniga FS, Seeberger PH, et al. Symbionts exploit complex signaling to educate the immune system. Proc Natl Acad Sci U S A. 2019;116(52):26157-66.
162. Donohoe DR, Garge N, Zhang X, Sun W, O'Connell TM, Bunger MK, et al. The microbiome and butyrate regulate energy metabolism and autophagy in the mammalian colon. Cell Metab. 2011;13(5):517-26.
163. Mirzaei R, Dehkhodaie E, Bouzari B, Rahimi M, Gholestani A, Hosseini-Fard SR, et al. Dual role of microbiota-derived short-chain fatty acids on host and pathogen. Biomed Pharmacother. 2022;145:112352.
164. Smith PM, Howitt MR, Panikov N, Michaud M, Gallini CA, Bohlooly YM, et al. The microbial metabolites, short-chain fatty acids, regulate colonic Treg cell homeostasis. Science. 2013;341(6145):569-73.

165. Sun M, Wu W, Chen L, Yang W, Huang X, Ma C, et al. Microbiota-derived short-chain fatty acids promote Th1 cell IL-10 production to maintain intestinal homeostasis. Nat Commun. 2018;9(1):3555.
166. Bachem A, Makhlouf C, Binger KJ, de Souza DP, Tull D, Hochheiser K, et al. Microbiota-Derived Short-Chain Fatty Acids Promote the Memory Potential of Antigen-Activated CD8(+) T Cells. Immunity. 2019;51(2):285-97 e5.
167. Feingold KR, Moser A, Shigenaga JK, Grunfeld C. Inflammation stimulates niacin receptor (GPR109A/HCA2) expression in adipose tissue and macrophages. J Lipid Res. 2014;55(12):2501-8.
168. Kaisar MMM, Pelgrom LR, van der Ham AJ, Yazdanbakhsh M, Everts B. Butyrate Conditions Human Dendritic Cells to Prime Type 1 Regulatory T Cells via both Histone Deacetylase Inhibition and G Protein-Coupled Receptor 109A Signaling. Front Immunol. 2017;8:1429.
169. Singh N, Gurav A, Sivaprakasam S, Brady E, Padia R, Shi H, et al. Activation of Gpr109a, receptor for niacin and the commensal metabolite butyrate, suppresses colonic inflammation and carcinogenesis. Immunity. 2014;40(1):128-39.
170. Kim M, Qie Y, Park J, Kim CH. Gut Microbial Metabolites Fuel Host Antibody Responses. Cell Host Microbe. 2016;20(2):202-14.
171. Vinolo MA, Rodrigues HG, Hatanaka E, Sato FT, Sampaio SC, Curi R. Suppressive effect of short-chain fatty acids on production of proinflammatory mediators by neutrophils. J Nutr Biochem. 2011;22(9):849-55.
172. Trompette A, Gollwitzer ES, Pattaroni C, Lopez-Mejia IC, Riva E, Pernot J, et al. Dietary Fiber Confers Protection against Flu by Shaping Ly6c(-) Patrolling Monocyte Hematopoiesis and CD8(+) T Cell Metabolism. Immunity. 2018;48(5):992-1005 e8.
173. Monaghan TM, Duggal NA, Rosati E, Griffin R, Hughes J, Roach B, et al. A Multi-Factorial Observational Study on Sequential Fecal Microbiota Transplant in Patients with Medically Refractory Clostridioides difficile Infection. Cells. 2021;10(11).
174. Weng NP, Akbar AN, Goronzy J. CD28(-) T cells: their role in the age-associated decline of immune function. Trends Immunol. 2009;30(7):306-12.
175. Noren Hooten N, Evans MK. Techniques to Induce and Quantify Cellular Senescence. J Vis Exp. 2017(123).
176. Galbiati A, Beausejour C, d'Adda di Fagagna F. A novel single-cell method provides direct evidence of persistent DNA damage in senescent cells and aged mammalian tissues. Aging Cell. 2017;16(2):422-7.
177. Rothkamm K, Barnard S, Moquet J, Ellender M, Rana Z, Burdak-Rothkamm S. DNA damage foci: Meaning and significance. Environ Mol Mutagen. 2015;56(6):491-504.
178. Campisi J, d'Adda di Fagagna F. Cellular senescence: when bad things happen to good cells. Nat Rev Mol Cell Biol. 2007;8(9):729-40.
179. Baldwin ASJ. The NF-kappa B and I kappa B proteins- new discoveries and insights. Annu Rev Immunol. 1996.
180. Di Mitri D, Azevedo RI, Henson SM, Libri V, Riddell NE, Macaulay R, et al. Reversible senescence in human CD4+CD45RA+CD27- memory T cells. J Immunol. 2011;187(5):2093-100.
181. Ma K, Chen G, Li W, Kepp O, Zhu Y, Chen Q. Mitophagy, Mitochondrial Homeostasis, and Cell Fate. Front Cell Dev Biol. 2020;8:467.
182. Correia-Melo C, Marques FD, Anderson R, Hewitt G, Hewitt R, Cole J, et al. Mitochondria are required for pro-ageing features of the senescent phenotype. EMBO J. 2016;35(7):724-42.
183. Callender LA, Carroll EC, Bober EA, Akbar AN, Solito E, Henson SM. Mitochondrial mass governs the extent of human T cell senescence. Aging Cell. 2020;19(2):e13067.
184. Ruano D. Proteostasis Dysfunction in Aged Mammalian Cells. The Stressful Role of Inflammation. Front Mol Biosci. 2021;8:658742.
185. Tai H, Wang Z, Gong H, Han X, Zhou J, Wang X, et al. Autophagy impairment with lysosomal and mitochondrial dysfunction is an important characteristic of oxidative stress-induced senescence. Autophagy. 2017;13(1):99-113.

186. Lee YK, Lee JA. Role of the mammalian ATG8/LC3 family in autophagy: differential and compensatory roles in the spatiotemporal regulation of autophagy. BMB Rep. 2016;49(8):424-30.
187. Kim YC, Guan KL. mTOR: a pharmacologic target for autophagy regulation. J Clin Invest. 2015;125(1):25-32.
188. Ruvinsky I, Sharon N, Lerer T, Cohen H, Stolovich-Rain M, Nir T, et al. Ribosomal protein S6 phosphorylation is a determinant of cell size and glucose homeostasis. Genes Dev. 2005;19(18):2199-211.
189. Davie JR. Inhibition of Histone Deacetylase Activity by Butyrate. Nutritional Proteomics in Cancer Prevention. 2003.
190. Schulthess J, Pandey S, Capitani M, Rue-Albrecht KC, Arnold I, Franchini F, et al. The Short Chain Fatty Acid Butyrate Imprints an Antimicrobial Program in Macrophages. Immunity. 2019;50(2):432-45 e7.
191. Folkerts J, Redegeld F, Folkerts G, Blokhuis B, van den Berg MPM, de Bruijn MJW, et al. Butyrate inhibits human mast cell activation via epigenetic regulation of FcepsilonRI-mediated signaling. Allergy. 2020;75(8):1966-78.
192. Pedersen SS, Prause M, Williams K, Barres R, Billestrup N. Butyrate inhibits IL-1beta-induced inflammatory gene expression by suppression of NF-kappaB activity in pancreatic beta cells. J Biol Chem. 2022;298(9):102312.
193. Pathak RU, Soujanya M, Mishra RK. Deterioration of nuclear morphology and architecture: A hallmark of senescence and aging. Ageing Res Rev. 2021;67:101264.
194. Heckenbach I, Mkrtchyan GV, Ezra MB, Bakula D, Madsen JS, Nielsen MH, et al. Nuclear morphology is a deep learning biomarker of cellular senescence. Nature Aging. 2022;2(8):742-55.
195. Ivanov A, Pawlikowski J, Manoharan I, van Tuyn J, Nelson DM, Rai TS, et al. Lysosome-mediated processing of chromatin in senescence. J Cell Biol. 2013;202(1):129-43.
196. Freund A, Laberge RM, Demaria M, Campisi J. Lamin B1 loss is a senescence-associated biomarker. Mol Biol Cell. 2012;23(11):2066-75.
197. Lopez-Otin C, Blasco MA, Partridge L, Serrano M, Kroemer G. Hallmarks of aging: An expanding universe. Cell. 2023;186(2):243-78.
198. Correa-Oliveira R, Fachi JL, Vieira A, Sato FT, Vinolo MA. Regulation of immune cell function by short-chain fatty acids. Clin Transl Immunology. 2016;5(4):e73.
199. Siddiqui MT, Cresci GAM. The Immunomodulatory Functions of Butyrate. J Inflamm Res. 2021;14:6025-41.
200. Arpaia N, Campbell C, Fan X, Dikiy S, van der Veeken J, deRoos P, et al. Metabolites produced by commensal bacteria promote peripheral regulatory T-cell generation. Nature. 2013;504(7480):451-5.
201. He Y, Fu L, Li Y, Wang W, Gong M, Zhang J, et al. Gut microbial metabolites facilitate anticancer therapy efficacy by modulating cytotoxic CD8(+) T cell immunity. Cell Metab. 2021;33(5):988-1000 e7.
202. Kang C. Senolytics and Senostatics: A Two-Pronged Approach to Target Cellular Senescence for Delaying Aging and Age-Related Diseases. Mol Cells. 2019;42(12):821-7.
203. Han YM, Bedarida T, Ding Y, Somba BK, Lu Q, Wang Q, et al. beta-Hydroxybutyrate Prevents Vascular Senescence through hnRNP A1-Mediated Upregulation of Oct4. Mol Cell. 2018;71(6):1064-78 e5.
204. Cavaglieri CR, Nishiyama A, Fernandes LC, Curi R, Miles EA, Calder PC. Differential effects of short-chain fatty acids on proliferation and production of pro- and anti-inflammatory cytokines by cultured lymphocytes. Life Sci. 2003;73(13):1683-90.
205. Wang CC, Wu H, Lin FH, Gong R, Xie F, Peng Y, et al. Sodium butyrate enhances intestinal integrity, inhibits mast cell activation, inflammatory mediator production and JNK signaling pathway in weaned pigs. Innate Immun. 2018;24(1):40-6.

206. Tang G, Du Y, Guan H, Jia J, Zhu N, Shi Y, et al. Butyrate ameliorates skeletal muscle atrophy in diabetic nephropathy by enhancing gut barrier function and FFA2-mediated PI3K/Akt/mTOR signals. Br J Pharmacol. 2022;179(1):159-78.
207. Goldberg EL, Asher JL, Molony RD, Shaw AC, Zeiss CJ, Wang C, et al. beta-Hydroxybutyrate Deactivates Neutrophil NLRP3 Inflammasome to Relieve Gout Flares. Cell Rep. 2017;18(9):2077-87.
208. Jiang L, Wang J, Liu Z, Jiang A, Li S, Wu D, et al. Sodium Butyrate Alleviates Lipopolysaccharide-Induced Inflammatory Responses by Down-Regulation of NF-kappaB, NLRP3 Signaling Pathway, and Activating Histone Acetylation in Bovine Macrophages. Front Vet Sci. 2020;7:579674.
209. Lanna A, Henson SM, Escors D, Akbar AN. The kinase p38 activated by the metabolic regulator AMPK and scaffold TAB1 drives the senescence of human T cells. Nat Immunol. 2014;15(10):965-72.
210. Songkiatisak P, Rahman SMT, Aqdas M, Sung MH. NF-kappaB, a culprit of both inflamm-ageing and declining immunity? Immun Ageing. 2022;19(1):20.
211. Aguilar EC, Leonel AJ, Teixeira LG, Silva AR, Silva JF, Pelaez JM, et al. Butyrate impairs atherogenesis by reducing plaque inflammation and vulnerability and decreasing NFkappaB activation. Nutr Metab Cardiovasc Dis. 2014;24(6):606-13.
212. Usami M, Kishimoto K, Ohata A, Miyoshi M, Aoyama M, Fueda Y, et al. Butyrate and trichostatin A attenuate nuclear factor kappaB activation and tumor necrosis factor alpha secretion and increase prostaglandin E2 secretion in human peripheral blood mononuclear cells. Nutr Res. 2008;28(5):321-8.
213. Napetschnig J, Wu H. Molecular basis of NF-kappaB signaling. Annu Rev Biophys. 2013;42:443-68.
214. José Alberto López-Domínguez SR-L, Ulises Ahumada-Castro, Pierre-Yves Desprez, Maria Konovalenko, Remi-Martin Laberge, César Cárdenas, José Manuel Villalba, Judith Campisi. Cdkn1a transcript variant 2 is a marker of aging and cellular senescence. Aging. 2021.
215. Bartkova JL, J.; Strauss, M.; Bartek, J. Cyclin D3- requirement for G1:S transition and high abundance in quiescent tissues suggest a dual role in proliferation and di erentiation. Oncogene. 1998.
216. Kwak SE, Shin HE, Zhang DD, Lee J, Yoon KJ, Bae JH, et al. Potential role of exercise-induced glucose-6-phosphate isomerase in skeletal muscle function. J Exerc Nutrition Biochem. 2019;23(2):28-33.
217. Westermann B. Mitochondrial fusion and fission in cell life and death. Nat Rev Mol Cell Biol. 2010;11(12):872-84.
218. Tailor D, Hahm ER, Kale RK, Singh SV, Singh RP. Sodium butyrate induces DRP1-mediated mitochondrial fusion and apoptosis in human colorectal cancer cells. Mitochondrion. 2014;16:55-64.
219. Yue S, Zheng X, Zheng Y. Cell-type-specific role of lamin-B1 in thymus development and its inflammation-driven reduction in thymus aging. Aging Cell. 2019;18(4):e12952.
220. Dou Z, Ghosh K, Vizioli MG, Zhu J, Sen P, Wangensteen KJ, et al. Cytoplasmic chromatin triggers inflammation in senescence and cancer. Nature. 2017;550(7676):402-6.
221. Kespohl M, Vachharajani N, Luu M, Harb H, Pautz S, Wolff S, et al. The Microbial Metabolite Butyrate Induces Expression of Th1-Associated Factors in CD4(+) T Cells. Front Immunol. 2017;8:1036.
222. Luu M, Weigand K, Wedi F, Breidenbend C, Leister H, Pautz S, et al. Regulation of the effector function of CD8(+) T cells by gut microbiota-derived metabolite butyrate. Sci Rep. 2018;8(1):14430.
223. Cong J, Zhou P, Zhang R. Intestinal Microbiota-Derived Short Chain Fatty Acids in Host Health and Disease. Nutrients. 2022;14(9).
224. Chambers ES, Viardot A, Psichas A, Morrison DJ, Murphy KG, Zac-Varghese SE, et al. Effects of targeted delivery of propionate to the human colon on appetite regulation, body weight maintenance and adiposity in overweight adults. Gut. 2015;64(11):1744-54.

225. Polyviou T, MacDougall K, Chambers ES, Viardot A, Psichas A, Jawaid S, et al. Randomised clinical study: inulin short-chain fatty acid esters for targeted delivery of short-chain fatty acids to the human colon. Aliment Pharmacol Ther. 2016;44(7):662-72.
226. Chambers ES, Byrne CS, Morrison DJ, Murphy KG, Preston T, Tedford C, et al. Dietary supplementation with inulin-propionate ester or inulin improves insulin sensitivity in adults with overweight and obesity with distinct effects on the gut microbiota, plasma metabolome and systemic inflammatory responses: a randomised cross-over trial. Gut. 2019;68(8):1430-8.
227. Thorakkattu P, Khanashyam AC, Shah K, Babu KS, Mundanat AS, Deliephan A, et al. Postbiotics: Current Trends in Food and Pharmaceutical Industry. Foods. 2022;11(19).
228. Vernero M, De Blasio F, Ribaldone DG, Bugianesi E, Pellicano R, Saracco GM, et al. The Usefulness of Microencapsulated Sodium Butyrate Add-On Therapy in Maintaining Remission in Patients with Ulcerative Colitis: A Prospective Observational Study. J Clin Med. 2020;9(12).
229. Maruyama M, Abe R, Shimono T, Iwabuchi N, Abe F, Xiao JZ. The effects of non-viable Lactobacillus on immune function in the elderly: a randomised, double-blind, placebo-controlled study. Int J Food Sci Nutr. 2016;67(1):67-73.
230. Akatsu H, Arakawa K, Yamamoto T, Kanematsu T, Matsukawa N, Ohara H, et al. Lactobacillus in jelly enhances the effect of influenza vaccination in elderly individuals. J Am Geriatr Soc. 2013;61(10):1828-30.
231. Bunout D, Barrera G, Hirsch S, Gattas V, de la Maza MP, Haschke F, et al. Effects of a nutritional supplement on the immune response and cytokine production in free-living Chilean elderly. JPEN J Parenter Enteral Nutr. 2004;28(5):348-54.
232. Boge T, Remigy M, Vaudaine S, Tanguy J, Bourdet-Sicard R, van der Werf S. A probiotic fermented dairy drink improves antibody response to influenza vaccination in the elderly in two randomised controlled trials. Vaccine. 2009;27(41):5677-84.

Appendix

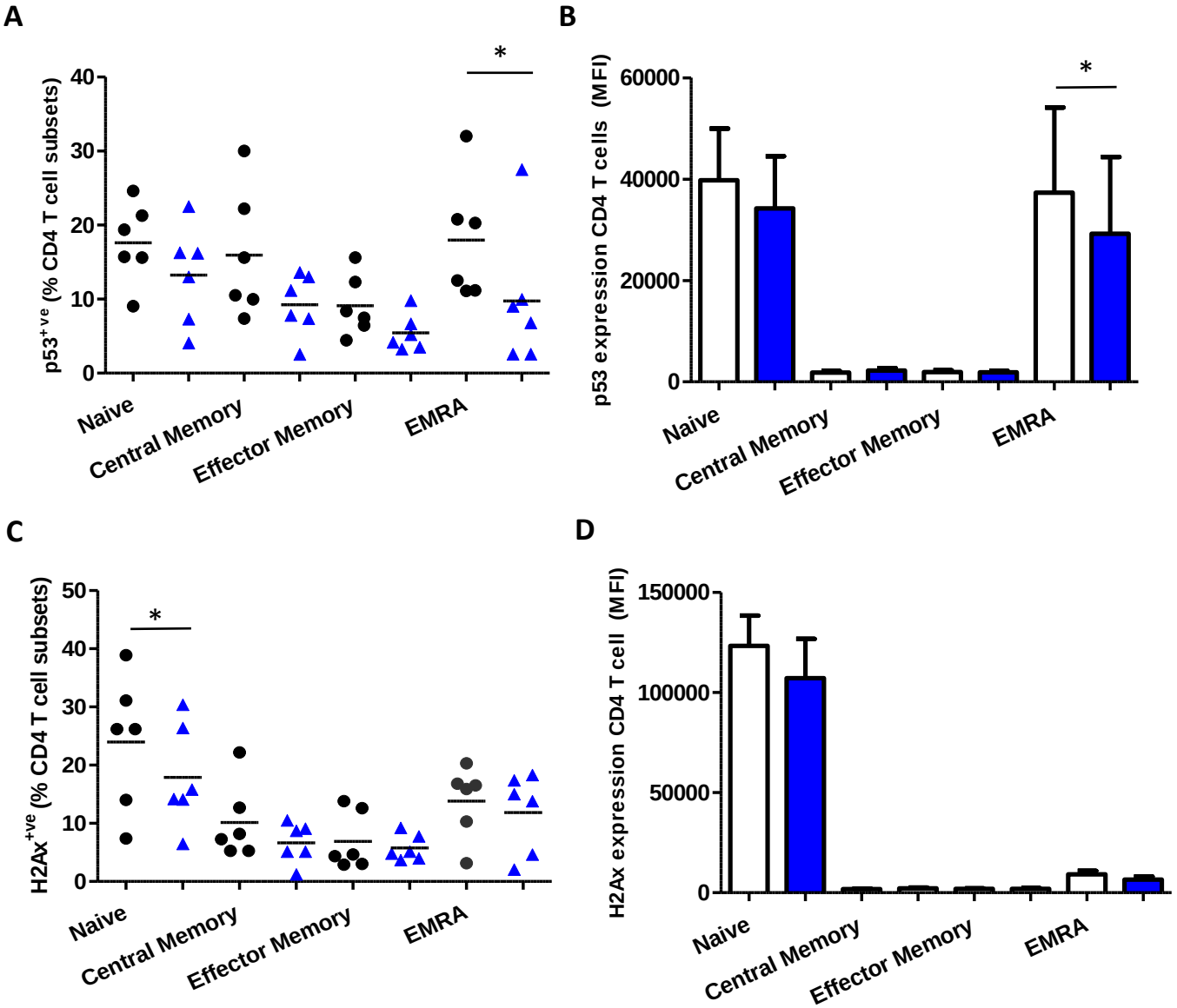

Supplementary Figure 1. Regulation of senescence phenotype by butyrate in aged CD4 T cells.
In vitro culture of PBMCs in CD3-coated wells for 3 days in the presence/absence of SCFA butyrate for **(A)** frequency of phosphorylated p53 expressing CD4 T cell subsets, **(B)** p53 expression levels in CD4 T cell subsets, **(C)** frequency of γH2AX expressing CD4 T cell subsets and **(D)** γ-H2AX expression levels (MFI) in CD4 T cell subsets. Statistical analysis was performed by a two-tailed paired Student's t-test. Data are shown as the mean ± SD *p <0.05.